

VOLTAGE STABILITY ANALYSIS USING CONVENTIONAL AND EVOLUTIONARY METHODS



Mitali Chakravorty

**Department of Electrical Engineering
Assam Engineering College
Guwahati-13**

**This thesis is submitted to
Gauhati University as requirement for the degree of
*Doctor of Philosophy***

Faculty of Engineering

June 2017

Dedicated to
my late father, my guiding light

DECLARATION

I hereby declare that this thesis is the result of my own research work which has been carried out under the guidance of Dr. (Mrs) Sarmila Patra of Assam Engineering College under Gauhati University. I further declare that this thesis as a whole or any part thereof has not been submitted to any university (or institute) for the award of any degree or diploma.

This thesis contains less than 90,000 (ninety thousand) words excluding bibliography and captions.



Mitali Chakravorty

June 2017



Government of Assam
ASSAM ENGINEERING COLLEGE
JALUKBARI :: GUWAHATI - 781013



Department of Electrical & Instrumentation Engineering

Dr. Sarmila Patra
Associate Professor

Email: sarmilapatra@yahoo.com
Mobile: +919864028052

CERTIFICATE

Certified that the thesis titled "**Voltage Stability Analysis Using Conventional and Evolutionary Methods**" is an authentic record of research carried out by **Mitali Chakravorty**, for the degree of Doctor of Philosophy in Engineering of Gauhati University, under my supervision and guidance.

I further certify that the candidate has fulfilled all criteria under existing norms for submission of current PhD thesis which is found to be original in kind and based on her own findings and close observation.

(Dr SARMILA PATRA)

Research Guide

June 2017

ACKNOWLEDGEMENTS

At the very outset, I express my deepest gratitude to Dr (Mrs) Sarmila Patra, my thesis supervisor, whose guidance and encouragement is unforgettable. She has been a great inspiration and a strong driving force, without which this work would not have been possible. Her wide knowledge, tremendous grasp of the subject and great motivational skills have been of immense value to me over the years.

I am very grateful to Dr D. Agarwal, Professor and HOD (Electrical Engineering), Assam Engineering College, Guwahati, for providing me with a healthy and productive environment to complete my thesis work successfully.

I am deeply indebted to Dr. D. Hazarika, Professor, Department of Electrical Engineering, Assam Engineering College, Guwahati, and Dr (Mrs) B. Goswami, Asso. Professor, Assam Engineering College, for their valuable inputs through the course of this work.

I would like to thank all faculty members of the Department of Electrical Engineering, Assam Engineering College, Guwahati, for their constant encouragement.

I gratefully acknowledge the various faculty members of IIT, Guwahati, for extending their help and support at different stages of my work.

Finally, I would like to express my ultimate gratitude to my husband Mr. S.N. Sarma and daughter Drishti, for being patient, supportive and encouraging throughout my period of research.



(MITAEI CHAKRAVORTY)

Table of Contents

List of Figures	xi-xiv
List of Tables	xv-xvi
Nomenclature	xvii-xix
Chapter 1: Introduction	1-15
1.1 Overview/ Problem Statement	1
1.2 Thesis objective/ Scope of work	2
1.3 Literature Review	3
1.4 Outline of the Thesis / Thesis Organisation	14
Chapter 2: Voltage Stability Analysis using Conventional Methods	
<i>(Weak Bus Identification)</i>	16-45
2.1. Introduction	16
2.2. Classification of Voltage Stability: Concepts and definitions	17
2.3. Analysis of Voltage stability	21
2.4. Methods of Voltage Stability Analysis: Weak Bus Identification:	23
2.4.1. P-V Curve method	26
2.4.2. Q-V Curve method	27
2.4.3. Modal analysis	29
2.4.4. Continuation Power Flow (CPF) method	32
2.4.5. Voltage Stability Indices	36
2.5. Results and Discussion	36
2.5.1. Case study: IEEE 30 bus system	37

2.5.1.1	Results of Modal Analysis	37
2.5.1.2	Results of Continuation Power Flow (CPF) Analysis	39
2.5.2.	Case study: IEEE 57 bus system	41
2.5.2.1	Results of Modal Analysis	41
2.5.2.2	Results of Continuation Power Flow (CPF) Analysis	43
2.6.	Conclusion	45
 Chapter 3: Bus Voltage Stability Analysis		
	<i>(Voltage Stability Enhancement using Reactive Power Compensation)</i>	46-72
3.1.	Introduction	46
3.2.	Flexible AC Transmission system (FACTS)	47
3.2.1.	Shunt FACTS controllers	48
3.2.2.	Series FACTS Controllers	51
3.2.3.	Series-shunt FACTS controller: United Power Flow Controller (UPFC)	54
3.3.	Bus Voltage Stability Analysis using Shunt FACTS controllers	55
3.3.1.	Modelling of SVC and STATCOM for power flow computations	56
3.3.2.	Chapter3: Objectives	59
3.4.	Results and Discussion	60
3.4.1.	Case study: IEEE 30 bus system	60

3.4.2.	Case Study: IEEE 57 bus System	65
3.4.3.	Summary / Analysis of Results	70
3.5.	Conclusion	72
Chapter 4: Line Voltage Stability Analysis		
	<i>(Application of FVSI and Series FACTS controllers)</i>	73-98
4.1.	Introduction	73
4.2.	Voltage Stability Indicators	74
4.2.1.	Bus voltage Stability Indices	75
4.2.2.	Line voltage Stability Indices	77
4.3.	Fast Voltage Stability Index (FVSI)	81
4.3.1.	Fast Voltage Stability Index Formulation	81
4.4.	Line stability analysis using series FACTS controllers	82
4.4.1.	Modelling of Thyristor controlled Series Compensator (TCSC)	83
4.4.2.	Modelling of Static Synchronous Series Compensator (SSSC)	85
4.4.3.	Chapter 4: Objectives	86
4.5.	Results and Discussion	87
4.5.1.	Case Studies	87
4.5.1.1.	Test case 1 : IEEE 30 bus system	87
4.5.1.2.	Results and Analysis (Test case 1)	88
4.5.1.3.	Test case 2 : IEEE 57 bus system	92
4.5.1.4.	Results and Analysis (Test case 2)	93
4.6.	Conclusion	98

Chapter 5: Voltage Stability Analysis using Evolutionary Methods	
<i>(Teaching Learning Based Optimization Method for Voltage Stability Analysis)</i>	99-126
5.1. Introduction	99
5.2. Evolutionary programming applied to Voltage Stability	100
5.3. The Teaching Learning Based Optimization (TLBO) Method	102
5.3.1. The Teaching Learning Based Optimization (TLBO) Algorithm	103
5.3.2. Multi-objective TLBO problem formulation	106
5.4. Chapter 5: Objectives	109
5.5. Results and Discussion	109
5.5.1. Case Study: IEEE 14 bus system	110
5.5.2. Case Study: IEEE 30 bus system	115
5.5.3. Case Study: IEEE 57 bus system	120
5.6. Conclusion	125
Chapter 6: Conclusion	
<i>(Summary of work and scope for future study)</i>	127-130
6.1 Summary of work	127
6.2 Scope for future study	130
References / Bibliography	131-144
Appendix A List of publications	145
Appendix B Flowcharts	146-149
Appendix C Test Data	150-158

List of Figures

2.1	Power System Stability- Classification	18
2.2	Single line representation of a two-bus system	22
2.3	Saddle-Node Bifurcation	25
2.4	P-V curve	27
2.5	Q-V curve	28
2.6	P-V curve solution using prediction-correction technique	32
2.7	Plot of Eigen values (real part) for IEEE 30 bus system	37
2.8	Highest Participation factor profile (IEEE 30 bus system)	38
2.9	Voltage magnitude profile of the weak buses (IEEE 30 bus system)	39
2.10	P-V curves for the PQ buses with minimum voltage Values (IEEE 30 bus system)	40
2.11	Plot of Eigen values (real part) for IEEE 57 bus system	41
2.12	Highest Participation factor profile (IEEE 57 bus system)	42
2.13	Voltage magnitude profile of the weak buses (IEEE 57 bus system)	44
2.14	P-V curves for the PQ buses with minimum voltage values (IEEE 57 bus system)	44
3.1	Basic structure of SVC (FC-TCR configuration)	49
3.2	Basic structure of SVC (TSC-TCR configuration)	50
3.3	Basic structure of STATCOM	51
3.4	Symbolic representation of SSSC	52
3.5	Basic structure of TCSC	53
3.6	Schematic of a Unified Power Flow Controller (UPFC)	54

3.7	Equivalent model of UPFC	55
3.8	Variable susceptance model of SVC	56
3.9	Model of STATCOM in Load flow calculations	57
3.10	Voltage Magnitude Profile of the weak buses (IEEE 30 bus system)	61
3.11	Voltage Magnitude Profile of the weakest (IEEE 30 bus system)	62
3.12	P-V curve for PQ buses with minimum voltages (IEEE 30 bus system) (Without compensation)	62
3.13	P-V curve for PQ buses with minimum voltages (IEEE 30 bus system) (With SVC in bus 30)	63
3.14	P-V curve for PQ buses with minimum voltages (IEEE 30 bus system) (With STATCOM in bus 30)	63
3.15	Reactive Power Profile of IEEE 30 Bus System (Without compensation)	64
3.16	Reactive Power Profile of IEEE 30 Bus System (With SVC in bus 30)	64
3.17	Reactive Power Profile of IEEE 30 Bus System (with STATCOM in bus 30)	65
3.18	Voltage Magnitude Profile of the weak buses (IEEE 57 bus system)	66
3.19	Voltage Magnitude Profile of the weakest bus (IEEE 57 bus system)	67
3.20	P-V curve for PQ buses with minimum voltages (IEEE 57 bus system) (Without compensation)	67
3.21	P-V curve for PQ buses with minimum voltages (IEEE 57 bus system) (SVC in bus 31)	68
3.22	P-V curve for PQ buses with minimum voltages (IEEE 57 bus system) (STATCOM in bus 31)	68

3.23	Reactive Power Profile of IEEE 57 Bus System (Without compensation)	69
3.24	Reactive Power Profile of IEEE 57 Bus System (With SVC in bus 31)	69
3.25	Reactive Power Profile of IEEE 57 Bus System (With STATCOM in bus 31)	69
4.1	Single line diagram of a two-bus system	78
4.2	TCSC Model	83
4.3	Circuit element model of SSSC	85
4.4	Real power flow profile of the compensated lines (IEEE 30 bus system)	89
4.5	Total Real Power Loss profile (IEEE 30 bus system)	89
4.6	Total Reactive Power Loss profile (IEEE 30 bus system)	90
4.7	Reactive power loss profile of compensated lines (IEEE 30 bus system)	90
4.8	Voltage profile of the connected buses (IEEE 30 bus system)	91
4.9	Real power flow profile of the compensated lines (IEEE 57 bus system)	94
4.10	Total Real power loss profile (IEEE 57 bus system)	94
4.11	Total Reactive power loss profile (IEEE 57 bus system)	95
4.12	Reactive power loss profile of the compensated lines (IEEE 57 bus system)	95
4.13	Voltage magnitude profile of the compensated lines (IEEE 57 bus system)	96
5.1	Voltage profile of the connected buses (IEEE 14 bus system)	111
5.2	Total Real Power Loss profile (IEEE 14 bus system)	112
5.3	Sum FVSI profile of compensated lines (IEEE 14 bus system)	113
5.4	Total Reactive Power Loss profile (IEEE 14 bus system)	114

5.5	Convergence characteristics of Multi-Objective TLBO & GA for IEEE 14 bus system	114
5.6	Voltage profile of the connected buses (IEEE 30 bus system)	116
5.7	Total Real Power Loss profile (IEEE 30 bus system)	117
5.8	Sum FVSI profile of compensated lines (IEEE 30 bus system)	118
5.9	Total Reactive Power Loss profile (IEEE 30 bus system)	119
5.10	Convergence characteristics of Multi-Objective TLBO & GA for IEEE 30 bus system	120
5.11	Voltage magnitude profile of the connected buses (IEEE 57 bus system)	121
5.12	Total Real Power Loss profile (IEEE 57 bus system)	122
5.13	Sum FVSI profile of compensated lines (IEEE 57 bus system)	123
5.14	Total Reactive Power Loss profile (IEEE 57 bus system)	124
5.15	Convergence characteristics of Multi-Objective TLBO & GA for IEEE 57 bus system	124

List of Tables

2.1	Minimum Eigen values for IEEE 30 bus system	38
2.2	Highest Participation factors (IEEE 30 bus system)	38
2.3	Voltage magnitudes of the weak buses (IEEE 30 bus system)	39
2.4	Minimum Eigen values for IEEE 57 bus system	41
2.5	Highest Participation factors (IEEE 57 bus system)	42
2.6	Voltage magnitudes of the weak buses (IEEE 57 bus system)	43
3.1	Voltage magnitudes of the weak buses (IEEE 30 bus System)	60
3.2	Voltage magnitudes of the weak buses (IEEE 57 bus system)	66
3.3	Maximum loading margin	70
3.4	Voltage magnitudes of weakest buses	70
3.5	State Variables of PSAT output	71
4.1	Results (IEEE 30 Bus system)	88
4.2	Results (IEEE 57 Bus system)	93
4.3	Line Compensation provided by FACTS devices	96
4.4	Real Power flow in adjacent lines	97
5.1	Voltage magnitudes of the connected buses (IEEE 14 bus system)	111
5.2	Result of Multi-Objective TLBO (IEEE 14 bus system)	112
5.3	Reactive Power Losses (IEEE 14 bus system)	113
5.4	Voltage magnitudes of the connected buses (IEEE 30 bus system)	116
5.5	Result of Multi-Objective TLBO (IEEE 30 bus system)	117
5.6	Reactive Power Losses (IEEE 30 bus system)	119

5.7	Voltage magnitudes of the connected buses (IEEE 57 bus system)	121
5.8	Result of Multi-Objective TLBO (IEEE 57 bus system)	122
5.9	Reactive Power Losses (IEEE 57 bus system)	123
5.10	Reactive Compensation provided by TCSC	125

Nomenclature

List of Symbols

V, I	:	Voltage, Current
P	:	Active Power
Q	:	Reactive Power
C	:	Capacitance
L	:	Inductance
Y	:	Bus Admittance Matrix
R	:	Resistance of line
X	:	Reactance of line
Z	:	Impedance of line
λ	:	(Lambda) Loading Factor of a bus
J	:	Jacobian Matrix of the power system
J_R	:	Reduced Jacobian Matrix
ξ	:	Right Eigen Vector matrix of J_R
η	:	Left Eigen Vector matrix of J_R
Λ	:	Diagonal Eigen value matrix of J_R
ΔV	:	Change in the voltage value.
ΔP	:	Change in the active power
ΔQ	:	Change in the reactive power
P_{Gm}	:	Active Power generation at m^{th} bus
Q_{Gm}	:	Reactive Power generation at m^{th} bus
P_{Dm}	:	Injected active power at m^{th} bus
Q_{Dm}	:	Injected reactor power at m^{th} bus
δ	:	Bus Voltage angle
ϕ	:	Power factor angle of the load
V_O	:	Base case load voltage
P_O	:	Base case load real power
Q_O	:	Base case load reactive power

P_L	:	Real power limit
Q_L	:	Reactive power limit
dV	:	Incremental change in V
dP	:	Incremental change in P
dQ	:	Incremental change in Q
θ	:	Impedance Angle
$\tan \theta$:	$= Q/P$
$ V_m , V_n $:	Voltage magnitudes of buses m and n
δ_m, δ_n	:	Voltage angles at buses m and n
X_{mn}	:	Reactance of Line m-n
i_s	:	Input current to the SVC
i_r	:	Current through the TCR of SVC
i_c	:	Current through the fixed capacitor, C of SVC
I_q	:	Current flow from the STATCOM output
E_s	:	Voltage of the STATCOM
E_t	:	Bus voltage to which the STATCOM is connected
V_C	:	SSSC output voltage
X_C	:	Capacitive reactor
V_{dc}	:	DC source voltage
V_{se}	:	Series voltage source output
V_{sh}	:	Shunt voltage source output
r and γ	:	UPFC control parameters
B_{SVC}	:	Susceptance of SVC
X_{ST}	:	STATCOM reactance
B_{ST}	:	STATCOM susceptance
Q_{ST}	:	Reactive power exchange between STATCOM
V_s	:	Sending end bus voltage
V_r	:	Receiving end bus voltage
P_r	:	Active power at the receiving end

Q_r	:	Reactive power at the receiving end
S_r	:	Apparent power at the receiving end
δ_s	:	Voltage angle at the sending end
δ_r	:	Voltage angle at the receiving end
X_{TCSC}	:	Equivalent reactance of the TCSC Controller
γ_{TCSC}	:	Compensation ratio of the TCSC

Acronyms

CPF	:	Continuation Power Flow
FACTS	:	Flexible AC Transmission System
FC	:	Fixed Capacitor
FVSI	:	Fast Voltage Stability Index
MLL	:	Maximum Loading Limit
RPF	:	Reactive Participation Factor
SNB	:	Saddle Node Bifurcation
STATCOM	:	Static Synchronous Compensator
SSSC	:	Static Synchronous Series Compensator
SVC	:	Static VAR Compensator
TCR	:	Thyristor Controlled Reactor
TCS	:	Thyristor Switched Capacitor
TCSC	:	Thyristor Controlled Series Compensator
UPFC	:	Unified Power Flow Controller
VCPI	:	Voltage Collapse Proximity Indicator
VSI	:	Voltage Stability Index
VSC	:	Voltage Source Converter
VSM	:	Voltage Stability Margin
TLBO	:	Teaching Learning Based Optimization
GA	:	Genetic Algorithm

Chapter 1

Introduction

This chapter is a general introduction to the thesis, importance of voltage stability analysis of transmission systems, the background of the work undertaken, its objectives and organisation of the thesis

1.1 Overview/Problem Statement

Power systems across the world today are subjected to heavy demands owing to widespread expansions in the networks. Environmental and economic constraints have forced the power systems to operate closer to their stability limits. Overloading of an already stressed system may lead to voltage collapse, when the bus voltage drops to such a level from which it cannot recover, and if ignored, may result in complete shutdown. Such blackouts have been witnessed in developed and developing countries in the recent past.

Voltage stability has, therefore, become a serious concern in power system operations. The complexity in the operation and structure of such networks is a

challenge that power engineers and researchers face frequently. Voltage Stability analysis is today considered very important for successful operation and planning of power systems and for reduction of losses.

It is known that the voltage instability phenomenon is dynamic in nature, and yet both static and dynamic methods are used for voltage studies. In most cases the system dynamics affecting voltage stability are usually quite slow and so static analysis is preferred, which gives information of the maximum loadability limit and factors contributing to the instability problem. Static analysis is found to involve less computational time and so it is faster than dynamic approach.

1.2 Thesis objective / Scope of work

Keeping in view the importance of voltage stability analysis for power system planners and engineers, the aim of this thesis is:

- ❖ Analysis of voltage stability with modern compensating devices like series and shunt FACTS controllers, using both conventional and evolutionary methods.

The thesis objectives are as mentioned below:

- To make an in-depth study of the voltage stability analysis of power system networks and the voltage collapse phenomenon.
- To study the conventional methods of voltage stability analysis and the voltage stability indices formulated for weak bus/line identification, satisfying the static voltage stability criteria.

- To investigate the impact of reactive power compensation on critical lines and bus using selected FACTS devices for different types of power system networks.
- To apply a new and effective evolutionary programming method i.e., the Teaching Learning Based Optimization (TLBO) method, for optimization of the ratings of the FACTS compensating device used for enhancing the voltage stability margin of weak lines.

1.3 Literature Review

With the fast development in urban areas and the subsequent overloaded and stressed conditions of our power system networks, Voltage Stability Analysis has gained importance in power system stability studies. Literature review indicates that sufficient work has been done in this aspect so far.

Static Voltage Stability Analysis was presented by H.G. Kwanty et.al in 1986, where steady-state stability and voltage collapse could be studied by considering them to arise from a common well-defined origin [1]. Kwanty showed that a state bifurcation exists that result in voltage collapse when the Jacobian is singular.

In 1988, I. Dobson and H.D. Chiang explained the loss of stability due to the disappearance of a stable equilibrium point in a saddle node bifurcation [2]. The voltage collapse model was demonstrated as a slow initial, and then a subsequent rapid voltage decrease. Subsequent works of the same author explored the voltage collapse phenomenon in diverse perspectives [3,4,5].

In 1989, V. Ajjarapu explored voltage stability via a multi-parameter perturbation technique [6]. The methodology took into consideration the Jacobian Matrix Eigen values for weak bus identification.

In 1992, B. Gao, G.K. Morrison, and P. Kundur proposed the Modal Analysis Method of Voltage Stability analysis [7]. The method used the Eigen values and Eigenvectors of a reduced matrix to provide a relative measure of proximity to voltage instability.

In 1992, V. Ajjarapu [8] presented a tool to examine the steady state voltage stability analysis of power systems: the Continuation Power Flow (CPF). The difficulty encountered in the Modal Analysis Method was that the Jacobian of the Newton Raphson Power Flow became singular at the Voltage Stability limit (or the critical/collapse point). To address and overcome this difficulty, the Continuation Power Flow method was developed, which employs the Predictor-Corrector scheme to find a solution path of the power flow equations.

It was therefore seen that voltage stability analysis methods could be categorised as direct methods and continuation methods.

Voltage Stability Analysis of power systems using static and dynamic techniques were discussed by G.K Morrison, B.Gao and P. Kundur [9]. Static Analysis was made using Modal Analysis method to determine the Voltage Stability of the power system under test. For the Dynamic analysis, the disturbance considered was the loss, without a fault, of one of the lines.

In 1993, C.A. Canizares and F.L. Alvarado discussed the implementation Point of Collapse and Continuation Methods for computation of voltage collapse points [10]. The tests were carried out on a variety of ac/dc systems. The Continuation Methods was observed as a method performed to provide additional information about the stability of the system and so was concluded that these two methods complement each other for accurate analysis of voltage stability of a power system.

C.A. Canizares, again in 1995, established a relation between bifurcations and power system stability [11]. Hopf and Saddle-node bifurcations had been recognised as some of the reasons for voltage stability problems. This paper concentrated on depicting the effects of Saddle-node bifurcations and their relationship to voltage collapse phenomenon, for different load models in different sample system. The results were further applied to a 115 bus S N I Ecuadorian system to discuss some of the applications and shortcomings of bifurcation theory.

C.A. Canizares et al., in their paper published in August 1996, made a comparative study of Performance Indices for detection of proximity of a node towards voltage collapse [12]. A new test function was proposed to be used in an existent performance index and it was compared with known singular values and Eigenvalue indices. The test was carried out on an IEEE 300 bus test system.

Definition and classification of Power System Stability had been put forward by P. Kundur et al., where the authors have defined and classified Power System Stability [13] to understand and mitigate the various forms of instabilities. The authors have

categorised Power System Stability into Rotor Angle Stability, Frequency Stability and Voltage Stability.

The knowledge of proximity of a particular line or bus to voltage collapse is of utmost importance in Voltage Stability studies. Some measuring indices had been formulated to identify the voltage-weak areas and their proximity to voltage collapse.

In 1986, P. Kessel and H. Glavitsch [14] formulated an indicator for online testing of a power system for voltage instabilities. This indicator used information of normal load flow to predict proximity of a node or bus to voltage collapse.

The authors [15] presented a technique where the system is reduced to a single-line network. A system stability factor was calculated to predict voltage collapse. Overall system stability could be checked through this process.

M. Moghavvemi and O. Faruque [16] formulated a voltage collapse proximity indicator (VCPI) based on the concept of maximum power transfer through a line, for an effective real-time monitoring of system status,

The same authors formulated another stability index (L_{mn}), to accurately predict voltage collapse of any line [17]. As long as L_{mn} remained less than 1, the system is considered stable and the system becomes unstable when the L_{mn} value exceeds 1, leading to voltage collapse.

Musirin, et al. developed the Fast Voltage Stability Index (FVSI) by obtaining the equation of current flow through a line in a 2-bus system [18]. This index was

capable of determining the point of voltage instability, the critical line referred to a bus and the weakest bus in the system. The results were compared with other line indices with favourable conclusions. Several similar indices were subsequently put forward by others, based on the same concept. Static Voltage Instability is mainly associated with reactive power imbalance. In 2004, A. Sode-Yome and N. Mithulananthan compared the traditional shunt capacitors with newly developed Flexible AC Transmission System (FACTS) devices like Static Var Compensators (SVC) and Static Synchronous Compensators (STATCOM), as reactive power compensators in static voltage stability margin enhancement [19]. It was found that FACTS devices provided better behaviour in terms of Loss reduction and Voltage profile improvement.

In 2005, the same authors extended the study to different types of FACTS devices (STATCOM, TCSC and SSSC) to compare their behaviour in Static voltage stability margin enhancement [20]. Earlier works considered only the A.C equations for voltage stability study. In this paper, the D.C. equations of the FACTS devices under study were incorporated in the Continuation Power flow (CPF) process in the voltage stability study. Voltage stability margin enhancement using the FACTS devices was compared.

In 2009, M. Ndubuka investigated the effects of Static Var Compensator (SVC) on Voltage Stability of a power system [21]. It was found that the FACTS controller; SVC provides fast-acting dynamic reactive compensation during contingencies. It also dampens power swings and reduces system losses by optimized reactive power control.

N.M. Ndubuka also studied the effects of STATCOM on voltage stability and transmission losses of power systems [22]. The test was carried out on the North West Nigerian Grid System (330KV) and it was observed that with STATCOM embedded in the system, the transmission losses were drastically reduced.

M. Kowsalya, et al, in 2009, presented a study on the voltage profile improvement in power system networks with optimal application of Unified Power Flow Controllers (UPFC) [23].

Champa Nandi, et al, studied the impact of SVC and STATCOM on voltage collapse and critical fault clearing time (CTFT) of the induction motor predominant load buses [24]. It was concluded that the stabilizing effect of SVC and STATCOM on the voltage helps in the fast recovery of the power network after fault clearing. It was also found that the critical fault clearing time for the system to regain voltage at stable state was lower with the application of STATCOM over SVC.

Since then, several comparative study of the performance of different FACTS controllers used for voltage stability margin improvement and loss minimization have been performed [25,26].

The power flow problem has also been treated as an optimization problem and in 1998, Canizares, et al. described several applications of optimization to voltage stability analysis [27]. The optimization problems stated here were those of voltage instability, chiefly those related to voltage collapse.

Considering voltage collapse as an optimization problem meant that many optimization techniques could be employed to compute the collapse point. One of them was the Interior Point Method [28], which had better limit handling capabilities and improved convergence characteristics than the Direct and Continuation Methods. In 2002, L.C.A. Ferreira et al. [28] used the Interior Point Optimization to improve the system operating conditions. Local shunt compensation was used for system loss minimization and load margin improvement.

Subsequent to these conventional optimization techniques, Evolutionary programming methods have been applied to power system stability studies from time to time. Artificial Intelligence (AI) techniques are modern research tools used to eliminate and/or minimize the limitations of conventional control methods. The FACTS controller ratings can be optimized to yield the best results, when applied to power system networks for the purpose of loss minimization or enhancement of voltage stability margin. The remarkable feature of these programming techniques is that no restrictions to the nature of the search space and the type of variables are found here.

Improvement of voltage stability margin with reactive power compensation had been highlighted by Y. Su et al. in 2006 [29]. The method proposed for the management of reactive power reserves was proposed as an optimization problem. Application of the evolutionary algorithm, Pseudo-gradient Evolutionary Programming had been used here, with Modal analysis technique used for the search direction.

The need to locate Type-1 load flow solutions, as they are closely associated with voltage collapse phenomenon was also highlighted [30]. In general, the load flow solution is considered Type K when there are K positive values for the real part of the Eigen values. Type-1 solutions have only one positive Eigen value (real part) and the rest are negative, indicating voltage instability. In this paper, the authors used a Hybrid Genetic Algorithm/ Particle Swarm Optimization Technique to find the Type-1 load flow solutions. The proposed method eliminated the need for tracing of solution curves.

In 2009, Liu Zhijian, et al. [31] presented a multi-objective designing method, based on fuzzy-satisfactory degree theory to establish co-ordination control of Power System Stabilizers (PSS), required for power angle stability; and Static VAR Compensators (SVC), required for voltage stability.

A.H. Khalazi, et al., applied an improved Harmony Search algorithm to an optimal reactive/voltage control problem [32]. The objectives of the problem were power transmission loss, voltage stability and voltage profile, which had been optimized separately. The results had then been compared with other evolutionary programs like Harmony search Algorithm (HSA) and Particle Swarm Optimization (PSO). The study was carried out on a standard IEEE 30 bus system.

Genetic Algorithm has been observed to be the most preferred among all other evolutionary programming methods used for voltage stability analysis. Application of Genetic algorithm to Optimal Reactive Power Dispatch with voltage stability

constraint has been put forward by S. Duriaraj, P.S. Kannam and D. Devaraj in 2005 [33].

Inclusion of FACTS devices like SVC etc in voltage stability studies have been carried out using Genetic algorithm and the results compared with the Direct and Continuation Power Flow methods [34,35,36,37,38,39]. Such evolutionary programming methods are used for optimal parameter setting of FACTS devices for voltage stability margin enhancement and loss minimization.

Comparison between Genetic Algorithm and Particle Swarm Optimization (PSO), when applied to voltage stability studies have been discussed by M. Kowsalya, K.K. Ray and D.P. Kothari [40]. The findings indicated that PSO gave better optimization and the best location for the compensating device used, while minimizing the series reactive power loss. Similiar comparison between GA and PSO were found in subsequent works [37, 41].

In 2011, P. Acharjee used a Security Constraint Genetic Algorithm (SCGA) to identify the maximum loadability limit of a network and the weak buses [42]. It was concluded that the performance of the proposed method was better than General Particle Swarm optimization (GPSO) and could be applied for steady state stability analysis.

In recent years, many new evolutionary methods have been developed that aim to simplify the optimization procedures. The Differential Evolution (DE) technique has been used in a multi-objective problem with loss minimization and voltage stability as objectives by J. Jithendranath and K.H. Reddy in 2013 [43]. Differential

Evolution is an improved version of GA which was first presented by Storn and Price. Its main advantage is its simple structure, robustness and superiority applied to optimization problems.

Luke Jebaraj, et al. in 2014, used the Firefly Algorithm for multi-objective optimization of extended voltage stability margin and minimization of Losses while using FACTS compensation [44]. The Firefly Algorithm (FA) is a metaheuristic and nature-inspired optimization based on the flashing behaviour of fireflies. It was developed in 2007, by Dr. Xin-She Yang at Cambridge University. This paper demonstrated the ease of use of the new optimization technique as compared to the DE and PSO.

The superiority of the Firefly algorithm when applied to Real Power Loss Minimization and Voltage Profile Improvement has been presented by H. Deenadhyalan [45].

Cuckoo Search Algorithm has been applied to a Voltage stability enhancement study for determining the appropriate location and size of SVCs [46]. Modal Analysis has been used for weak bus identification. The Cuckoo Search (CS) Algorithm was first proposed in 2009 as a multi-objective optimization technique based on birds with an aggressive reproductive strategy. In this paper it was concluded that the Improved Cuckoo search Algorithm performed better, in terms of accuracy and speed, when compared with other optimization techniques like GA, PSO, and HS (Harmony Search) Algorithms.

Similar work using Cuckoo Search with Levy Flight Algorithm for Voltage Stability improvement has been performed by C. Mwaniki, et al. [47].

Voltage Stability studies using many new evolutionary nature-inspired techniques have been carried out in the recent years (Ant-Lion Optimizer [48], Jaya Algorithm [49], etc) with a fair amount of success.

Thesis Justification:

In this thesis, Conventional and Evolutionary methods are used for Static Voltage Stability Analysis on standard test systems. Keeping in view the recent work on voltage stability studies using the mentioned methods, a novel approach is made towards the voltage stability studies of power systems i.e., Weak Bus Identification, Bus Voltage Stability Analysis and Line Voltage Stability Analysis. The impact of FACTS compensation on voltage stability is also highlighted.

A new evolutionary programming method, the Teaching Learning Based Optimization (TLBO) technique is adopted in this work to address a multi-objective problem of Voltage stability.

The contribution of this work is a new approach to static voltage stability analysis of transmission systems; and a new evolutionary programming technique used to optimize multiple objectives leading to improvement of voltage stability and enhancement of performance of the test systems used.

1.4 Outline of the Thesis / Thesis Organisation

Chapter 1 is dedicated to an introduction to the topic of this thesis. The voltage stability problem and its importance in the power system stability studies, is highlighted.

A literature review, discussing the previous work done on static as well as dynamic voltage stability analysis, voltage collapse problem and its mitigation and various stability indices formulated, is made here. The history of the application of Flexible AC Transmission System (FACTS) controllers to voltage stability enhancement is included. Evolution of conventional optimization techniques to evolutionary population and nature-based algorithms used for parameter optimization of compensating devices are also discussed in brief.

The scope of work and the objectives of this thesis are included in this chapter.

Chapter 2 gives a general background of voltage stability, its definitions and classifications, voltage collapse phenomenon and the different conventional methods of voltage stability analysis. Case studies implementing these methods for weak bus identification are carried out in this chapter.

Chapter 3 presents Bus Voltage Stability Analysis using conventional methods. Importance of Reactive Power Compensation using shunt FACTS controllers, in voltage stability enhancement is discussed in this chapter. Case studies for different test systems and using different FACTS compensators are carried out.

Chapter 4 emphasizes on Line Voltage Stability Analysis of critical lines. Voltage stability indices used for weak bus and line identification are discussed here. Line stability index FVSI is used for critical line identification and series FACTS controllers, TCSC and SSSC are used for series compensation. The case studies are carried out on IEEE test systems.

Chapter 5 is devoted to the second part of the thesis i.e. Evolutionary methods applied to voltage stability analysis. The Teaching Learning Based Optimization (TLBO) technique is discussed here. Multi-objective optimization applied to Voltage stability studies is highlighted in this chapter.

Case studies are performed on IEEE test systems using Multi-objective TLBO method for simultaneous minimization of system real power loss and total FVSI of compensated lines using TCSC. The simplicity and effectiveness of Multi-objective TLBO technique over Genetic Algorithm (GA) is also presented here.

Chapter 6 contains the conclusions of this thesis. It also includes the scope of future work in the current field of study.

Chapter 2

Voltage Stability Analysis using Conventional Methods

(Weak Bus Identification)

2.1. Introduction

Modern power systems are subjected to growing load demand and increasing power transfers over long geographical distances. Rapid industrial development and urbanization of the suburban areas all over the world has led to excessive dependence on electrical energy and an ever increasing power demand. Power shortage has led to expansion of existing networks and establishment of new ones. With ever increased demand of the power system utilities in countries all over the globe, the lines become heavily stressed and this leads to a low voltage condition or voltage collapse.

In recent years voltage instability has attracted the attention of power system planning and operating engineers as well as researchers. This is due to the frequent voltage collapse incidents occurring in different parts of the world. Therefore

Voltage Stability Analysis is important for researchers and power system planners to prevent such incidents from occurring.

Development of power markets have created situations where electrical utilities face voltage stability-imposed limits and therefore, for the power system to be more protected and secure it is compelled to operate within these limits.

On the other hand, if these limits are violated it can lead to generator synchronism loss, transmission line outage or might result in a phenomenon called voltage collapse.

This chapter deals with the basic concepts of voltage stability. The terms voltage stability / instability, weakest bus and voltage collapse are defined here. The different methods of static voltage stability analysis are discussed and the voltage collapse indicators are briefly introduced. Case studies on different test systems, for static voltage stability analysis and critical bus identification are carried out using the methods mentioned in this chapter.

2.2. Classification of Voltage Stability: Concepts and definition

Voltage stability is a sub-set of overall power system stability. We can define power system stability as: *“that property of a power system that enables it under normal operating conditions, to remain in a state of operating equilibrium and after being subjected to a disturbance, to regain the state of equilibrium”* [50].

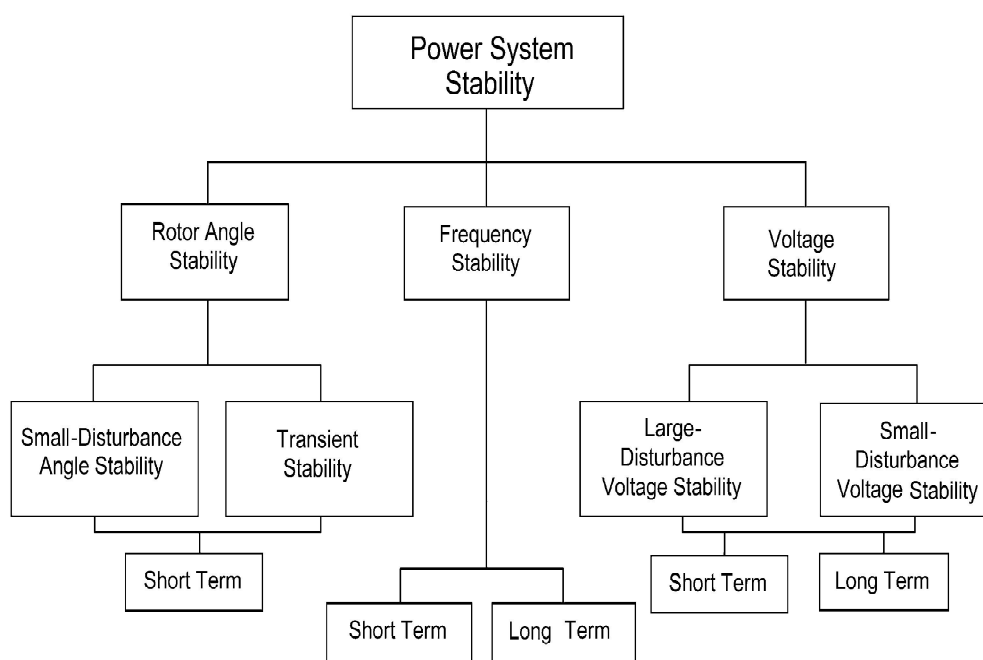


Fig 2.1 Power System Stability- Classification [13]

Several definitions of Voltage have been put forward in literature. One definition is given by the IEEE/CIGRE report “Definition and Classification of Power System Stability” [13] as:

“Voltage Stability is the ability of a power system to maintain steady acceptable voltages at all buses in the system under normal operating conditions and after being subjected to a disturbance.”

Voltage Instability, the opposite of voltage stability, is defined as [51]:

“Voltage instability stems from an attempt of load dynamics to restore power consumption beyond the capability of the combined transmission and generation system”

Voltage instability is manifested as a fall or rise of voltages of weak buses, progressively and results in loss of load, or tripping of transmission lines and other elements leading to cascading line outages [13].

Voltage Collapse:

Voltage collapse is one of the outcomes of voltage instability. Rotor angle instability may cause progressive fall in bus voltage due to gradual loss of synchronism of machines. But, it is seen at times that there is sustained falling bus voltage even when rotor angle stability is not the problem. This can be attributed to voltage instability [50]. Voltage collapse is an outcome of voltage instability that is identified by a low undesired voltage profile in a significant part of the power system [50].

Instances of voltage collapse are mostly observed on power systems that are either overloaded, faulted and/or have reactive power shortages [52]. Such instances are likely to occur when a power system is operated close to its capacity limits, resulting in bus voltage drops to such a level from which it cannot recover, and if ignored, may result in complete system shutdown.

Voltage collapse is known to be caused by the following changes in the power system [53]:

- Overloading of lines
- reactive power limits violated by generators or synchronous condensers
- Action of tap-changing transformers
- Dynamics of load recovery
- Tripping of lines or generator outages

As most of these changes influence reactive power production, consumption and transmission, hence reactive power compensation is used as a countermeasure against voltage collapse.

Classification of Voltage stability is essential for analyzing the problem and identifying the factors relating to voltage instability or in some cases, voltage collapse.

➤ From the view point of techniques, voltage stability is classified as [50]:

- Large disturbance or large-signal voltage stability
- Small-disturbance or small-signal voltage stability

Small disturbance (or small-signal) voltage stability: These disturbances are continuous occurrence caused by small variations in generation and load. This type of voltage stability can be defined as the ability of the power system to maintain synchronism under small disturbances.

Large disturbance voltage stability: It refers to the voltage stability of the system after being subjected to a large disturbance, like system faults, contingencies, loss of generation etc.

➤ From the point of viewpoint of time span of a disturbance in a power system, voltage stability is further classified as:

- Short term and
- Long term voltage stability.

- **Short term voltage (or transient) stability** refers to the stability of fast-acting load components like automatic voltage regulators, induction motors and electronically operated load (fast-acting load components) and HVDC interconnections. The time period of study is in the order of several seconds. For a stable system, short term disturbances die and thereafter, system enters a stage of slow long term dynamics [53]. Operator intervention is not required in short-term or transient voltage instability and automatic emergency measures are adopted to mitigate such voltage instability e.g. protective devices.
- **Long term voltage stability** refers to slow acting components like tap-changing transformers, generator excitation limiters. In this case, the time period of study is in the order of several minutes [13]. Voltage stability of heavily loaded systems usually occurs in the long-term time-frame, with large electrical disturbance between generators and load and is thus, dependent on the detailed topology of the power system [53]. With reactive power compensation or load shedding at appropriate positions and instances this type of voltage instability may be prevented.

2.3. Analysis of Voltage stability:

A simple 2-bus system representing a transmission line of a power system network is shown in Fig 2.2. This system can be used to explain the basic concept of voltage stability [53, 54].

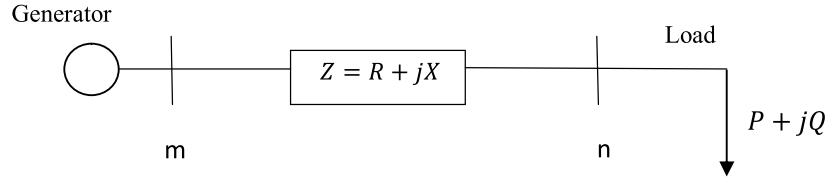


Fig 2.2: Single line representation of a two-bus system

Where,

$V_m < \delta$: voltage magnitude & phase angle at bus m

$V_n < 0$: voltage magnitude & phase angle at bus n

X : line impedance (neglecting resistance)

P : active power load

Q : reactive power load

δ : phase difference between the generator and load voltages (*power angle or load angle*)

Using Load flow equations, real power transfer from bus m to bus n is given by [50]:

$$P = \frac{V_m V_n}{X} \sin \delta \quad (2.1)$$

$$Q = -\frac{V_n^2}{X} + \frac{V_m V_n}{X} \cos \delta \quad (2.2)$$

Solving Eqns. (2.1) and (2.2) yields voltage V_n as:

$$V_n = \sqrt{\frac{V_m^2}{2} - QX \pm \sqrt{\left(\frac{V_m^2}{4} - X^2 P^2 - X V_m^2 Q\right)}} \quad (2.3)$$

Eqn. (2.3) implies that there are two solutions for voltage V_n . The higher value represents the stable solution and the lower value implies the unstable solution. The solutions to this load voltage is represented in P-V and Q-V curves (*discussed in Sections 2.4.1 and 2.4.2*), also referred to as nose curves. The P-V curves represent the bus voltage profiles.

Voltage stability analysis for a given system state comprises of two stages - [55]

- (i) Proximity to voltage instability- nearness of the system to voltage collapse
- (ii) Mechanism of voltage instability- i.e. factors contributing to voltage instability, identification of weak buses, and effective measures for improving voltage instability.

2.4. Methods of Voltage Stability Analysis: Weak Bus Identification

Voltage instability is a non-linear phenomenon, having various types of dynamics associated with it. Hence, static as well as dynamic analyzing techniques can be used to effectively analyze the problem [55]. However, sensitivity information or the degree of stability, required for dynamic analysis, is not easily provided by transient stability simulations. This is due to the time consumed in terms of computers and engineering effort and analysis of system conditions and the contingencies [1]. Therefore, the steady state voltage stability analysis is more suitable for voltage collapse prediction and reactive power load problems [9, 56, 57].

Some of the conventional methods used for steady state voltage stability analysis are:

- (i) P-V curve method for Real power loading
- (ii) V-Q curve method for Reactive power loading
- (iii) Modal Analysis
- (iv) Continuation Power Flow (CPF) method
- (v) Voltage Stability Indices

Weakest Bus

The weakest bus is identified as the bus that is closest to a voltage collapse situation. It is the bus that is nearest to the turning point or 'Nose' point of the P-V (received power versus bus voltage) curve. The Saddle-node bifurcation (SNB) point or voltage collapse point is shown in Fig 2.3. At this point, only one solution of voltage occurs and beyond this point no solution exists. The system can therefore be loaded only up to this point, which is why the SNB point is also known as the maximum loading point. The distance AB in Fig 2.3 represents the static voltage stability margin of the weakest bus.

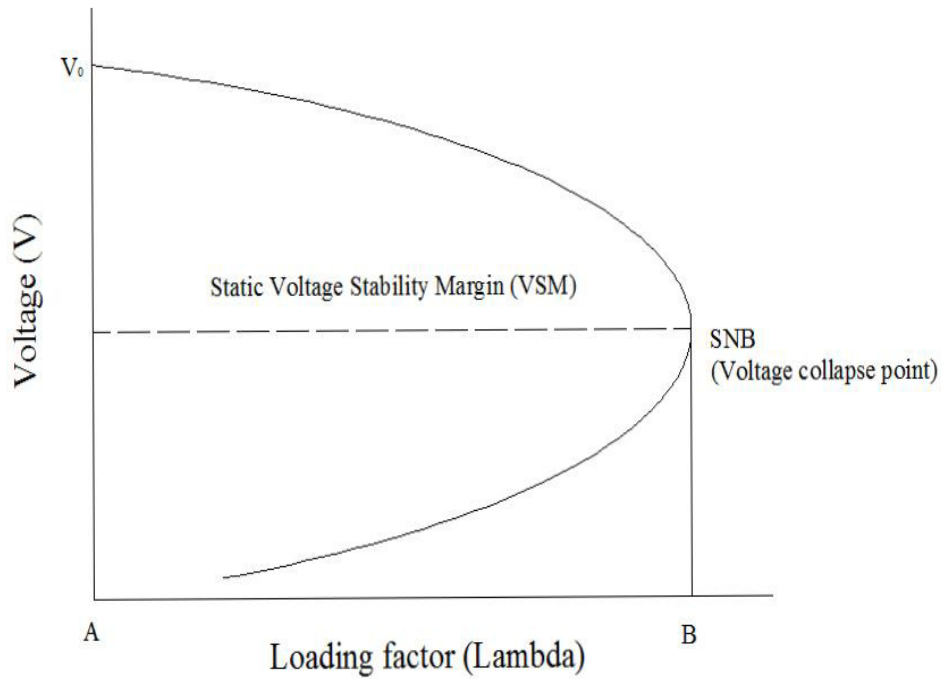


Fig 2.3 Saddle-node bifurcation [58]

The weakest bus can be identified by the following:

- (i) It is the bus that has a large ratio of differential change in load (dV/dP_{\max}). For a particular bus, the predictor steps of the Continuation Power Flow process yield the bus voltage change for a given change of loading (*details in section 2.4.4*).
- (ii) The voltage stability critical point is obtained when, for a certain value of the main system parameter, solution does not exist for the load flow algorithm.

Singularity of the Jacobian matrix of the load flow equations is observed and the bus corresponding to the smallest Eigen value is the weakest bus and closest to voltage collapse.

The right Eigenvector indicates the buses close to voltage collapse. The biggest element of the right Eigenvector corresponds to the most critical bus (*details in section 2.4.3*).

2.4.1. P-V Curve method

This is one of the simplest and most widely used methods of determining voltage instability. This method is used both on a radial and interconnected networks [53, 55]. Eqn. (2.3), representing a 2-bus system (shown in Fig 2.2), gives two solutions of V ; one is the high voltage or stable solution, representing the actual bus voltage, and the other one is the low voltage or unstable solution.

For this analysis, the real power (P) at a particular bus or node is increased in steps and the voltage (V) of some critical load buses is observed. The curves for these particular buses are plotted to determine the behaviour of the voltage with increasing real power load. The bus or node that experiences a rapid reduction in voltage magnitude with increasing load is identified as a weak bus or a critical node, which is approaching voltage collapse. The Voltage Stability Margin (VSM) or Active Power Margin can also be determined from the P-V curve.

The P-V curve is shown in Fig. 2.4, which represents the voltage variation with change in total active power load at a bus.

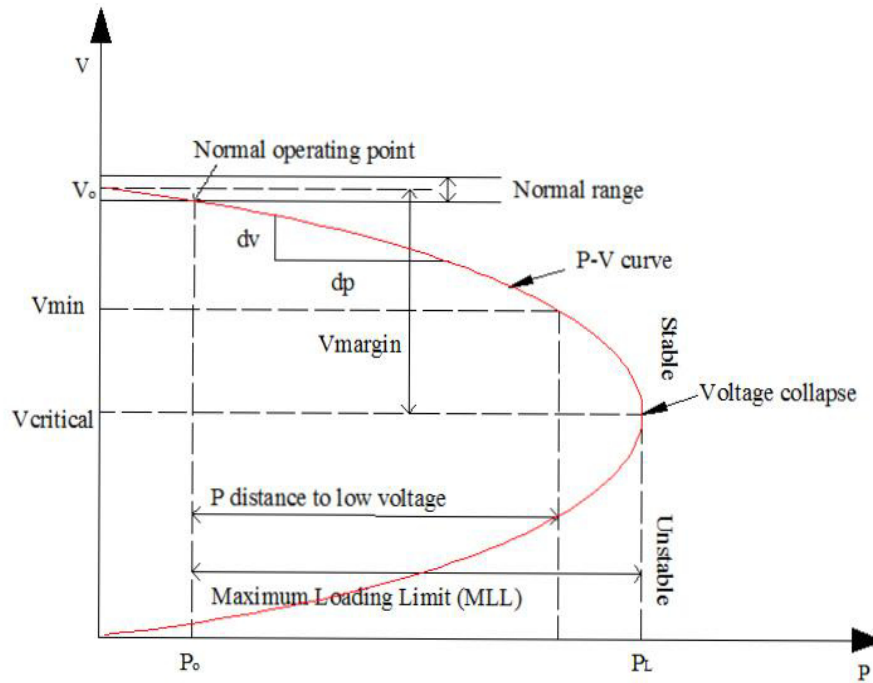


Fig 2.4: P-V curve

2.4.2. Q-V Curve method

Voltage instability can be attributed to reactive power deficit to a great extent. It has been established that to maintain a good and acceptable voltage profile, reactive power support must be provided at the requisite locations of a power system. Unlike P-V curve method, the system need not be represented as two-bus equivalent here. The critical bus is identified and the Q-V curves are generated by a series of power flow simulations [59, 60]. The voltages at the critical bus versus the reactive powers are then plotted.

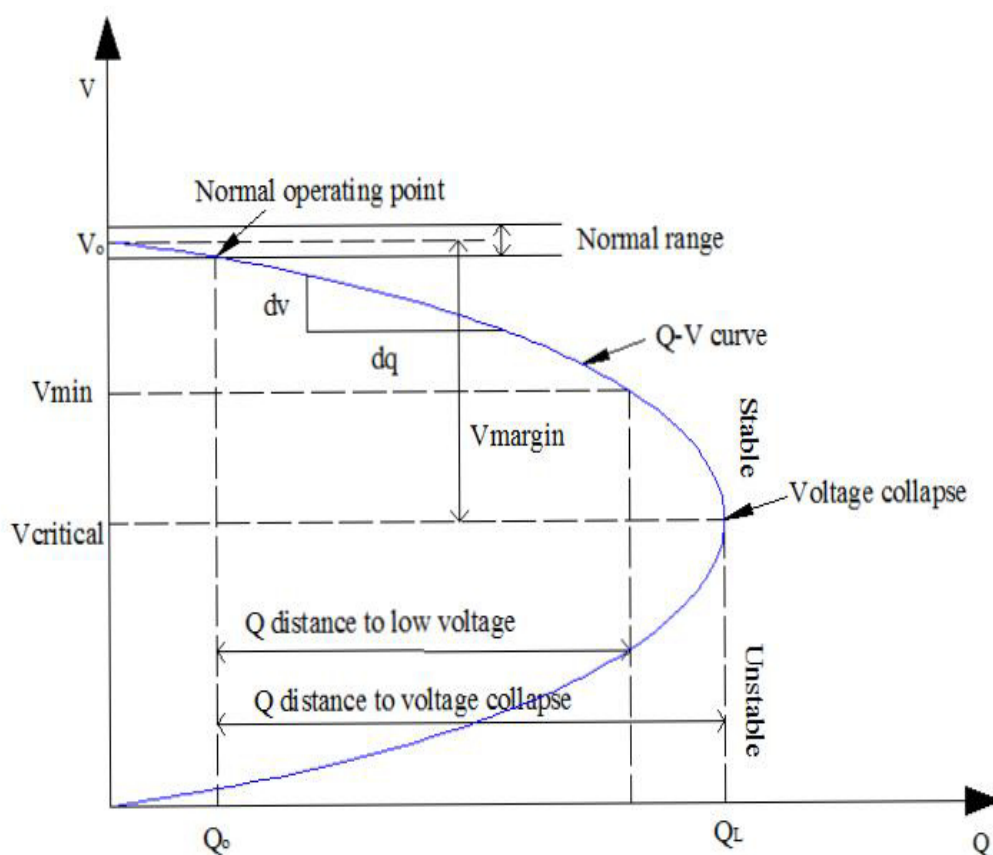


Fig 2.5: Q-V curve

Fig 2.5 shows the Q-V curve, which is a variation of the bus voltage with increasing reactive power.

The reactive power margin is the MVAR distance between the operating point and the nose point of the Q-V curve. Weak buses in the system can be identified by the slope of the curve. The greater the slope is, the less stiff is the bus and therefore more vulnerable to voltage collapse. The main drawback with Q-V curves is that it is difficult to identify the weak buses previously at which these curves should be generated [60].

2.4.3. Modal analysis

Modal Analysis is one of the most popular methods and has been widely used for weak bus identification [54, 60]. Modal analysis of the Jacobian matrix was first proposed by Gao, et al. [7], and its singularity at the point of voltage collapse was used for voltage stability analysis. In this method, the Eigen value and the associated Eigenvectors of the reduced Jacobian matrix are computed. The smallest Eigen value gives the weakest bus of the system, as the Eigen values are associated with a mode of voltage and reactive power variation [61].

For voltage stability analysis the conventional Newton Raphson power flow equations are used as [54, 57, 59]:

$$\begin{bmatrix} \Delta P \\ \Delta Q \end{bmatrix} = \begin{bmatrix} J_{P\theta} & J_{PV} \\ J_{Q\theta} & J_{QV} \end{bmatrix} \begin{bmatrix} \Delta \theta \\ \Delta V \end{bmatrix} \quad (2.4)$$

Where,

- $J_{P\theta}, J_{PV}, J_{Q\theta}, J_{QV}$: Jacobian sub-matrices
- $\Delta P, \Delta Q$: vectors of incremental changes of active and reactive power of buses
- $\Delta \theta, \Delta V$: vectors of incremental changes of bus voltage angle and Magnitudes

When power is kept constant, Eqn. (2.4) is rearranged as follows:

$$\Delta Q = J_R \Delta V \quad (2.5)$$

Eqn. (2.5) represents the reduced Jacobian matrix of the system as:

$$J_R = [J_{QV} - J_{Q\theta} J_{P\theta}^{-1} J_{PV}] \quad (2.6)$$

$$\text{And} \quad J_R = \xi \Lambda \eta \quad (2.7)$$

Where,

ξ = Right Eigenvector matrix of J_R

η = Left Eigenvector matrix of J_R

Λ = Diagonal Eigen value matrix of J_R

From equation (2.7) we get:

$$J_R^{-1} = \xi \Lambda^{-1} \eta \quad (2.8)$$

$$\Delta V = \xi \Lambda^{-1} \eta \Delta Q \quad (2.9)$$

The i^{th} mode of the Q-V response is defined by Eigen value Λ_i and corresponding right and left Eigen vectors. Therefore, voltage stability of the system can be analysed by computation of the Eigen values and Eigen vectors of the reduced Jacobian matrix J_R .

The system is stable if all the Eigen values are positive and thus the V-Q sensitivities are also positive. The system is unstable, if some of the Eigen values of J_R are negative.

Therefore, the Eigen values and Eigenvectors of the reduced Jacobian matrix are calculated in order to specify the condition of the power system in context with its voltage stability.

Reactive Participation factor (RPF)

Information regarding the voltage stability of a power system network can be obtained from the left and right eigenvectors corresponding to the critical modes in the system.

For any critical mode i , the reactive participation factor (RPF) of bus k , is given by the bus participation factor as [54, 57]:

$$RPF_i = P_{ki} = \xi_{ki} \eta_{ik} \quad (2.10)$$

Where,

ξ : right eigenvector matrix

η : left eigenvector matrix

P_{ki} : reactive participation factor of the i^{th} Eigen value at bus k .

The magnitude of the participation factor represents the contribution of a bus to voltage collapse under stressed conditions. Higher the value of P_{ki} , greater is the contribution of that bus and closest is it to voltage collapse [54]. Hence, Reactive participation factor is very useful for identifying weak buses and therefore helps in identifying the appropriate location for reactive power compensation of a system undergoing stress.

The main advantage of applying Modal Analysis technique for Voltage stability studies is that reactive power compensation can be limited to less number of buses as this method helps in accurate identification of groups of buses contributing to the instability [54, 62].

2.4.4. Continuation Power Flow (CPF) method

The drawback of the Modal analysis method is that it is difficult to obtain a power flow solution near the voltage collapse point, which shows divergence and error. This is because the Jacobian matrix of the Newton Raphson power flow becomes singular at the voltage stability limit or maximum loading point [50, 55, 63].

Continuation power flow (CPF) is a technique by which the power flow equations converge near or at the voltage collapse point. [53, 55, 64] .

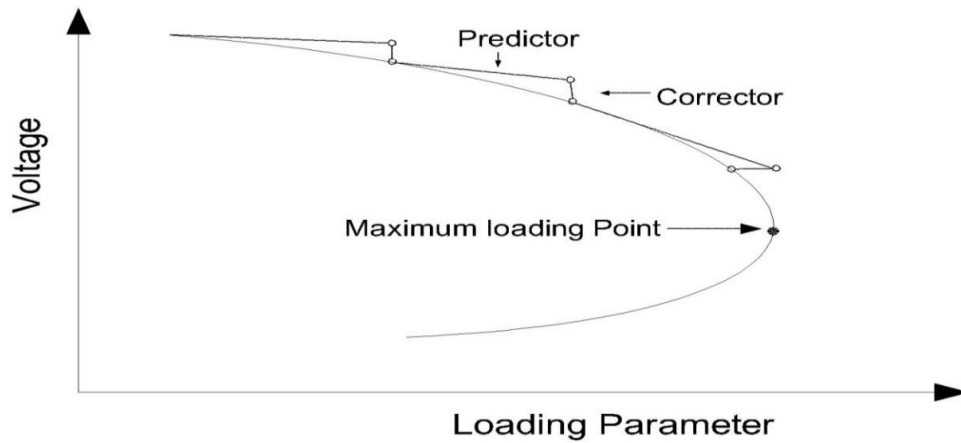


Fig 2.6: P-V curve solution using prediction-correction technique [65]

This method was first proposed by V. Ajjarapu, et al. [8] and it overcomes the problem of Jacobian matrix singularity, by reformulating the power flow equations. A predictor-corrector scheme is employed here to find a solution path (as shown in Fig. 2.6). The health of the power system network under study, in terms of voltage stability, can be assessed by the intermediate results of this process. Local parameterization, used in this method, allows the increased load parameter and together with the state variables, to be used as continuation parameters [66].

The prediction step, the tangent parameter, estimates the next P-V curve solution based on a known solution. Prediction is unnecessary at the flat part of the P-V curve, but is very valuable around the nose point. The corrector step is then used to rectify this inexact estimate. It determines the exact solution using the conventional Newton Raphson power flow technique. After that, for a specific increase in load, a new predictor step is taken. The step size should be taken keeping in view the radius of convergence of the corrector, i.e., the predicted solution should be within that radius [55, 65]. This process is repeated until critical point is reached, i.e. where the tangent vector is zero.

Mathematical formulation: [64, 67]

Reformulation of the load flow equations is done by inserting load parameter λ , to enable local parameter application.

Using constant power load, the general form of power flow equation is: [55, 67]

$$P_m = \sum_{k=1}^n |V_m| |V_k| (G_{mk} \cos \theta_{mk} + B_{mk} \sin \theta_{mk}) \quad (2.11)$$

$$Q_m = \sum_{k=1}^n |V_m| |V_k| (G_{mk} \sin \theta_{mk} - B_{mk} \cos \theta_{mk}) \quad (2.12)$$

$$P_m = P_{Gm} - P_{Dm} \quad (2.13)$$

$$Q_m = Q_{Gm} - Q_{Dm} \quad (2.14)$$

Where,

P_{Gm} : active power generation at m^{th} bus

Q_{Gm} : reactive power generation at m^{th} bus

P_{Dm} : injected active power at m^{th} bus

Q_{Dm} : injected reactive power at m^{th} bus

A load parameter λ is incorporated with demand power P_{Dm} and Q_{Dm} for load change simulation as,

$$P_{Dm} = P_{Dmo} + \lambda(P_{\Delta base}) \quad (2.15)$$

$$Q_{Dm} = Q_{Dmo} + \lambda(Q_{\Delta base}) \quad (2.16)$$

Where,

P_{Dmo} and Q_{Dmo} : initial load demand on the m^{th} bus

$P_{\Delta base}$ and $Q_{\Delta base}$: powers chosen to scale λ appropriately.

The reformulation power-flow equation, with provision for increased generation as the load increases is represented as:

$$F(\delta, V) = \lambda K \quad (2.17)$$

Where,

λ is the load parameter,

δ is the vector of bus voltage angles,

V is the vector of bus voltage magnitudes.

K is the vector representing present load change at bus.

The set of nonlinear equations in Eqn. (2.17) is solved for a specified value of λ such that $0 \leq \lambda \leq \lambda_{\text{critical}}$.

Predictor step:

In the predictor step, a linear approximate prediction of the next solution is made for a change in one of the state variable [7].

Differentiating both sides with respect to the state variable corresponding to the initial solution, yields following equations:

$$F_{\delta}d\delta + F_vdV + F_{\lambda}d\lambda = 0 \quad (2.18)$$

$$[F_{\delta}F_vF_{\lambda}] \begin{bmatrix} d\delta \\ dV \\ d\lambda \end{bmatrix} = 0 \quad (2.19)$$

With the addition of the unknown variable λ to the load flow equations, Eqn. (2.19) is solved setting one of the tangent vector components to +1 or -1. This is also known as the continuation parameter.

Corrector Step:

In the corrector step, local parameterization is used to correct the predicted step. The original set of equation is increased by one equation that specifies the state variable selected as the continuation parameter [7].

Thus new set of equations is,

$$\begin{bmatrix} F(\delta, V, \lambda) \\ x_k - x'_k \end{bmatrix} = [0] \quad (2.20)$$

where,

x_k : the state variable (continuation parameter)

x'_k : the predicted value of x_k .

With the introduction of the additional equation specifying x_k , the Jacobian becomes non-singular at the critical operating point.

Loading margin is defined as the distance between the critical point and the current operating point. The Continuation Power Flow is very useful in the estimation of the loading margin of a power system [56].

The exact location of the maximum loading point requires a lot of searching, using decreasing step size around that point. Therefore, it is seen that optimization method is found to be more effective in finding the exact voltage collapse point [65].

2.4.5. Voltage Stability Indices

In addition to the methods discussed so far, some indices have been found in literature that has been formulated for on-line voltage stability monitoring [16, 17, 18]. They have proved to be useful in finding the voltage stability margin or assessing the proximity to voltage collapse.

Some of the common Voltage Stability indices used in research have been discussed in Chapter 4.

2.5 Results and Discussion

In this section, voltage stability analysis of standard IEEE test systems is presented. The tests have been carried out to study the effectiveness of the Conventional methods mentioned in this chapter and to identify the weak buses. Modal Analysis is carried out on standard IEEE 30 and 57 bus systems. The Eigen values and Eigen vectors of the reduced Jacobian matrix are calculated. The Participation factors of each mode are then calculated which helps in identifying the weak load buses. The bus having the highest participating factor is identified as the weakest bus, having maximum contribution and proximity to voltage collapse. The results of Modal

Analysis are compared with those of the Continuation Power Flow (CPF) Analysis performed on the same test systems.

2.5.1 Case study: IEEE 30 bus system:

The standard IEEE 30 bus test system used here consists of 30 buses, 41 lines, 4 transformers and 6 generators (connected to the PV buses 2, 5, 8, 11 and 13) and bus 1 considered as the slack / swing buses.

2.5.1.1 Results of Modal Analysis:

Modal Analysis is performed on this system and Eigen values are calculated and plotted for V-Q sensitivity analysis.

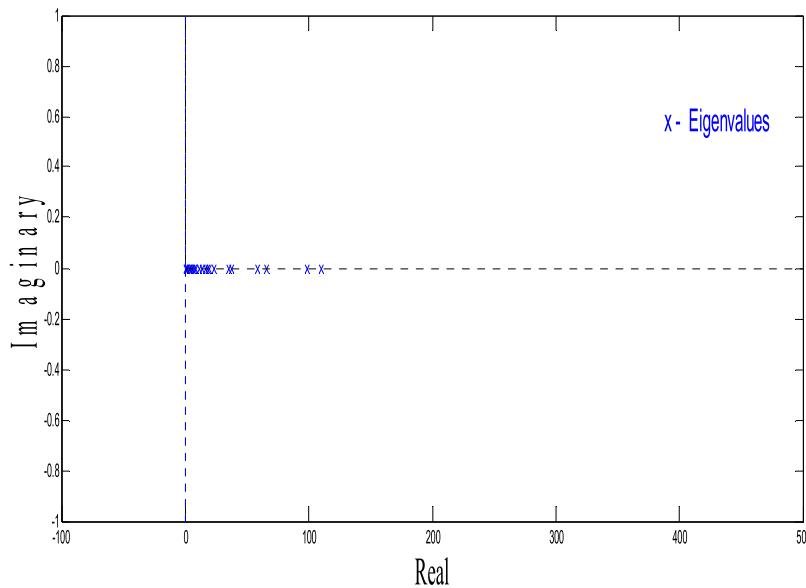


Fig 2.7: Plot of Eigen values (real part) for IEEE 30 bus system

The real part of the Eigen values are positive as seen in Fig 2.7, implying that the IEEE 30 bus system is voltage stable.

Table 2.1: Minimum Eigen values for IEEE 30 bus system

Bus no.	30	19	26	19	14
Eigen value mode	Eig Jlfr #13	Eig Jlfr #14	Eig Jlfr #15	Eig Jlfr #19	Eig Jlfr #20
Eigen values	0.50496	1.02882	1.76511	3.54778	4.02295

The minimum values of the Eigen values are shown in Table 2.1. The minimum Eigen value ($\lambda = 0.50496$) is the most critical mode (13) and is associated with bus number 30. The participation factors for this mode (=13) are computed.

Table 2.2: Highest Participation factors (IEEE 30 bus system)

Bus No.	30	29	26	25	27
Participation factor of the most associated bus	0.20874	0.19144	0.173192	0.106947	0.10489

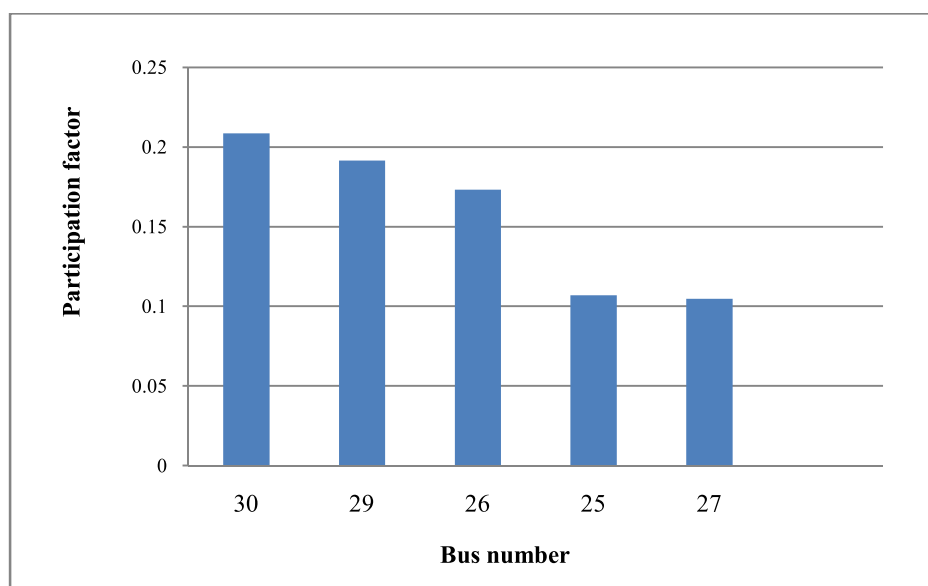
**Fig 2.8: Highest Participation factor profile (IEEE 30 bus system)**

Table 2.2 shows the highest participation factors of the critical mode (=13) and the associated buses. The results show that the buses 25, 26, 27, 29 and 30 have highest Participation factors in the critical mode.

The largest Participation factors value (0.2.874) is associated with bus 30, implying that it is the weakest bus, as seen in Fig 2.8, and therefore, having highest contribution to voltage collapse.

Hence, it can be concluded from Modal analysis, that bus 30 is the weakest bus, and is the optimum location for corrective measures.

2.5.1.2 Results of Continuation Power Flow (CPF) Analysis

Continuation Power Flow analysis on the system yields the following results:

Table 2.3: Voltage magnitudes of the weak buses (IEEE 30 bus system)

Bus No.	30	29	26	25
Voltage (p.u.)	0.497227842	0.574011094	0.585780919	0.674363235

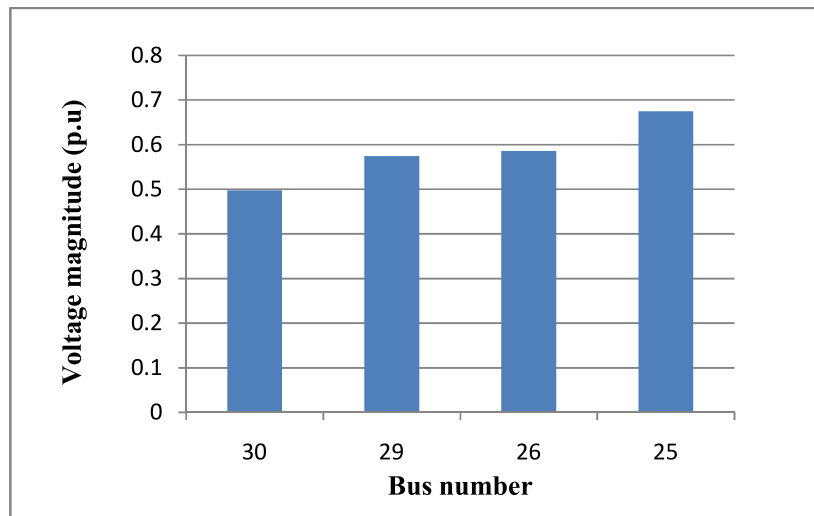


Fig 2.9: Voltage magnitude profile of the weak buses (IEEE 30 bus system)

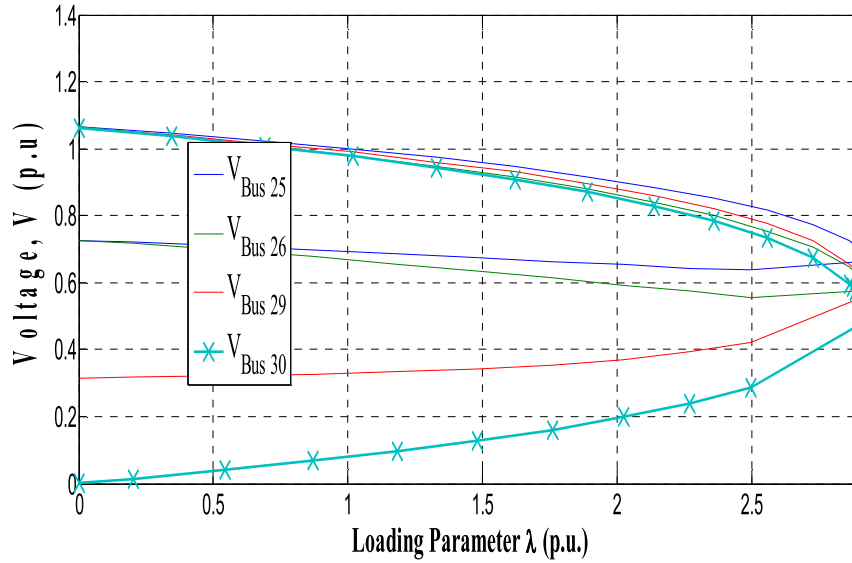


Fig 2.10 P-V curves for the PQ buses with minimum voltage values (IEEE 30 bus system)

Table 2.3 indicates the voltage magnitudes of the weakest buses of the system at critical loading condition. Bus 30 is the critical bus as it has the minimum voltage magnitude, as seen in Fig 2.9.

Fig 2.10 shows the plot of Bus voltage V Vs Loading parameter λ . The maximum loading parameter λ is found to be $=2.9039$. Bus 30 reaches the critical loading point (nose point) the earliest at minimum voltage value ($=0.4972$ p.u.). This indicates that bus 30 is on the verge of experiencing voltage collapse at this loading condition. The CPF Analysis, for both the test cases, is performed using PSAT toolbox of MATLAB [68]. Fig 2.10 represents both the stable and unstable part of the P-V curve (*which cannot be obtained using load flow method*), i.e. the complete nose curve. It is traced using this toolbox with λ negative (retracting the upper part) for the unstable portion of the curve.

The findings of the two conventional methods applied to the IEEE 30 bus system yield the same result; that bus 30 is the weakest bus and most prone to voltage collapse. Therefore, bus 30 is identified for reactive power compensation.

2.5.2 Case study: IEEE 57 bus system:

The standard IEEE 57 bus test system used here consists of 57 buses, 63 lines, 7 transformers and 7 generators (connected to the PV buses 2,3,6,8, 9 and 12) and bus 1 considered as the slack / swing bus.

2.5.2.1 Results of Modal Analysis:

Similar test, as in section 2.5.1.1 is performed on this system yielding the following results:

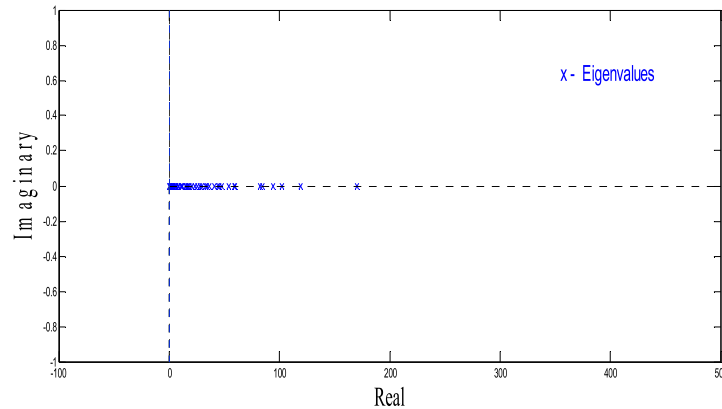


Fig 2.11: Plot of Eigen values (real part) for IEEE 57 bus system

Table 2.4: Minimum Eigen values for IEEE 57 bus system

Bus no.	33	57	20	19	33
Eigen value mode	Eig Jlfr #28	Eig Jlfr #29	Eig Jlfr #30	Eig Jlfr #31	Eig Jlfr #32
Eigen values	0.24851	0.62428	0.88728	1.23369	1.07068

Table 2.5: Highest Participation factors (IEEE 57 bus system)

Bus No.	31	33	32	30	25
Participation factor of the most associated buses	0.177394	0.178006	0.173853	0.12398	0.091812

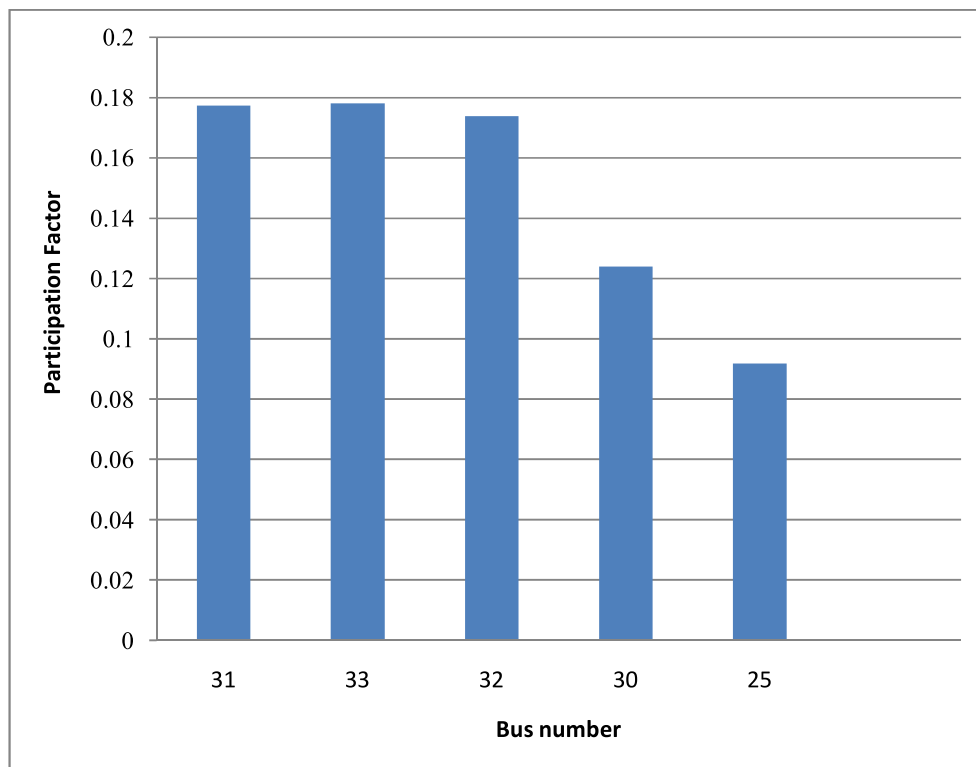
**Fig 2.12: Highest Participation factor profile (IEEE 57 bus system)**

Fig 2.11 indicates that the IEEE 57 bus system is voltage stable; as all the real parts of the Eigen values are positive.

Table 2.4 shows the minimum Eigen values and the associated modes. The minimum Eigen value ($\lambda=0.24851$) is associated with bus 33 and is the most critical mode (=28). Bus participation factors associated with the most critical mode are calculated.

Table 2.5 and Fig 2.12 indicate that bus 33 has the largest participation factor, although bus 31 has a very close value of participation factor with bus 33.

It may therefore be concluded that both bus 33 and 31 have the highest contribution to voltage collapse. This ambiguity is addressed while performing the CPF method.

2.5.2.2 Results of Continuation Power Flow (CPF) Analysis

Continuation power flow analysis on this test system yields the following results:

Table 2.6: Voltage magnitudes of the weak buses (IEEE 57 bus system)

Bus No.	30	31	32	33
Voltage (pu)	0.545302119	0.457560252	0.53988	0.532152291

The ambiguity of Modal Analysis results, as observed in section 2.5.2.1, is cleared by performing the CPF analysis on the same test system. The results, as shown in Table 2.6, reveal that bus 31 has the minimum voltage; closely followed by 33, 32 and 30. This indicates that bus 31 is the weakest and prone to voltage collapse under critical loading conditions.

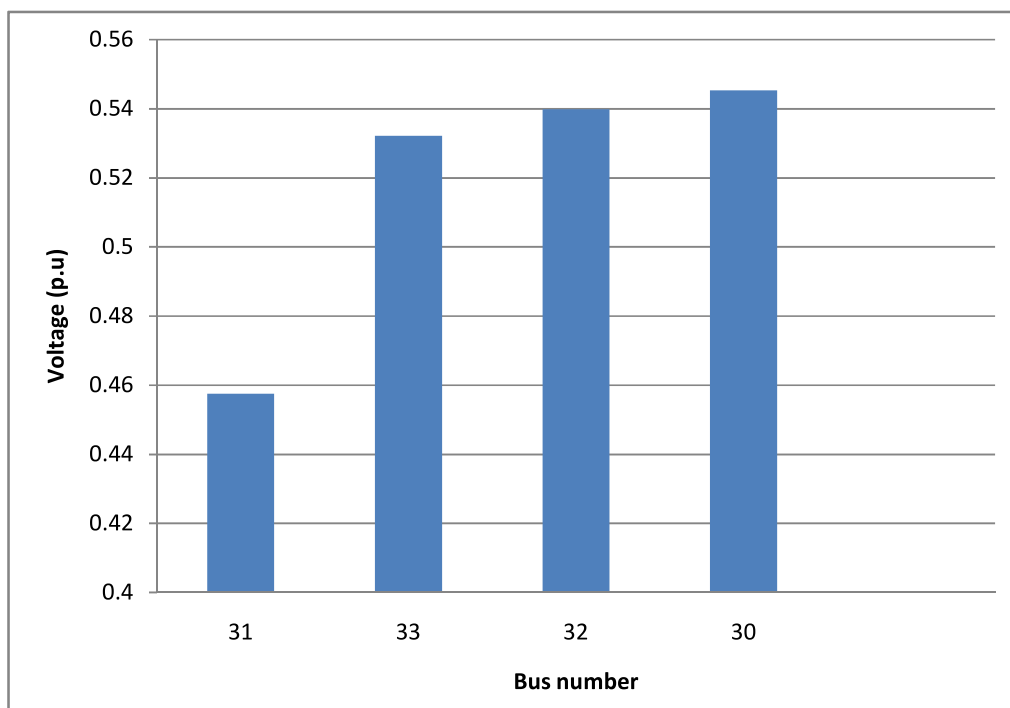


Fig 2.13: Voltage magnitude profile of the weak buses (IEEE 57 bus system)

Fig 2.13 shows the voltage profile of the weak buses of this system. Bus 31 reaches the critical loading point (nose point) at the minimum voltage value ($=0.4576$ pu).

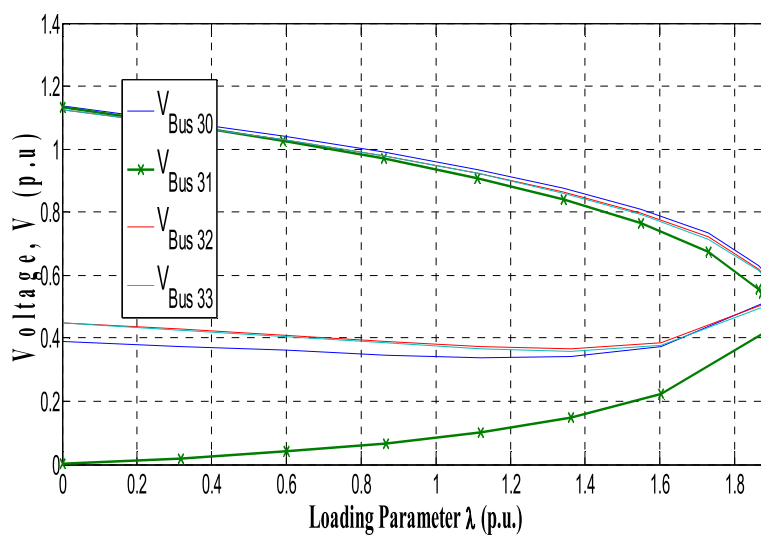


Fig 2.14: P-V curves for the PQ buses with minimum voltage values (IEEE 57 bus system)

Fig 2.14 shows the plot of voltage magnitude Vs loading factor λ . The maximum loading parameter λ has a value of 1.8921, as seen in Fig 2.14.

The results of the CPF analysis has helped remove the ambiguity of the Modal analysis method performed on the same test system.

2.6 Conclusion

This chapter has been devoted to the Conventional Methods of voltage stability analysis, where the Jacobian induced parameters are used for the purpose. It reveals the importance of Load Flow analysis, particularly the Newton Raphson load flow technique for weak bus identification and proximity to voltage collapse. The implementation of these methods on standard test systems highlights the effectiveness of these techniques for proper and accurate voltage stability studies.

Chapter 3

Bus Voltage Stability Analysis

(Voltage Stability Enhancement using Reactive Power Compensation)

3.1 Introduction

This chapter deals with bus voltage stability analysis or node voltage stability analysis. The primary cause leading to voltage instability is the reactive power imbalance in the power system network. Reactive power in surplus leads to over voltage and in deficit results in low voltage. After the weak points having reactive power imbalance are identified, it is essential to mitigate preventive action to avoid cascading failures. Occurrence of voltage collapse can only be prevented by either reducing the reactive power load or by providing additional supply of reactive power before the system reaches the points of voltage collapse [50]. Traditional utilities have used fixed compensators in the form of fixed capacitors and inductors for reactive power compensation. But the nature of modern loads makes such compensation less relevant. Therefore a fast acting efficient and variable source of reactive power compensation is required [64].

Flexible AC transmission systems (FACTS) devices are being used to improve the overall performance of the power system network. FACTS devices help improve voltage profile, provide flexibility to system operation and manipulate power flows, without compromising the reliability and securing of the system [69]. FACTS was a concept proposed by N.G. Hingorani for higher controllability in power systems using power electronic devices [70].

3.2 Flexible AC Transmission system (FACTS)

Voltage stability can be enhanced by the following [65]:

- (i) Reactive power support using passive shunt compensators
- (ii) Line length compensation
- (iii) Load shedding during contingencies
- (iv) Adding more transmission lines i.e. network expansion.
- (v) Using FACTS controllers.

Application of methods (i) and (ii) are simple and most preferred due to their efficiency and cost. Method (iii) is least preferred although effective, as it involves temporary power discontinuity. Method (iv) is a viable but costlier option. Method (v) has become a preferred choice in recent times, as it improves voltage stability and in addition can control real power flows [65].

FACTS (Flexible AC Transmission System) are defined as “*an alternating current transmission incorporating semiconductor- based power electronics and other static controllers*”. They enhance the capacity of power transfer through transmission lines, in addition to reactive power compensation and voltage stability margin enhancement [71]. N. Hingorani, et al. defined as:

“The concept of using solid –state power electronic devices, mainly thyristors for power flow control at transmission level” [58]

FACTS devices have been defined by the IEEE as:

“Alternating current transmission system incorporating power electronic – based and other static controllers to enhance controllability and increase transfer capacity.”

Voltage stability of a system can be most effectively improved by introducing FACTS controllers at the appropriate locations.

Some well known Facts devices utilized for this purpose are classified as [65]:

(1) Shunt FACTS controllers:

- (i) Static VAR Compensator (SVC):
- (ii) Static Synchronous Compensator (STATCOM)

(2) Series FACTS controllers:

- (iii) Thyristor –Controlled Series Capacitor (TCSC)
- (iv) Static Synchronous Series Compensator (SSSC)

(3) Series-shunt FACTS controllers:

- (v) Unified Power Flow Controller (UPFC)

3.2.1 Shunt FACTS Controllers

3.2.1.1 Static VAR Compensator (SVC)

Static VAR Compensator (SVC) is one of the most important shunt FACTS devices used for power system studies. It is a shunt connected static VAR generator (or absorber) whose output is adjusted to draw capacitive or inductive current so as to maintain or control a specific power system variable at the bus to

which it is connected [72]. The power system control variable in this work is the terminal bus voltage. Thyristors without gate turn-off capability are used in SVC design.

There are two configurations of SVC found in literature [19]:

(a) Fixed capacitor (FC) - Thyristor controlled reactor (TCR)

configuration:

It is the commonest form of SVC. Here, a thyristor controlled reactor (TCR) is connected in parallel with fixed capacitor C . The equivalent shunt admittance applied to the power system is varied through firing angle control of the thyristor banks (*Fig 3.1*). L_s is the line reactance, L_r is the TCR reactance, i_s , i_r and i_c are the currents through the line, TCR and C respectively.

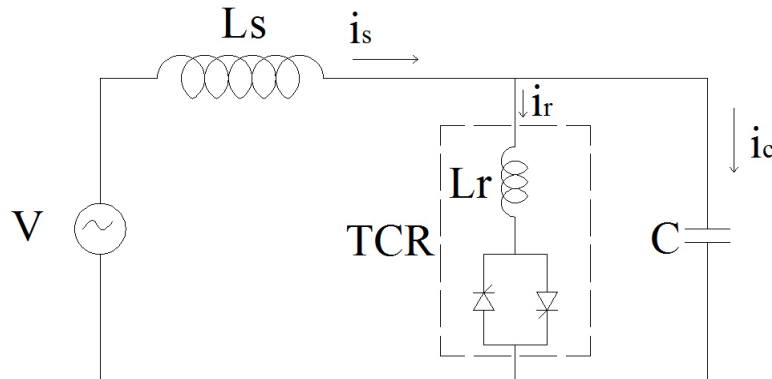


Fig 3.1: Basic structure of SVC (FC-TCR configuration) [73]

(b) Thyristor Switched Capacitor (TCS) and Thyristor Controlled Reactor (TCR) configuration:

For better control, the fixed capacitors are replaced by a thyristor-switched capacitor (TSC) (*as shown in Fig 3.2*). Here, the capacitors are switched in or out (without firing angle control) as per requirement.

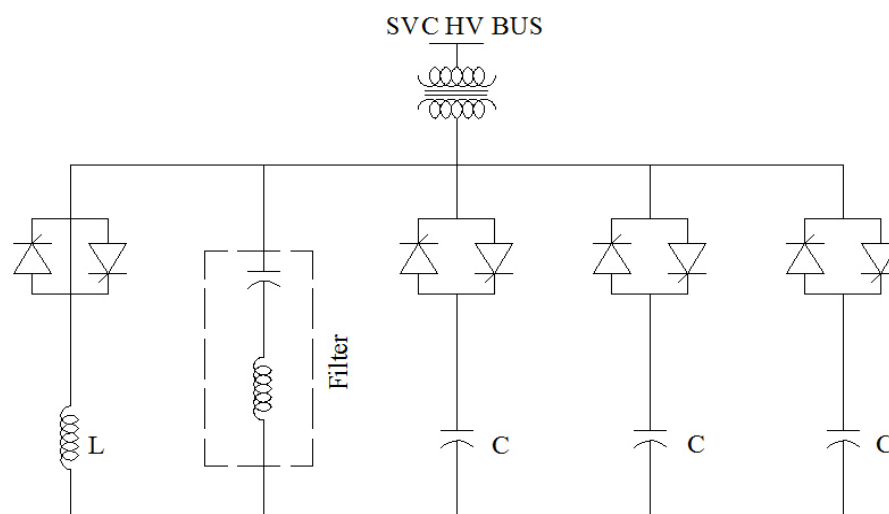


Fig 3.2: Basic structure of SVC (TSC-TCR configuration) [73]

3.2.1.2 STATCOM (Static Synchronous Compensator)

The Static Synchronous Compensator (STATCOM) is another shunt connected FACTS device. It is a voltage-source converter (static synchronous generator operated as a static VAR compensator) based device which can inject lagging or leading VAR into the system to compensate its active and reactive needs [19, 74]. Conversion of a DC input voltage into an AC output voltage is done by the STATCOM, which is injected into the system to control the specific parameter under study [24]. An interface reactor or the leakage inductance of a coupling transformer couples the DC converter to the corresponding AC system [22, 58]. An energy –storage capacitor provides the DC voltage (*Fig. 3.3*).

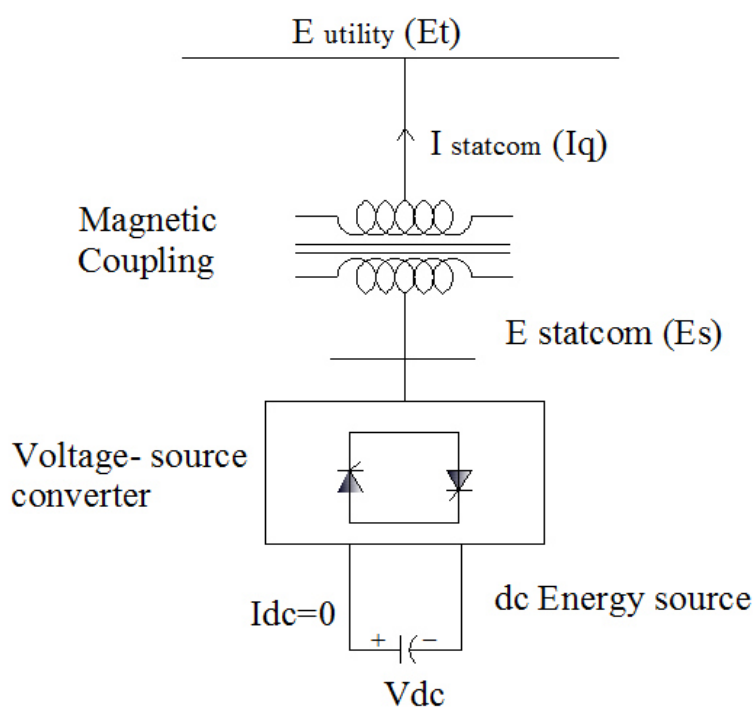


Fig 3.3: Basic structure of STATCOM [75, 76]

The exchange of reactive power between the converter and the AC system is controlled by varying the AC output voltage E_s of the converter [65]

Hence during low load conditions, if the line voltage E_t is more, the converter absorbs lagging VAR from the system. Conversely under heavy loaded conditions, if output of the converter (E_s) is more than the line voltage E_t , then converter supplies lagging VAR into the transmission system.

3.2.2 Series FACTS Controllers

Series FACTS Controllers are connected in series with the line and are used to inject voltage along it. They are useful in controlling the voltage drop between two buses and can also control the power flow through the line connecting them [65].

Some important series FACTS Controllers are:

- (i) Static Synchronous Series Compensator (SSSC)
- (ii) Thyristor Controlled Series Capacitor (TCSC)

Static Synchronous Series Compensator (SSSC)

SSSC is one of the most important series FACTS controllers. It is a solid-state synchronous generator operated without an electrical energy source. It uses an appropriate DC to AC inverter having thyristors with gate turn-off facility. The SSSC acts as a series compensator whose output voltage of the SSSC is in quadrature with the line current. As a result, the reactive voltage drop in the line can be increased or reduced, thereby controlling the transmitted power. Hence the main objective of the SSSC is to directly control the current and indirectly control the real power flow through the line by injecting the series voltage into it; in addition to controlling the reactive power exchange between the device and the AC system [20].

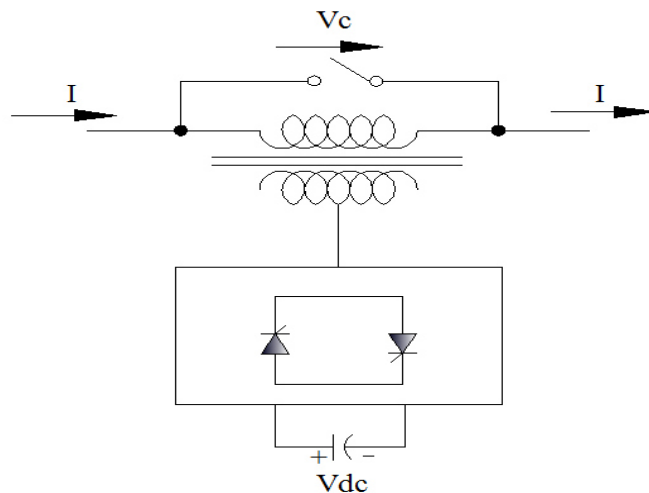


Fig 3.4: Symbolic representation of SSSC [73]

The line inductive reactance is compensated by the series connected capacitor. Due to this, the power transfer capability is increased [73]. The main advantage of this controller over TCSC is that there is no resonance problem, as SSSC does not have significant effect on the impedance of the transmission system [20]. The detailed modelling of SSSC is discussed in Chapter 4.

3.2.2.1 Thyristor Controlled Series Capacitor (TCSC)

The Thyristor Controlled Series Capacitor (TCSC) is the next variety of series FACTS controllers. This device uses a series capacitor bank reactance connected in parallel with a thyristor controlled reactor (TCR) [70].

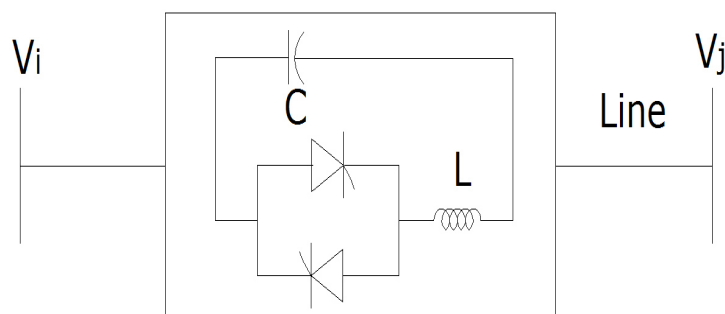


Fig 3.5: Basic structure of TCSC [77]

The structure of the TCSC shown in Fig 3.5 consists of a series capacitor C connected in parallel with a Thyristor controlled reactor L [78].

A practical TCSC module incorporates protective equipment (metal-oxide varistor (MOV)), which is connected across the capacitors. like. The MOV, which is a non-linear resistor, limits voltage across the capacitor under fault conditions, and helps improve transient stability [77].

Thyristors with gate turn – off capability are not required in the TCSC circuit, as the reactor is controlled by controlling the firing angles of the anti – parallel thyristors [65].

3.2.3 Series-shunt FACTS controller: United Power Flow

Controller (UPFC)

The United Power Flow Controller (UPFC) is developed by coupling a STATCOM and a SSSC through a dc link. It is normally incorporated in a system to provide simultaneous real and reactive series line compensation without any external electric energy source, and can also be used as an independent shunt controller [65].

Fig 3.6 represents the schematic of a UPFC.

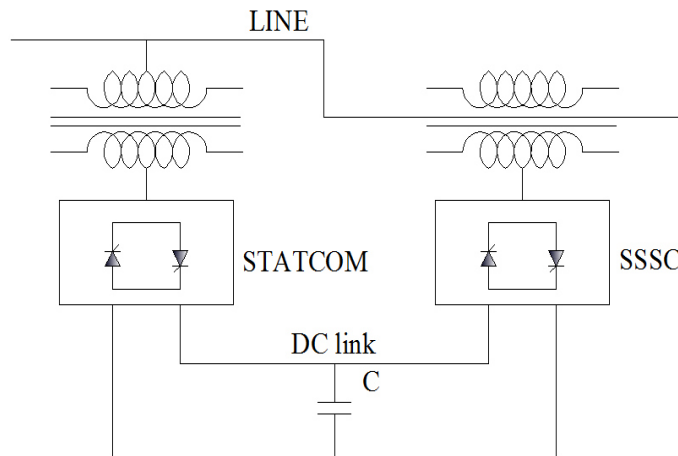


Fig 3.6: Schematic of a Unified Power Flow Controller (UPFC) [73]

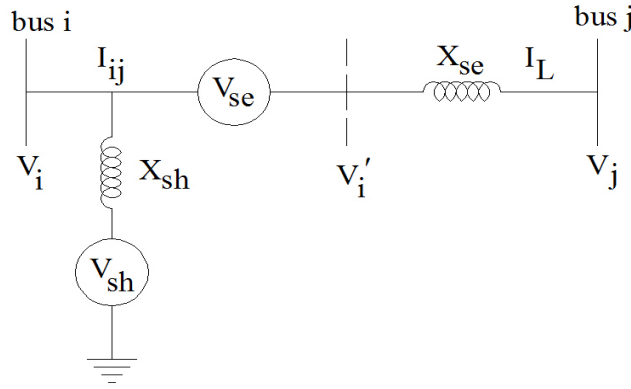


Fig 3.7: Equivalent model of UPFC [23]

With the reference voltage for the i^{th} bus considered as $V_i \angle 0$, modified system voltage is represented by (Fig 3.7):

$$V_i' = V_{se} + V_i \quad (3.1)$$

The voltage source V_{se} and V_{sh} are controllable both in magnitude and angle. The control parameters of UPFC are r and γ , which operates within the following specific limits [23]:

$$0 \leq r \leq r_{\max} \quad \text{and} \quad 0 \leq \gamma \leq 2\pi$$

3.3 Bus Voltage Stability Analysis using Shunt FACTS

controllers:

In this chapter bus voltage stability analysis is performed with the application of reactive power compensation. Shunt FACTS devices, SVC and STATCOM are chosen for this purpose, as it is observed that these FACTS controllers have become alternatives to a fixed reactive source [79].

It is observed that in post contingency situation, even if the fault is cleared the voltage level remains within the instability zone [24]. But with the application of a SVC or a STATCOM, this type of instability can be avoided. Shunt FACTS

controllers are located at the identified weakest bus and in the midpoint of the critical line for injecting current into the system where these are connected [69].

3.3.1 Modelling of SVC and STATCOM for power flow computations:

Modelling of SVC:

Fig 3.8 [69] represents the variable susceptance model of SVC applied to bus j . The SVC is represented as a reactance adjustable within limits. The shunt susceptance B_{SVC} , represents the amount of SVC susceptance required to maintain the voltage of specified value at the bus. Inclusion of SVC at any bus converts it into a voltage-controlled (PV) bus and the variable susceptance B_{SVC} is operated as a state variable [65]. If B_{SVC} is maintained within limits, the specified voltage is obtained and the bus operates as a PV bus. If B_{SVC} exceeds the minimum or maximum limits, it is then fixed at the violated limit and the node operates as a PQ bus again.

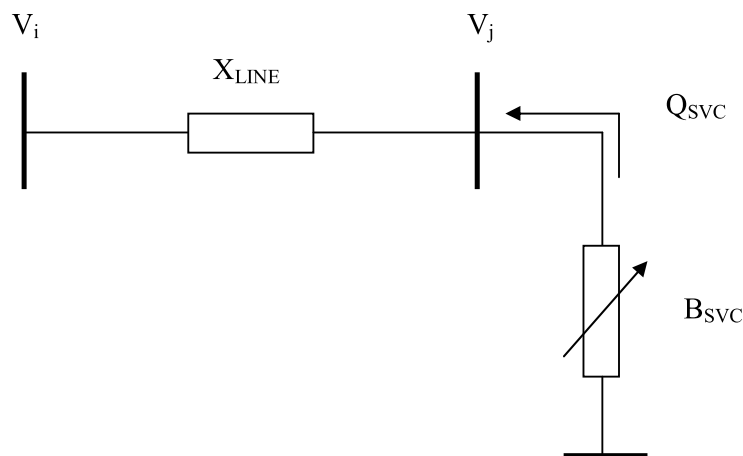


Fig 3.8: Variable susceptance model of SVC [25]

Current drawn by the SVC connected to bus j is given as:

$$I_{svc} = jB_{svc} V_j \quad (3.2)$$

And the reactive power drawn by the SVC is given as,

$$Q_{svc} = Q_j = -|V_j|^2 B_{svc} \quad (3.3)$$

The power mismatches are as shown below:

$$\begin{bmatrix} \Delta P_j \\ \Delta Q_j \end{bmatrix} = \begin{bmatrix} 0 & 0 \\ 0 & Q_j \end{bmatrix} \begin{bmatrix} \Delta \delta_j \\ \Delta B_{svc} / B_{svc} \end{bmatrix} \quad (3.4)$$

For each iteration f, the variable susceptance B_{SVC} is updated accordingly to,

$$B_{svc}^f = B_{svc}^{(f-1)} + (\Delta B_{svc} / B_{svc})^{(f)} B_{svc}^{(f-1)} \quad (3.5)$$

The varying susceptance represents the total SVC susceptance required for maintaining the bus voltage magnitude.

Modelling of STATCOM:

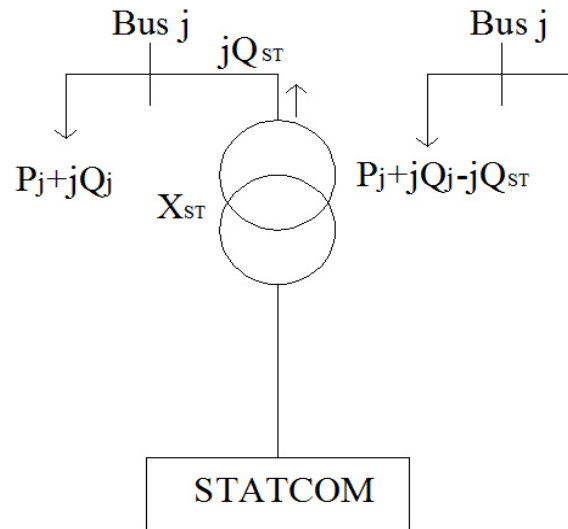


Fig 3.9: Model of STATCOM in Load flow calculations [64]

Fig 3.9 shows STATCOM connected to bus j where,

$V_j \angle \delta_j$: bus voltage at bus j

$V_{ST} \angle \delta_{ST}$: STATCOM output voltage (ac), referred to the jth bus side

X_{ST} : STATCOM reactance

B_{ST} : STATCOM susceptance

Q_{ST} : Reactive power exchange between STATCOM and the line

If we assume STATCOM to be loss less, there will be no active power flow.

Thus,

$$P_{ST} = 0, \quad \delta_{ST} \cong \delta_j$$

$$\begin{aligned} \therefore Q_{ST} &= \frac{|V_j|^2}{X_{ST}} - \frac{|V_j||V_{ST}|}{X_{ST}} \cos(\delta_j - \delta_{ST}) \\ &= \frac{|V_j|^2}{X_{ST}} - \frac{|V_j||V_{ST}|}{X_{ST}} \quad (\text{for lossless STATCOM}) \end{aligned} \quad (3.6)$$

$$\therefore Q_{ST} = -|V_j|^2 B_{ST} - |V_{ST}||V_j| B_{ST} \quad (3.7)$$

The power mismatches are as shown in Eqn (3.8):

$$\begin{bmatrix} \Delta P_j \\ \Delta Q_{ST} \end{bmatrix} = \begin{bmatrix} \frac{\partial P_j}{\partial \delta_j} & \frac{\partial P_j}{\partial |V_{ST}|} \\ \frac{\partial Q_{ST}}{\partial \delta_j} & \frac{\partial Q_{ST}}{\partial |V_{ST}|} \end{bmatrix} \begin{bmatrix} \Delta \delta_j \\ \Delta |V_{ST}| \end{bmatrix} \quad (3.8)$$

For each iteration f, variable voltage $|V_{ST}|$ is updated as,

$$|V_{ST}|^{(f+1)} = |V_{ST}|^{(f)} + \Delta |V_{ST}|^{(f)} \quad (3.9)$$

3.3.2 Chapter3: Objectives

In this chapter bus voltage stability analysis is being performed with the application of shunt FACTS controllers.

The weakest buses (bus 30 for IEEE 30 bus system and bus 31 for IEEE 57 bus system) has been chosen for reactive power compensation, as these buses have the highest tendency to collapse under overload conditions, as indicated by the CPF results (Section 2.5.1 and Section 2.5.2). Moreover, the Eigenvalue (Modal) Analysis have inferred that bus 30 (in IEEE 30 bus system) and bus 31 (in IEEE 57 bus system) has the highest participation factor among the weak buses and therefore has the maximum contribution voltage collapse (ref Section 2.5.1.1 and Section 2.5.2.1).

Therefore, these buses have been chosen for reactive power compensation using SVC and STATCOM. The performances of the other weak buses with compensation applied to the weakest bus, have also been observed. Continuation Power Flow (CPF) method is used to identify the weakest bus of each system under test (*as in section 2.5.2*). SVC and STATCOM are applied at the weakest bus and the behaviour of the power system is observed. Bus voltage stability analysis with application of shunt FACTS compensation is performed, and the voltage magnitude improvement is observed. PSAT toolbox of MATLAB is used to perform the CPF analysis [80, 81] with SVC applied to the weakest bus and then with STATCOM, and the results are being compared with those of the uncompensated systems (*section 2.5*). The flowchart of CPF Process with FACTS is shown in Appendix B (*Fig B.1*).

3.4 Results and Discussion

Bus voltage stability analysis has been carried out on IEEE 30 and 57 bus systems. The results of section 2.5 are used for weak bus identification and the maximum loading margin of the test systems, without reactive power compensation.

Shunt FACTS devices SVC and STATCOM are then applied to the weakest bus, to compensate for the reactive power deficit, improve the voltage profile and increase the maximum loading margin. Continuation power flow (CPF) analysis is performed on the compensated systems under study, once with application of SVC and then with STATCOM connected to the weakest bus. The voltage profile, real and reactive power profiles and the maximum loading margin are observed for each case. Comparisons are then made with the uncompensated systems.

3.4.1 Case study: IEEE 30 bus system

Results of Section 2.5.1 identify bus number 30 of IEEE 30 bus test system as the weakest bus, having minimum voltage magnitude under critical loading conditions and having the highest value of participation factor. Therefore, bus 30 is selected for reactive power compensation. Static VAR Compensator (SVC) and Static Synchronous Compensator (STATCOM) are applied separately, on this bus.

Table 3.1: Voltage magnitudes of the weak buses (IEEE 30 bus System)

Bus No.	Voltage (pu)		
	Without compensation	with SVC in bus 30	with STATCOM in bus 30
30	0.497227842	0.982735742	0.973736097
29	0.574011094	0.862739959	0.853795738
26	0.585780919	0.852473543	0.853795738
25	0.674363235	0.690291178	0.68178783

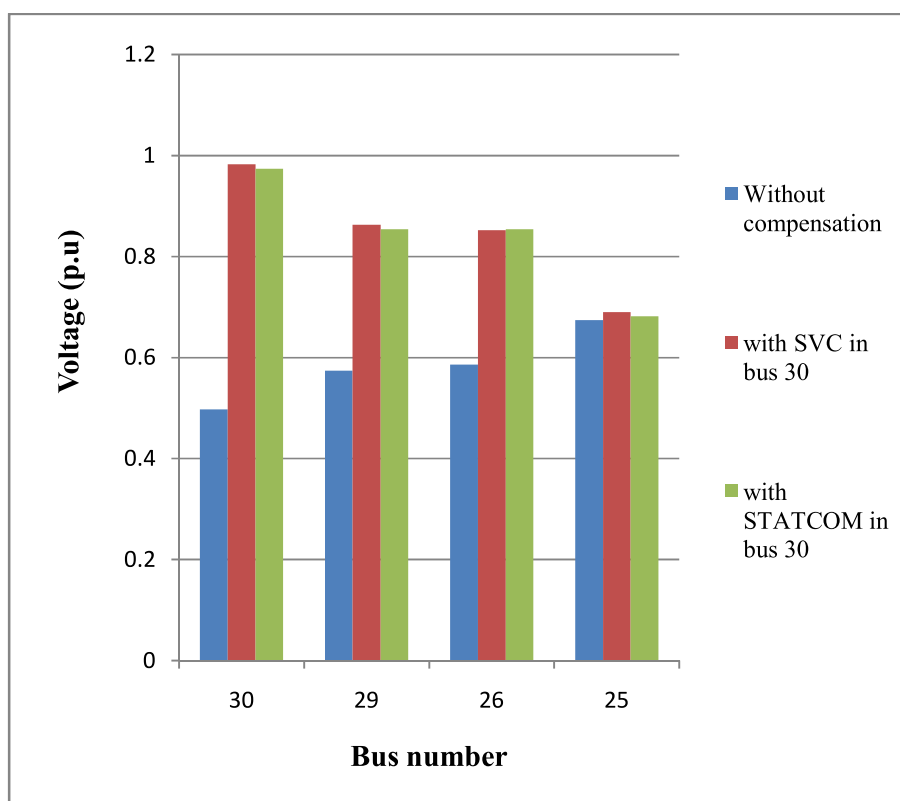


Fig 3.10: Voltage Magnitude Profile of the weak buses (IEEE 30 bus system)

Table 3.1 shows the voltage magnitudes of the weakest buses, having minimum voltage values, without compensation, with SVC and then with STATCOM applied to bus 30. It is observed in Fig 3.10, that there is an improvement in the voltage magnitudes of the weak buses, including the critical bus 30, when SVC and STATCOM are applied. This indicates that with the application of shunt FACTS devices in the most critical bus, the voltage profiles of the other weak buses are also improved.

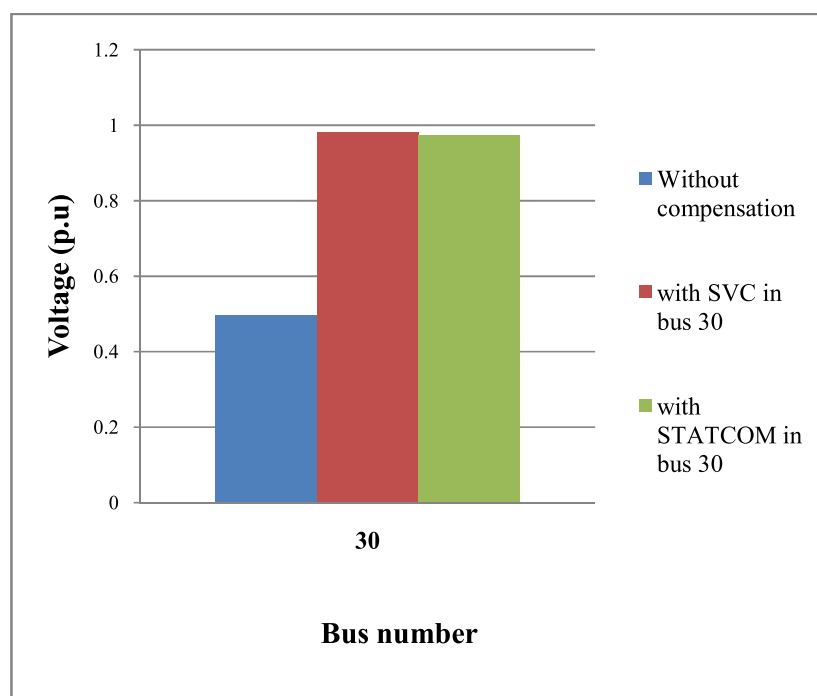


Fig. 3.11: Voltage Magnitude Profile of the weakest bus (IEEE 30 bus system)

Fig. 3.11 represents the voltage profile of bus 30 under different types of shunt compensation. The voltage profile is improved by nearly the same amount with the use of SVC and STATCOM.

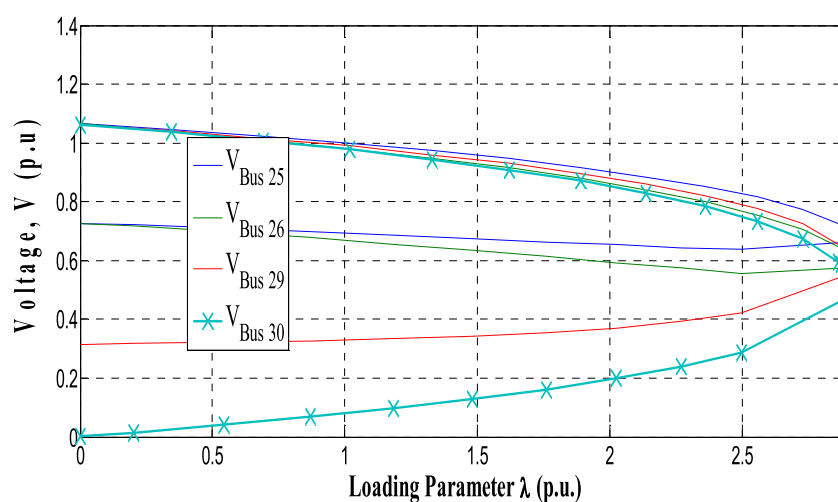


Fig. 3.12: P-V curve for PQ buses with minimum voltages (IEEE 30 bus system) (Without compensation)

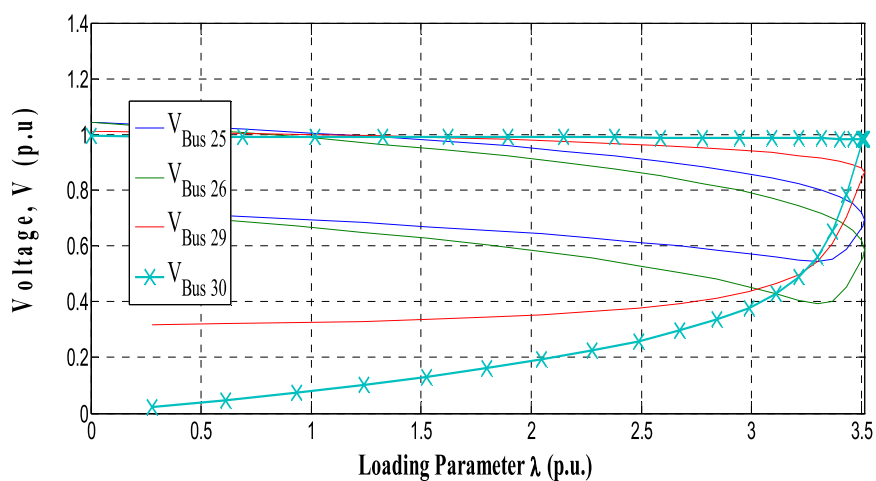


Fig 3.13: P-V curve for PQ buses with minimum voltages (IEEE 30 bus system)
(With SVC in bus 30)

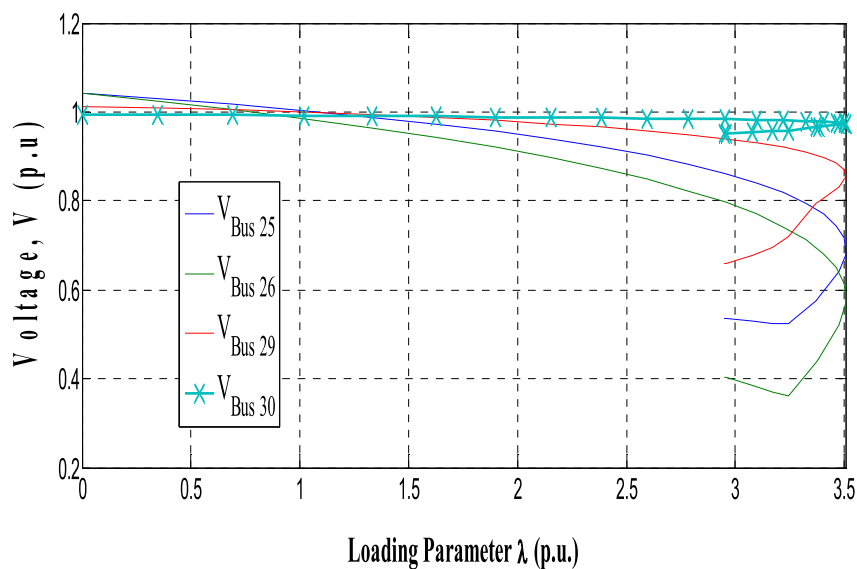


Fig. 3.14: P-V curve for PQ buses with minimum voltages (IEEE 30 bus system)
(With STATCOM in bus 30)

Fig. 3.12, Fig.3.13 and Fig. 3.14 represent the P-V curves of the system under different types of compensation. These indicate the increase in voltage magnitude

and enhancement in the maximum loading margin when SVC and STATCOM are applied to the weakest bus 30.

The maximum loading level λ is increased from 2.9.39 p.u. without compensation to 3.5111 p.u with SVC and 3.508 p.u with STATCOM in bus 30.

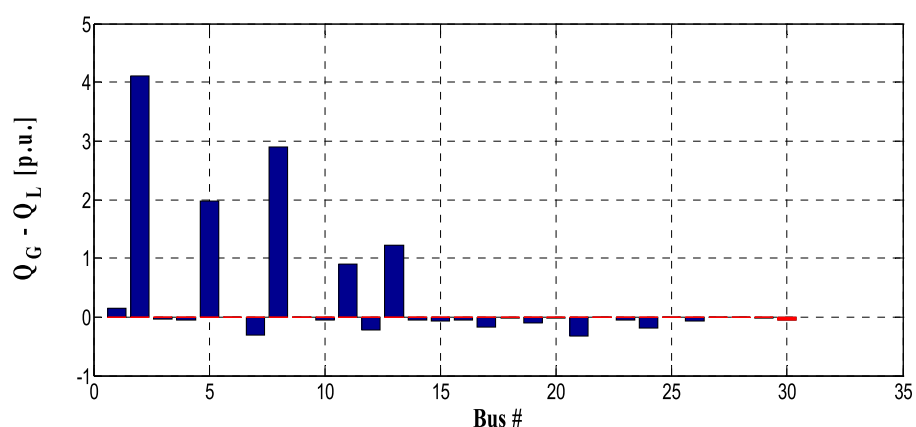


Fig 3.15: Reactive Power Profile of IEEE 30 Bus System (Without compensation)

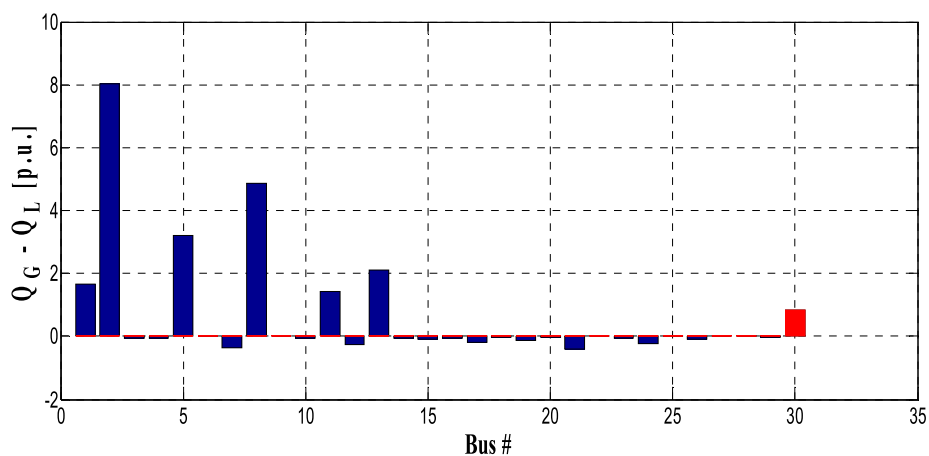


Fig 3.16: Reactive Power Profile of IEEE 30 Bus System (With SVC in bus 30)

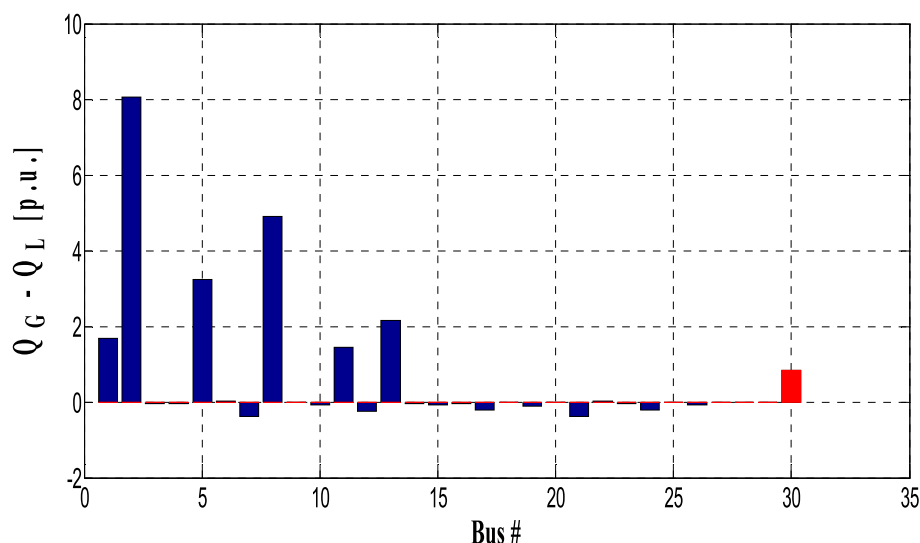


Fig 3.17: Reactive Power Profile of IEEE 30 Bus System (With STATCOM in bus 30)

Fig. 3.15, Fig. 3.16 and Fig. 3.17 represent the reactive power profiles of the IEEE 30 bus system with different types of compensation applied to the weakest bus (bus 30).

The above figures reflect the reactive power boost in the weakest bus (bus 30) with application of SVC and STATCOM to it.

Bus voltage stability analysis with the application of shunt FACTS devices have been successfully carried out in this exercise. Voltage profile and reactive power profile improvement has been observed and maximum loading margin enhanced with application of these devices.

3.4.2 Case Study: IEEE 57 bus System

It has been found in section 2.5.2, that the weakest bus in IEEE 57 bus test system is bus 31. Therefore, bus 31 is selected for reactive power compensation. SVC and STATCOM are applied to this bus separately and CPF analysis is performed on it.

The voltage magnitudes from this exercise are then tabled as below:

Table 3.2: Voltage magnitudes of the weak buses (IEEE 57 bus system)

Bus No.	Voltage (pu)		
	Without compensation	with SVC in bus 31	with STATCOM in bus 31
31	0.457560252	0.93	0.913912924
33	0.532152291	0.941027273	0.717815353
32	0.539879665	0.943337322	0.725422177
30	0.545302119	0.957793159	0.773651656

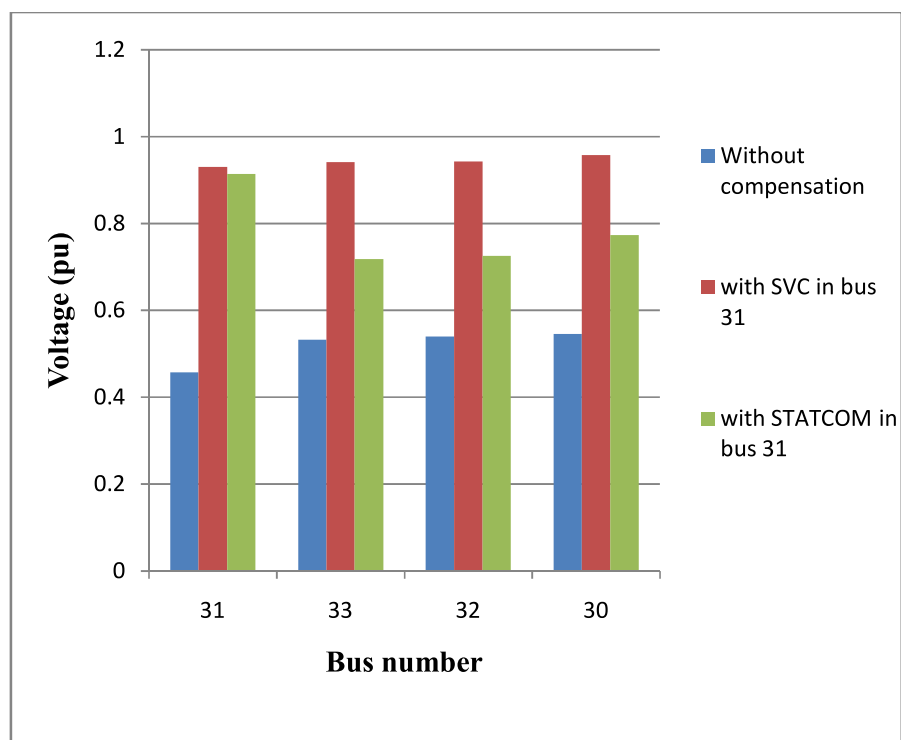


Fig 3.18: Voltage Magnitude Profile of the weak buses (IEEE 57 bus system)

It is observed in Fig 3.18, that there is substantial improvement of voltage magnitudes in the weak buses with application of FACTS devices in only the weakest bus. Application of SVC yields slightly better results than STATCOM.

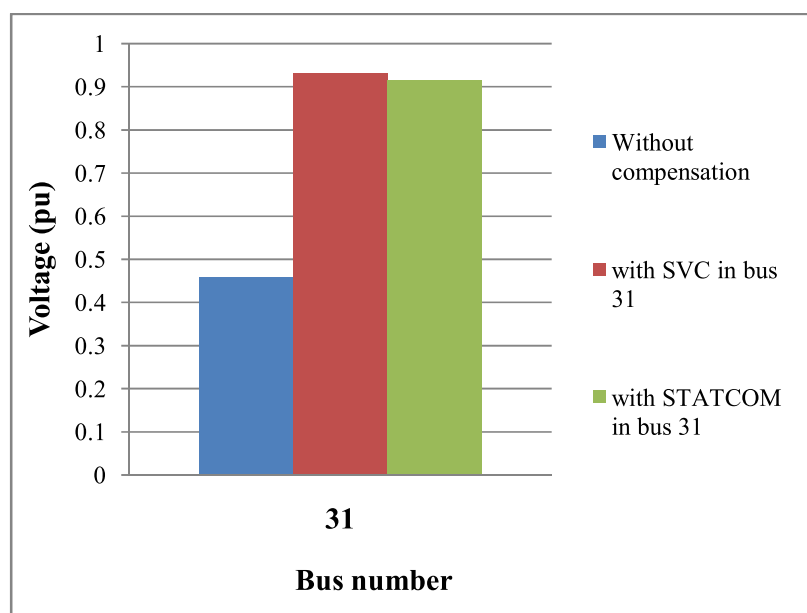


Fig 3.19: Voltage Magnitude Profile of the weakest bus (IEEE 57 bus system)

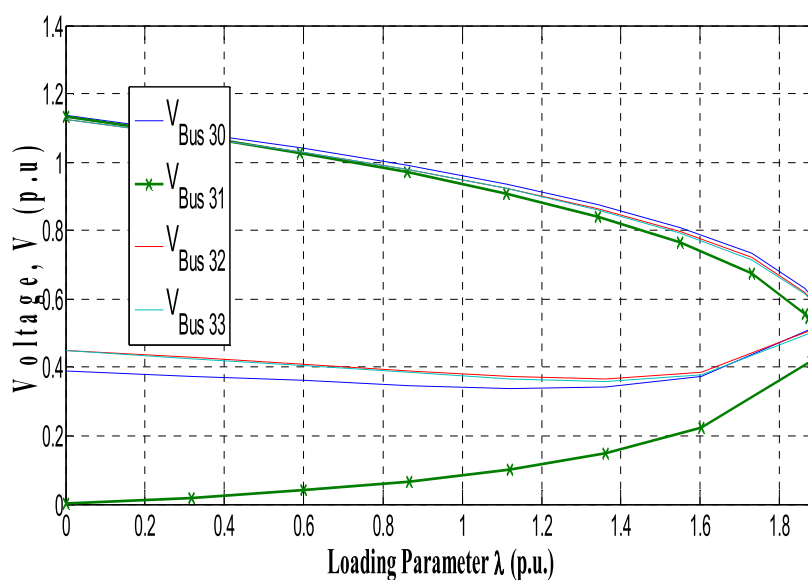


Fig 3.20: P-V curve for PQ buses with minimum voltages (IEEE 57 bus system)
(Without compensation)

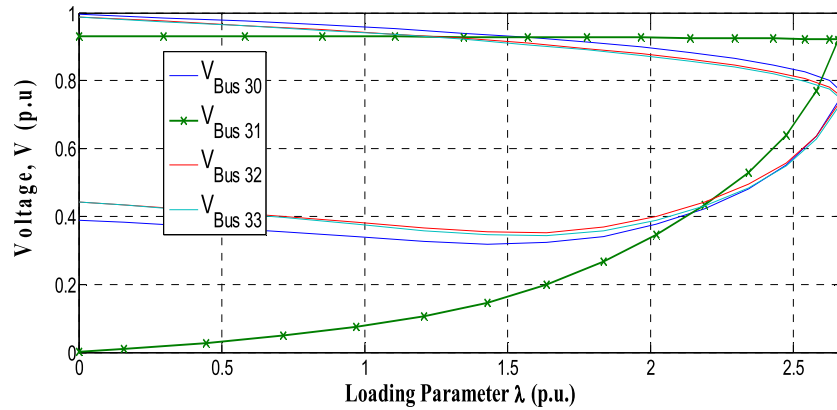


Fig 3.21: P-V curve for PQ buses with minimum voltages (IEEE 57 bus system)
(SVC in bus 31)

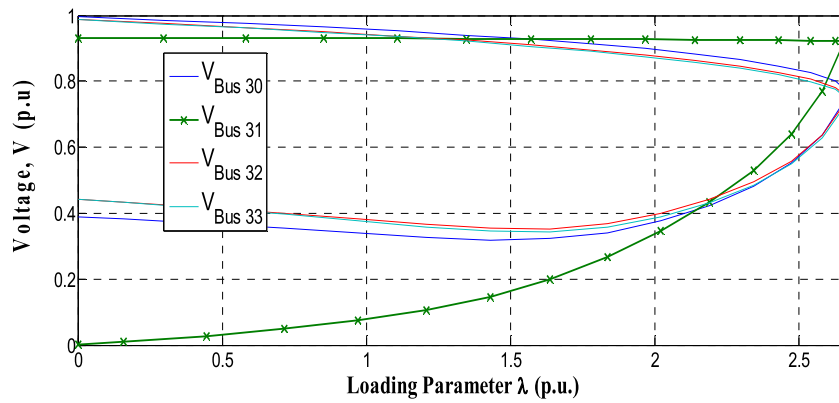


Fig 3.22: P-V curve for PQ buses with minimum voltages (IEEE 57 bus system)
(STATCOM in bus 31)

Fig. 3.19 shows the voltage profile improvement of the weakest bus. Fig 3.20, Fig 3.21 and Fig 3.22 are the P-V curves for the test system for different types of shunt compensation. These curves are drawn using PSAT [82]; the end criterion for the CPF being set for complete nose curve.

The P-V curves indicate that there is an improvement in the maximum loading limit, i.e. the voltage collapse point (or nose point) of the weakest bus is extended with application of SVC and STATCOM. The maximum loading parameter λ , increase

from 1.8921 p.u. (*without compensation*) to 2.6711 p.u. (*with SVC*) and 2.511 p.u. (*with STATCOM*).

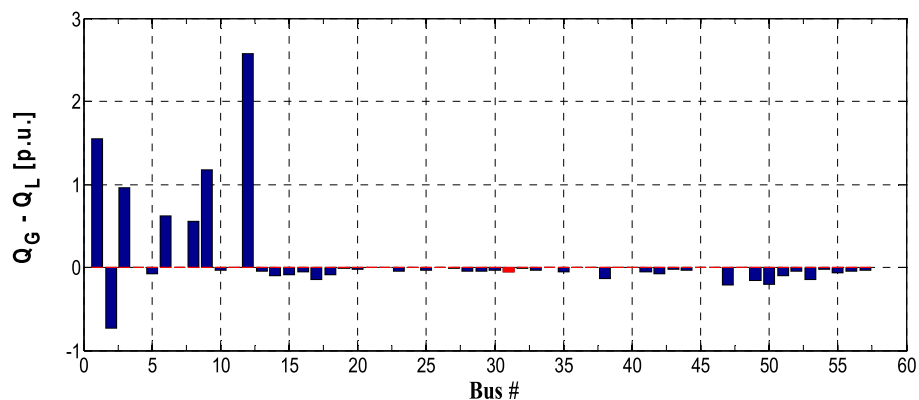


Fig 3.23: Reactive Power Profile of IEEE 57 Bus System (Without compensation)

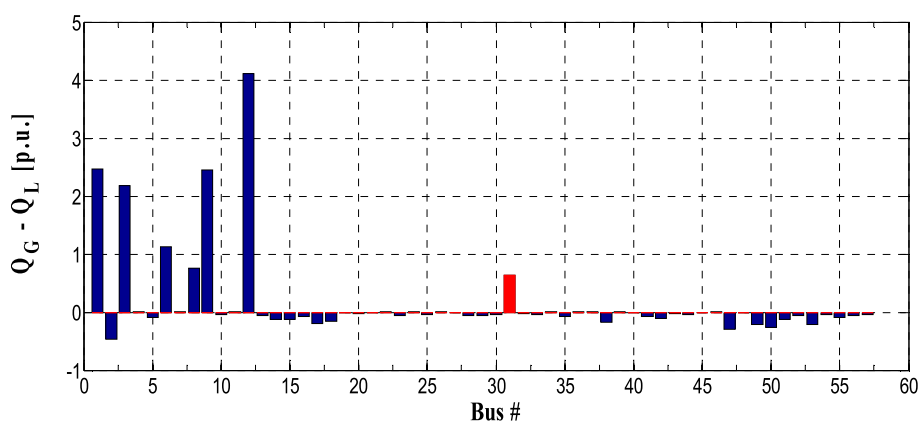


Fig 3.24: Reactive Power Profile of IEEE 57 Bus System (With SVC in bus 31)

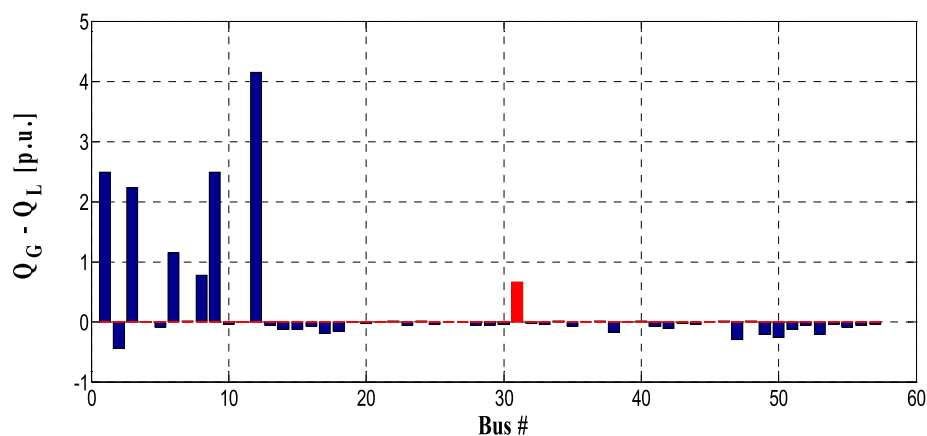


Fig 3.25: Reactive Power Profile of IEEE 57 Bus System (With STATCOM in bus 31)

Fig. 3.23, Fig. 3.24 and Fig. 3.25 are the reactive power profiles of the IEEE 57 bus system for different types of compensation. The reactive power boost in the weakest bus (bus 31) is observed from these figures.

IEEE 57 bus system also shows an improvement in the voltage profile and reactive power profile with the use of these compensating devices. Voltage stability margin is enhanced and the maximum loadability limit is improved.

3.4.3 Summary / Analysis of Results:

Table 3.3: Maximum loading margin

Test System	Maximum loading parameter, λ (p.u.)		
	Without compensation	with SVC	with STATCOM
IEEE 30 Bus	2.9039	3.5111	3.508
IEEE 57 Bus	1.8921	2.6711	2.511

Table 3.4: Voltage magnitudes of weakest buses

Test System	Weakest bus (No.)	Voltage (p.u.)		
		Without compensation	with SVC	with STATCOM
IEEE 30 Bus	30	0.497227842	0.982735742	0.973736097
IEEE 57 Bus	31	0.457560252	0.93	0.913912924

Table 3.3 shows the maximum loading margin of the two systems under test. It is seen that there is substantial improvement of maximum loadability limit in all the

three systems, with application of shunt FACTS devices on the buses approaching voltage collapse. Table 3.4 shows the voltage improvement in the most critical buses of the two systems under test. Voltage stability of these systems has therefore been enhanced by this process.

Table 3.5: State Variables of PSAT output

Test System	Bus No.	State Variables	
		SVC Susceptance (b_{SVC}) (pu)	STATCOM injected Current (pu)
IEEE 30 Bus	30	0.018452	0.018304
IEEE 57 Bus	31	-0.00631	-0.00587

Table 3.5 shows the amount of compensation provided by the SVC and STATCOM applied to the buses. The state variables have been obtained from the PSAT output.

3.5 Conclusion

Bus voltage stability analysis has been successfully performed on the IEEE 30 and 57 bus test systems.

Reactive power compensation with the help of shunt FACTS controllers helps improve the voltage profile of the system, especially the buses under stress and approaching voltage collapse. SVC and STATCOM have been selected for this purpose because of their superior performance (*as discussed in section 3.2*).

The results of this study have shown that, with the application of shunt FACTS devices at the most appropriate locations, improvement in voltage profile and reactive power profile, and enhancement of maximum loading limit of the systems under test can be achieved.

Hence, reactive power compensation plays a major role in voltage stability studies and voltage stability improvement is achieved with application of shunt FACTS devices.

Chapter 4

Line Voltage Stability Analysis

(Application of FVSI and Series FACTS controllers)

4.1 Introduction:

Power system networks are so designed that the number of lines in the system are usually more than the number of buses. This is done to assure delivery of power to main load centres and to ensure reliability and security of the system. In an overloaded and stressed system, the transmission line outages are therefore, more common as compared to bus failure. Hence, the study of line voltage stability is of utmost importance as part of power system stability studies. Voltage profile of a transmission system can be improved by controlling the reactive power absorption and flow through its lines [25, 83]. Jacobian matrix based voltage stability analysis is found to require high computational time and are more suitable for off-line monitoring purpose [84]. They are more useful in finding the voltage stability margin or proximity to voltage collapse [44].

In this chapter, Line voltage stability analysis is demonstrated with the application of Voltage Stability Indicators for critical line identification and series FACTS controllers for power flow improvement.

4.2 Voltage Stability Indicators

Different voltage stability indicators have been used to assess the proximity of a particular line or bus to voltage collapse; as formulated and presented in literature [61, 51, 55]. These indicators are used to forecast the possibility of a voltage unstable situation. Based on the power flow equation solutions, Kessel, et al. [14] introduced the first voltage stability index. Thereafter, many such indices were formulated [87] for real-time monitoring of system status. The voltage stability indicators can be classified as Jacobian matrix based voltage stability indicators and system variables based voltage stability indices [88]. These indicators are also used to classify different power system conditions. The system variables based indices require less computational time and are suitable for on-line monitoring purpose [88].

These indices may further be classified as bus voltage stability indices (those that identify the critical bus or node) and line voltage stability indices (those that reveal the stability of a line connected between two buses). Some common and effective voltage stability indices are mentioned in the next section

4.2.1 Bus voltage Stability Indices

(i) L index

Kessel, *et al.* first described the L index [14]. Here, the transmission system was represented in the form of hybrid matrix equations as shown in Eqn (4.1).

$$\begin{bmatrix} V_L \\ I_G \end{bmatrix} = H \begin{bmatrix} I_L \\ V_G \end{bmatrix} = \begin{bmatrix} Z_{LL} & F_{LG} \\ K_{GL} & Y_{GG} \end{bmatrix} \begin{bmatrix} I_L \\ V_G \end{bmatrix} \quad (4.1)$$

Where

V_L, I_L : load bus voltage and current vectors

V_G, I_G : generator bus voltage and current vectors

$Z_{LL}, K_{GL}, F_{LG}, Y_{GG}$: sub-matrices of the hybrid matrix H.

A voltage stability indicator is thus defined using this representation at each load bus j ($j \in L$).

$$L_j = \left| 1 + \frac{V_{0j}}{V_j} \right| \quad (4.2)$$

$$\text{Where,} \quad V_{0j} = -\sum_{i \in G} F_{ji} V_i \quad (4.3)$$

The index value of a load bus is 1 whenever it approaches a collapse point. The other weaker buses of the system are those having higher values of this index.

(ii) V/V₀ Index

A very simple index, the ratio V/V₀ index for bus voltage stability indication, has been presented in [89],

where,

V : bus voltage values obtained by performing the load flow on the system or by state estimation

V_o : new bus voltages computed after performing load flow for the same system, with the connected loads equated to zero.

The ratio is computed at each node of the power system and a voltage stability map is obtained, which yields the weak spots or the critical buses. The drawback of this index is that it does not help in accurate prediction of the bus voltage collapse proximity, as the profile presented with respect to the key system parameter, is highly non-linear [90].

(iii) Voltage Stability index (VSI)

This index has been formulated by M.H. Haque [91]. The index is based on the theory that changes in the apparent power of the load results in change of load current and voltage, therefore satisfying the relationship:

$$S_i = V_i I_i \quad (4.4)$$

Using Taylor's theorem, the following equation is derived,

$$\Delta S_i = \frac{\partial S_i}{\partial I_i} \Delta I_i + \frac{\partial S_i}{\partial V_i} \Delta V_i + \text{higher order terms} \quad (4.5)$$

Where,

ΔS_i : Incremental change in load apparent power

ΔV_i : Incremental change in load voltage

ΔI_i : Incremental change in load current

From Eqn. 4.4 and Eqn. 4.5 (neglecting higher order terms) we have:

$$\Delta S_i = V_i \Delta I_i + I_i \Delta V_i \quad (4.6)$$

ΔS_i approaches zero when critical load is encountered at any bus.

Therefore, to assure stability:

$$0 \leq V_i \Delta I_i + I_i \Delta V_i \quad (4.7)$$

If Eqn. 4.7 is divided by $V_i \Delta I_i$:

$$0 \leq 1 + \frac{I_i \Delta V_i}{V_i \Delta I_i} \quad (4.8)$$

Thus, the VSI at any bus i can be represented as:

$$VSI_i = \left[1 + \frac{I_i \Delta V_i}{V_i \Delta I_i} \right]^\alpha \quad (4.9)$$

VSI equals unity at no load and its value is zero at the voltage collapse point. Simplicity in evaluation of this VSI is because only the magnitude of bus voltage and load current at two different operating points are required. The expression is raised to a power of α (≥ 1) in order that the index achieves a linear characteristic. The system determines the value of α .

4.2.2 Line voltage Stability Indices

The power transmission concept in a single line has been used to formulate most of line stability indices available in literature. Fig. 4.1 is an illustration of a single line in an interconnected network.

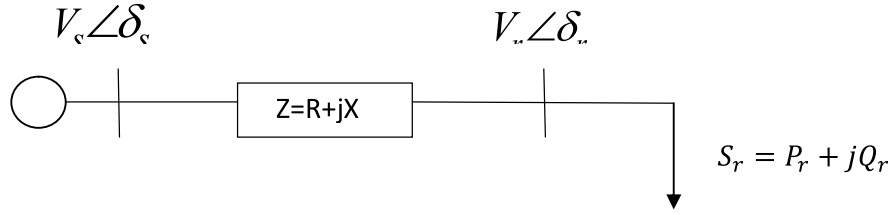


Fig 4.1: Single line diagram of a two-bus system

Where,

V_s and V_r : sending end and receiving end voltages

δ_s and δ_r : phase angle at the sending and receiving buses

Z : line impedance

R : line resistance

X : line reactance

θ : line impedance angle

Q_r : reactive power at the receiving end

P_r : active power at the receiving end

S_r : apparent power at the receiving end

(i) Lmn

This index was proposed by M. Moghavemmi, et al. [17] by adopting the technique of representing the power system network as a single line (Fig. 4.1).

From the power flow equation,

$$S_r = \frac{|V_s||V_r|}{Z} \angle(\theta - \delta_s + \delta_r) - \frac{|V_r|^2}{Z} \angle\theta \quad (4.10)$$

Where,

$$P_r = \frac{V_s V_r}{Z} \cos(\theta - \delta_s + \delta_r) - \frac{|V_r|^2}{Z} \cos \theta \quad (4.11)$$

$$Q_r = \frac{V_s V_r}{Z} \sin(\theta - \delta_s + \delta_r) - \frac{|V_r|^2}{Z} \sin \theta \quad (4.12)$$

Solving the Eqns. for V_r , we get,

$$V_r = \frac{V_s \sin(\theta - \delta) \pm \{[V_s \sin(\theta - \delta)]^2 - 4ZQ_r \sin \theta\}^{0.5}}{2 \sin \theta} \quad (4.13)$$

Where, $\delta = \delta_s - \delta_r$

Substituting $Z \sin \theta = X$ and considering only the positive square root value, we get Eqn. (4.13) as:

$$[V_s \sin(\theta - \delta)]^2 - 4Q_r X \geq 0 \quad (4.14)$$

Or,

$$L_{mn} = \frac{4XQ_r}{[V_s \sin(\theta - \delta)]^2} \leq 1 \quad (4.15)$$

This stability index is calculated for each line connecting two bus bars in an interconnected network. The system is stable if L_{mn} remains less than 1.

(ii) LQP index

This index has been derived by A. Mohamed, et al. [88] and uses the same concept of power flow through a single line. Using the notations as in section 4.2.2, the proposed index is calculated as below:

$$LQP = 4 \left(\frac{X}{V_s^2} \right) \left(\frac{X}{V_s^2} P_s^2 + Q_r \right) \quad (4.16)$$

(iii) Fast Voltage Stability Index (FVSI)

This index was proposed by I. Musirin et al. [18], and it is also based on the same concept as mentioned above. The stability index is calculated as:

$$FVSI_{sr} = \frac{4Z^2 Q_r}{V_s^2 X} \quad (4.17)$$

The line that has FVSI value closest to 1 is the most critical line of the system.

(v) Voltage Collapse Point Indicators (VCPI)

The voltage collapse point indicators (VCPI) proposed by M. Moghavemmi et al. [16], are based on the concept of maximum power transferred through a line.

$$VCPI(real) = \frac{P_r}{P_{r(max)}} \quad (4.18)$$

$$VCPI(react) = \frac{Q_r}{Q_{r(max)}} \quad (4.19)$$

Where,

P_r , Q_r : real or reactive power transferred to the receiving end

$P_{r(max)}$, $Q_{r(max)}$: maximum power that can be transferred to the receiving end
at a particular instant

P_r & Q_r depend on the system parameters, interconnections, network topology and load demand of the system.

$P_{r(max)}$ & $Q_{r(max)}$ can be calculated the following ways:

$$P_{r(max)} = \frac{V_s^2}{Z} \frac{\cos \phi}{4 \cos^2 \left(\frac{\theta - \phi}{2} \right)} \quad (4.20)$$

$$Q_{r(max)} = \frac{V_s^2}{Z} \frac{\sin \phi}{4 \cos^2 \left(\frac{\theta - \phi}{2} \right)} \quad (4.21)$$

Where,

Z : load impedance

$\phi = \tan^{-1}(Q_r/P_r)$.

The stability indices of the line are defined as [41]:

$$VCPI(Power) = \frac{P_r}{P_{r(max)}} \quad (4.22)$$

$$VCPI(Losses) = \frac{P_{losses}}{P_{losses(max)}} \quad (4.23)$$

With overloaded lines and increasing power flow through them, the values of $VCPI(Power)$ and $VCPI(Losses)$ increase, and when they reach 1, voltage collapse occurs. The VCPI indices varies from 0 (no load condition) to 1 (voltage collapse). Therefore it is possible to predict voltage collapse if any line of the network reaches the maximum value.

4.3 Fast Voltage Stability Index (FVSI)

Line voltage stability indices are suitable for on-line voltage stability analysis of transmission lines. Literature review suggests that, among all other line voltage stability indices, the Fast Voltage Stability Index (FVSI) is the most efficient, ensuring accuracy and less computational time [88]. FVSI is therefore used in this chapter for line voltage stability analysis and for weak bus identification.

4.3.1 Fast Voltage Stability Index Formulation

This index has been developed by taking the sending bus as the reference and using the general current equation [92]:

$$I = \frac{V_s \angle 0 - V_r \angle \delta}{R + jX} \quad (4.24)$$

The receiving voltage is computed as:

$$V_r = \frac{\left(\frac{R}{X}\sin\delta + \cos\delta\right)V_s \pm \sqrt{\left[\left(\frac{R}{X}\sin\delta + \cos\delta\right)V_s\right]^2 - 4\left(X + \frac{R^2}{X}\right)Q_r}}{2} \quad (4.25)$$

To obtain the real roots for V_r , the discriminant has to be set greater than or equal to zero, then:

$$\frac{4Z^2Q_rX}{V_s^2(R\sin\delta + X\cos\delta)^2} \leq 1 \quad (4.26)$$

The angle difference is normally very small and therefore the following simplification is done:

$$\delta \approx 0 \rightarrow \sin\delta = 0 \text{ \& } \cos\delta = 1 \quad (4.27)$$

Then a stability index is calculated as:

$$FVSI_{sr} = \frac{4Z^2Q_r}{V_s^2X} \quad (4.28)$$

The line that exhibits FVSI closest to 1 is the weakest or the most critical line of the system.

4.4 Line stability analysis using series FACTS controllers

FACTS controllers have often been used for improvement of voltage stability margin and boosting of bus voltage magnitudes under overload conditions. Series FACTS controllers like TCSC and SSSC are used to improve the real power flow through transmission lines in addition to reactive power compensation [38]. The line losses are significantly reduced and voltage profile of the system is improved [77, 93].

4.4.1 Modelling of Thyristor Controlled Series Compensator (TCSC)

The structure of the TCSC has been described in Section 3.2.2.2. To incorporate TCSC into the NR load flow, modelling of the device is required. Modelling of TCSC is done in two ways [94]:

- (i) Variable Reactance model
- (ii) Firing Angle model

In this thesis, the variable reactance model is used for line voltage stability analysis. The TCSCs are connected in series with the most critical lines under test. The model is shown in Fig 4.2

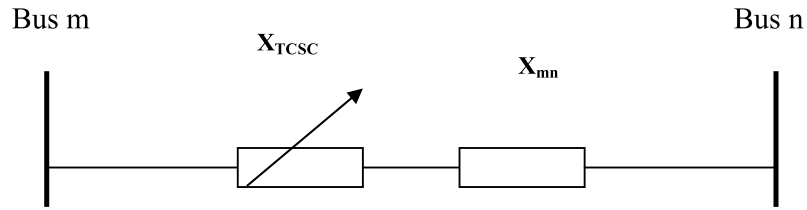


Fig 4.2: TCSC Model

The TCSC is used here as a real power flow controller between nodes i and j. The expression of power flow $P_{mn(reg)}$ is given by [65]:

$$P_{mn(reg)} = \frac{|V_m||V_n|}{X_{TCSC}} \sin(\delta_m - \delta_n) \quad (4.29)$$

Where,

$V_m \angle \delta_m$: voltage magnitude and phase of bus m

$V_n \angle \delta_n$: voltage magnitude and phase of bus n

X_{TCSC} : equivalent reactance of the TCSC controller

X_{line} : transmission line reactance without compensation

The equations of the variable series compensator are represented in matrix form as [25]:

$$\begin{bmatrix} I_m \\ I_n \end{bmatrix} = \begin{bmatrix} jB_{mm} & jB_{mn} \\ jB_{nm} & jB_{nn} \end{bmatrix} \begin{bmatrix} V_m \\ V_n \end{bmatrix} \quad (4.30)$$

For inductive operation,

$$B_{mm} = B_{nn} = -\frac{1}{X_{TCSC}} \quad (4.31)$$

$$B_{mn} = B_{nm} = \frac{1}{X_{TCSC}} \quad (4.32)$$

Reversal of signs is incorporated in the equations for capacitive operation.

The real power flow mismatch equation in TCSC is given by:

$$\Delta P_{mn} = P_{mn(reg)} - P_{mn(calculated)} \quad (4.33)$$

The value of X_{TCSC} of the TCSC controller is updated at the end of the iteration f, as [65]:

$$X_{TCSC}^{(f+1)} = X_{TCSC}^{(f)} + \Delta X_{TCSC}^{(f)} \cdot X_{TCSC}^{(f)} \quad (4.34)$$

Where, $\Delta X_{TCSC}^{(f)}$ is the incremental TCSC reactance.

The reactance of the TCSC depends on its compensation ratio (γ_{TCSC}) and the reactance of the transmission line where it is connected. The value of X_{TCSC} can be adjusted to control the real power flow across TCSC.

The TCSC modeled by the reactance, X_{TCSC} is given as follows: [70, 95, 96]:

$$X_{mn} = X_{line} + X_{TCSC} \quad (4.35)$$

$$X_{TCSC} = \gamma_{TCSC} \cdot X_{line} \quad (4.36)$$

Where, X_{line} : transmission line reactance.

To avoid overcompensation of lines, the compensation ratio γ_{TSC} is adjusted between 20% inductive reactance and 80% capacitive reactance [34]. Arbitrary values of γ_{TSC} within this range are used in this work to improve the voltage stability margin.

4.4.2 Modelling of Static Synchronous Series Compensator (SSSC):

In this chapter, SSSC is used to control the real power flow through the lines. As discussed in Section 3.2.2, no external energy source is required for SSSC operation and it is fully controllable. It can be used for regulating the reactive power drop across the line without any dependence on the transmission line current, thereby controlling the electric power flow.

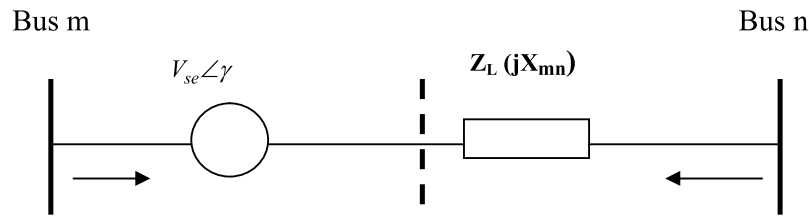


Fig4.3: Circuit element model of SSSC [44]

The Jacobian matrix of the NR load flow equations has to be modified in order to incorporate the SSSC controller in the line. Only the bus admittance matrix changes when the simplified model of SSSC is used and hence it makes the formulation simpler [44].

The complex power exchange between the SSSC and the line is given as:

$$S_{se} = V_{se} I \quad (4.37)$$

Where,

V_{se} : complex voltage injected into the line by SSSC

I : current through the line

$$I = \frac{V_m \angle \delta_m + V_{se} \angle \gamma - V_n \angle \delta_n}{Z_L} \quad (4.38)$$

The total active and reactive power flow through line m-n with SSSC is given as [82]:

$$P_{mn} = (1 + \epsilon) \frac{V_m V_n}{X_{mn}} \sin(\delta_m - \delta_n) \quad (4.39)$$

$$P_{mn} = -P_{nm} \quad (4.40)$$

$$Q_{mn} = (1 + \epsilon) \frac{V_m}{X_{mn}} (V_m - V_n \cos(\delta_m - \delta_n)) \quad (4.41)$$

$$Q_{nm} = (1 + \epsilon) \frac{V_n}{X_{mn}} (V_n - V_m \cos(\delta_m - \delta_n)) \quad (4.42)$$

Where,

$$\epsilon = \frac{V_{se}}{\sqrt{V_m^2 + V_n^2 - 2V_m V_n \cos(\delta_m - \delta_n)}} \quad (4.43)$$

The main control objective of the SSSC is to directly control the current and thereby the power flow by regulating the reactive power exchange between the SSSC and the line. The main advantage of SSSC over a TCSC is that the transmission line impedance is not impacted much and so the danger of resonance problem is eliminated [20].

4.4.3 Chapter 4: Objectives

In this chapter, line stability analysis using series FACTS compensators, TCSC and SSSC are carried out. Fast Voltage Stability Index (FVSI) is selected here for critical

lines identification, as it is found to be widely used in literature. These critical lines are then selected as optimal location for series FACTS compensation. The objective of this chapter is to enhance the real power flow through the critical lines as well as improve the bus voltage magnitudes. A comparison is made between the performances of the two compensating devices.

4.5 Results and Discussion

Line Voltage stability analysis is carried out on the two IEEE standard test systems selected for this thesis. Fast Voltage stability Index (FVSI) is computed for each line (*details in section 4.3*) and the two lines having the highest values of FVSI are identified as weak or critical lines. The lines chosen for Line voltage stability analysis are those connecting at least one load bus [97], as these are the lines where series FACTS compensation is to be provided. As discussed in the previous sections of this chapter, series FACTS devices are used on critical lines for real power flow enhancement, in addition to reactive power compensation. NR load flow analysis is performed on the systems, first without line compensation and then after application of series FACTS controllers, TCSC and SSSC separately to the stressed lines.

4.5.1 Case Studies

4.5.1.1 Test case 1 : IEEE 30 bus system

For IEEE 30 bus system, FVSI computation yields that line number 15 (connecting load buses 4 and 12) and line number 36 (connecting PQ buses 28 and 27) are the most critical lines. Therefore these lines are selected for line voltage stability analysis. NR load flow analysis is performed on the system with no compensation,

then with TCSC connected to the lines 15 and 36 and finally, with SSSC connected to the same lines. Real power flow, line losses and voltage magnitudes of the lines under test, and the connected buses are computed and tabled.

4.5.1.2 Results and Analysis (Test case 1):

The results of this case study are as shown below:

Table 4.1: Results (IEEE 30 Bus system)

		No compensation	with TCSC	with SSSC
Real Power flow in critical lines (p.u.)	Line 15	0.452248614	0.565637	0.509451
	Line 36	0.184893856	0.199852	0.197833
Bus Voltages (p.u.)	Bus 4 (line 15)	1.014353	1.023063	1.017141
	Bus 12 (line 15)	1.051024	1.029486	1.020232
	Bus 27 (line 36)	1.013721	1.007726	0.994064
	Bus 28 (line 36)	1.006326	1.010417	1.00578
Reactive Power Losses of critical lines	Line 15	0.04688622	0.016362	0.032120
	Line 36	0.01287219	0.003198	0.008447
Total Losses (p.u.)	Real Power Loss	0.175569	0.175053	0.174814
	Reactive Power Loss	0.329833	0.270228	0.310564
Sum FVSI in weak lines (p.u.)	Lines 15 & 36	1.1722	0.5640	0.5962

The result profiles are as shown below:

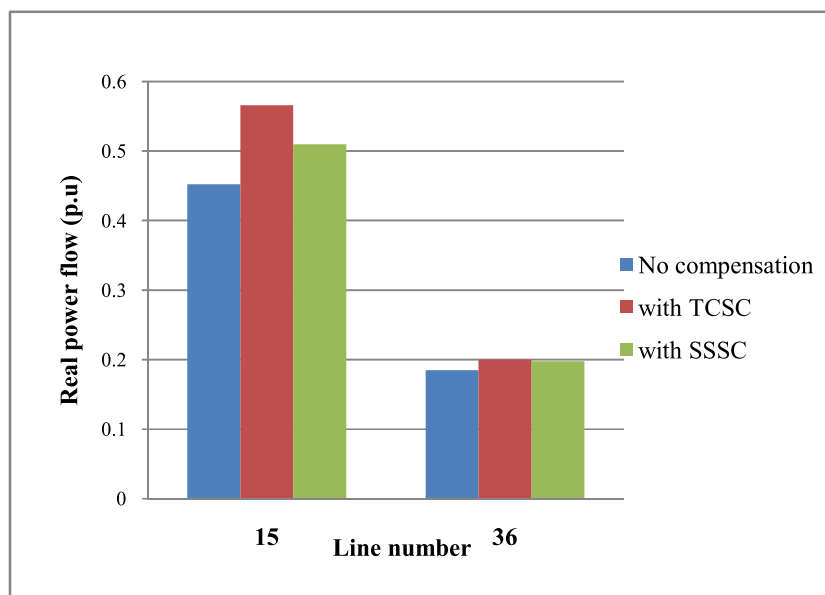


Fig 4.4: Real power flow profile of the compensated lines (IEEE 30 bus system)

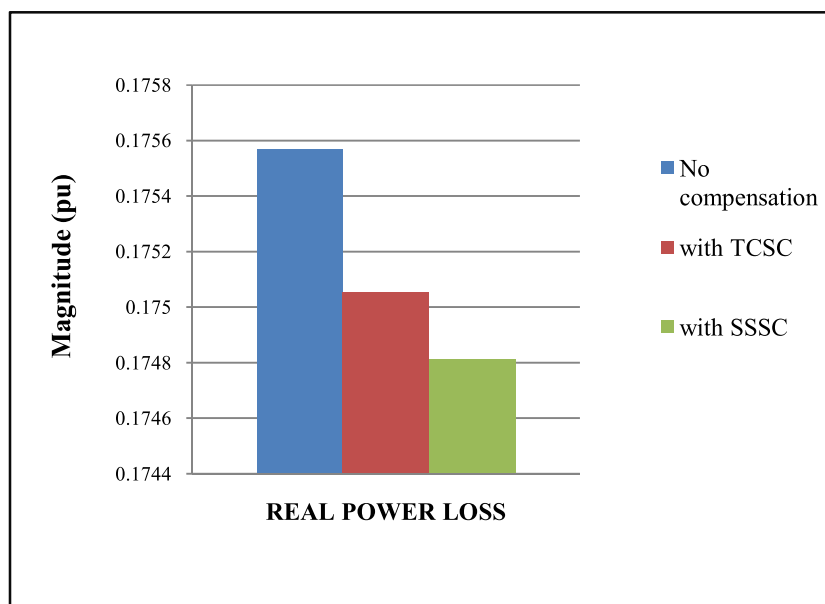


Fig 4.5: Total Real Power Loss profile (IEEE 30 bus system)

Table 4.1 and Fig 4.4 show the real power flows through the stressed lines, without compensation and with series FACTS compensation. These indicate that real power flow has increased in the stressed lines 15 and 36 with application of series FACTS controllers.

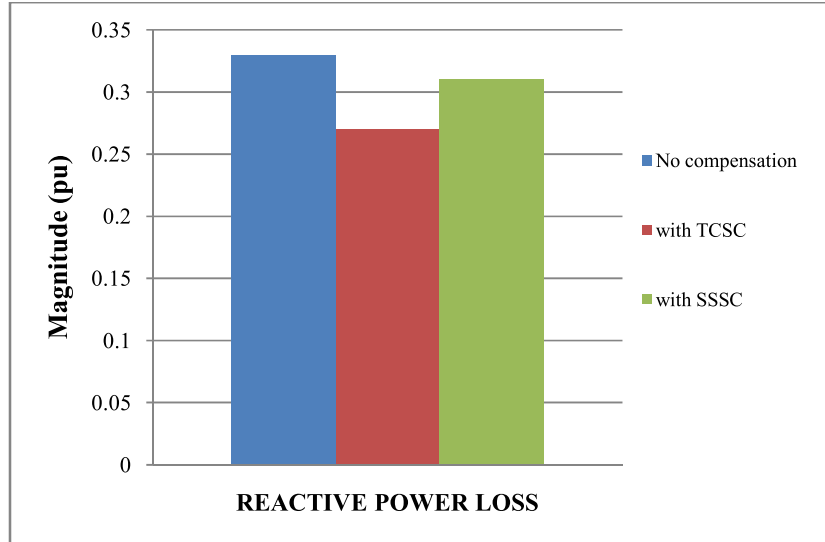


Fig 4.6: Total Reactive Power Loss profile (IEEE 30 bus system)

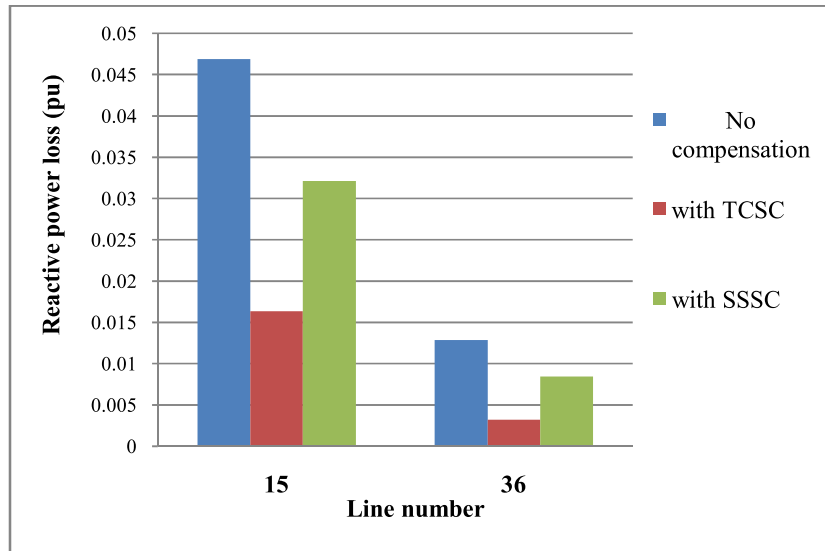


Fig 4.7: Reactive power loss profile of compensated lines (IEEE 30 bus system)

Fig 4.5 and Fig 4.6 represent the overall system losses. Fig 4.7 represents the reactive power losses of the stressed lines under test.

These results indicate that system loss minimization is achieved with reactive power compensation using series FACTS devices. The reactive power loss in the compensated lines is also minimized in this process, ensuring a voltage stable system.

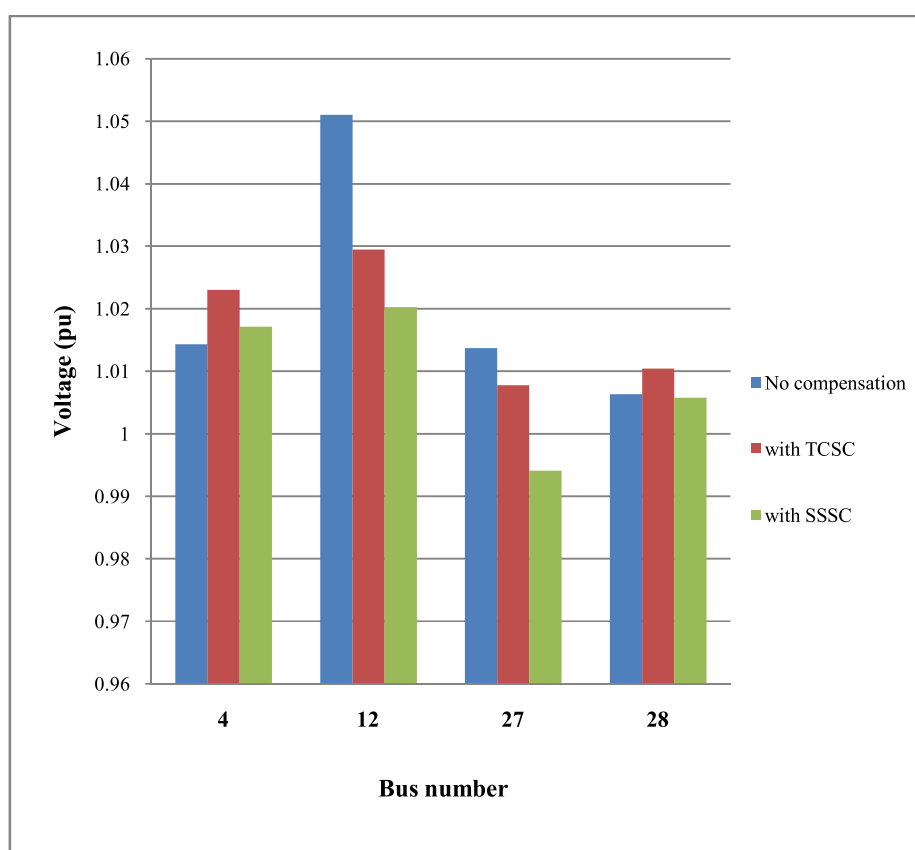


Fig 4.8: Voltage profile of the connected buses (IEEE 30 bus system)

Table 4.1 and Fig 4.8 represent the voltage magnitudes and voltage profile of the buses connected by the lines 15 and 36. The results indicate voltage improvement in the sending end buses, while a nominal drop is observed in the receiving end buses. This leaves a scope of further study, in terms of the optimum percentage of compensation to be used (*to be discussed in Chapter 5*) for maximum voltage stability enhancement. The total FVSI value of the critical lines is reduced as shown in Table 4.1. Therefore, line voltage stability improvement is achieved in this case study.

4.5.1.3 Test case 2 : IEEE 57 bus system

Fast Voltage Stability Index (FVSI) is calculated for the load lines of the IEEE 57 bus system. Here, it is seen that lines 35 and 46 (connecting PQ buses 24-25 and 32-34) have the highest FVSI values, both under normal and overload conditions. Therefore, lines 35 and 46 are identified for carrying out the similar test.

NR power flow analysis is performed on the system, without and with the series FACTS controllers TCSC and SSSC and the results are tabled.

4.5.1.4: Results and Analysis (Test case 2):

The results of this case study are as shown below:

Table 4.2: Results (IEEE 57 Bus system)

		No compensation	with TCSC	with SSSC
Real Power flow in critical lines (p.u.)	Line 35	0.070674	0.107584	0.105345
	Line 46	0.074603	0.074689	0.077519
Bus Voltages (p.u.)	Bus 24 (line 35)	0.99923304	1.00064511	1.00104644
	Bus 25 (line 35)	0.98252078	0.99312276	0.9934947
	Bus 32 (line 46)	0.94987472	0.95443453	0.95706597
	Bus 34 (line 46)	0.95920004	0.96270163	0.96244266
Reactive Power Losses of critical lines (p.u.)	Line 35	0.00626077	0.00429114	0.00411908
	Line 46	0.0068915	0.00197503	0.00139519
Total Losses (p.u.)	Real Power Loss	0.278638	0.278002	0.278002
	Reactive Power Loss	0.06328	0.048794	0.049623
Sum FVSI in weak lines (p.u.)	Lines 35 & 46	0.9101	0.6069	0.5250

The result profiles are as shown below:

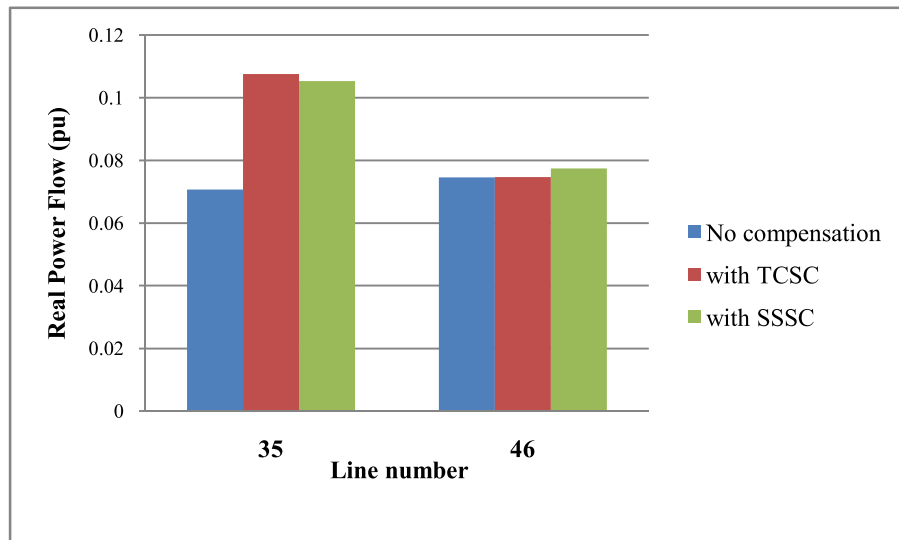


Fig 4.9: Real power flow profile of the compensated lines (IEEE 57 bus system)

Table 4.2 and Fig 4.9 show the real power flow improvement through the stressed/critical lines with the application of TCSC and SSSC. Real power flow enhancement is more in line 35 than in line 46 for the same percentage of compensation. With TCSC power flow enhancement is higher for line 35 and with SSSC it is higher for line 46.

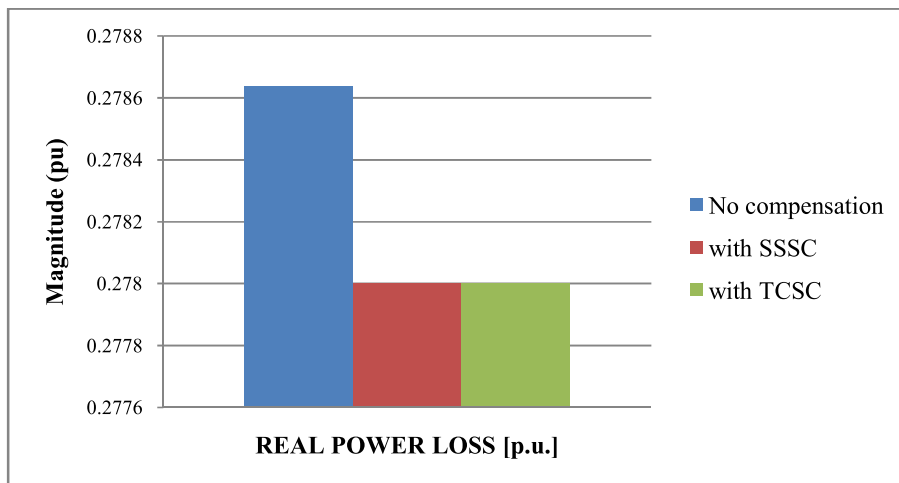


Fig 4.10: Total Real power loss profile (IEEE 57 bus system)

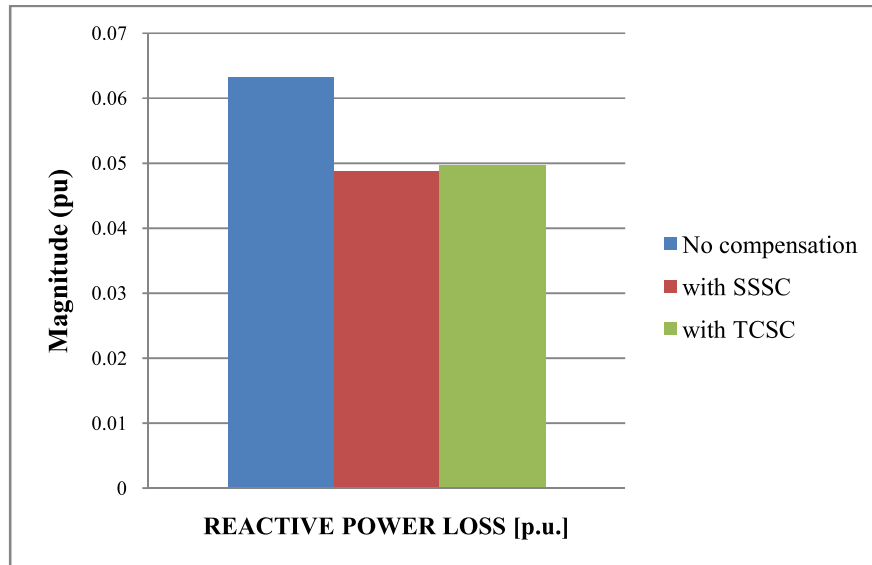


Fig 4.11: Total Reactive power loss profile (IEEE 57 bus system)

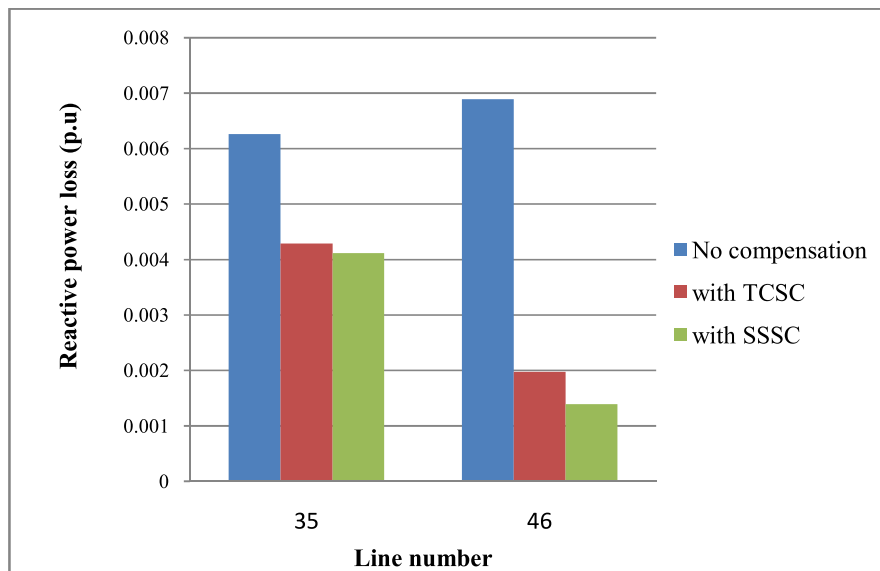


Fig 4.12: Reactive power loss profile of the compensated lines (IEEE 57 bus system)

Figs 4.10 and 4.11 represent the total system losses. Fig 4.12 represents the reactive power losses of the tested lines. The reactive power loss minimization is greater in line 46 with application of TCSC and SSSC to these lines, as shown in Table 4.2.

Total system real power loss minimization is greater than total reactive power loss with series FACTS compensation.

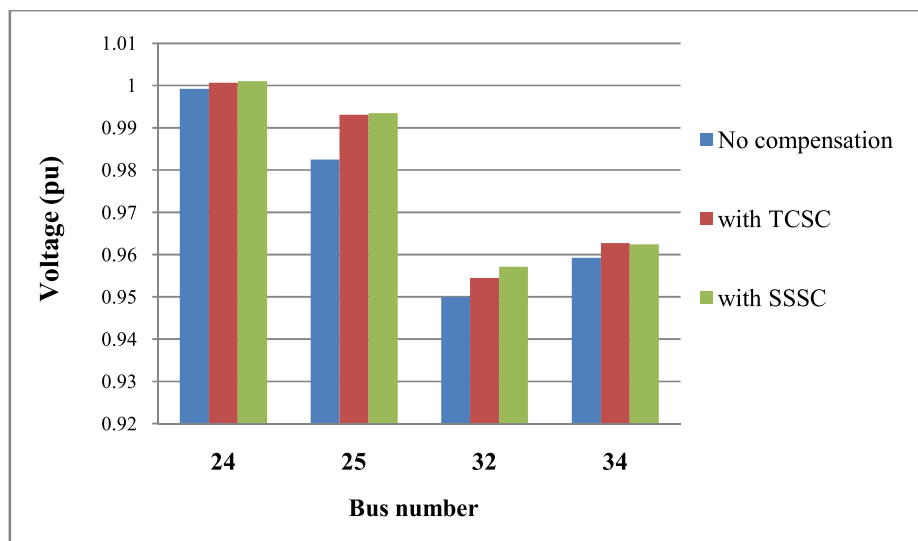


Fig 4.13: Voltage magnitude profile of the compensated lines (IEEE 57 bus system)

Table 4.2 and Fig 4.13 represent the voltage magnitudes of the buses connecting critical lines for different types of compensation.

Table 4.3: Line Compensation provided by FACTS devices

Test System	Line No.	Reactive Compensation (pu)	
		with TCSC	with SSSC
IEEE 30 Bus	15	0.0512	0.128
	36	0.0792	0.198
IEEE 57 Bus	35	0.3546	0.2364
	46	0.2859	0.1906

Table 4.3 shows the line compensation provided by the TCSC and SSSC. The state variables have been obtained from the PSAT output.

Table 4.4: Real Power flow in adjacent lines

System	Line No.	Connected Bus	Real Power Flow (p.u.)		
			Without compensation	with TCSC	with SSSC
IEEE 30	4	3-4	0.821419011	0.83598952	0.829184625
	17	12-14	0.078575198	0.088364572	0.084890375
	35	27-25	0.047628454	0.066455445	0.064317629
	37	27-29	0.061899457	0.061941222	0.061979076
IEEE 57	34	23-24	0.033439848	0.033535714	0.033512351
	44	32-31	0.020279214	0.020374171	0.023137231
	47	34-35	0.074603248	0.07468871	0.077519273

Table 4.4 represents the real power flows in the adjacent lines. It is found that the lines connected to the compensated lines too experience improvement in real power flow with the application of FACTS devices in the critical lines.

In this study, the bus voltages are successfully improved with application of TCSC and SSSC. The total FVSI value of the critical lines is also reduced, as shown in Table 4.2. Therefore, line voltage stability improvement is achieved in this case study.

4.6 Conclusion

Series FACTS controllers are often used for voltage stability enhancement, because in addition to reactive power compensation, they also help increase the real power flow through the lines directly, by varying the line reactance. System losses are reduced and voltage profile of the connected buses is improved by usage of series FACTS devices like TCSC and SSSC.

In this chapter, Line Voltage Stability Analysis has been successfully performed on standard IEEE test systems. Real power flow enhancement and system loss minimization have been achieved in this exercise. The effectiveness of FVSI for weak line identification and voltage stability improvement is also highlighted here.

Chapter 5

Voltage Stability Analysis using Evolutionary Methods

(Teaching Learning Based Optimization Method for Voltage Stability Analysis)

5.1 Introduction

It is seen in the previous chapters that improvement of voltage profile and prevention of voltage collapse can be achieved with the application of Flexible AC Transmission Systems (FACTS) at strategic and appropriate locations. The power transfer capability is also enhanced and line losses minimized by introduction of FACTS devices.

Power flow problem can also be treated as an optimization problem. Parameter optimization is one of the chief goals of engineering design where the emphasis is laid on maximization or minimization of objectives. Traditional or classical optimization methods have been used in literature and have been found to be easy to apply and require comparatively less iterations. But their limitations lie in their inherent search mechanisms. Generic solution approaches required for solving

problems having different types of constraints, variables and problem objectives, are seldom provided by classical methods [98]. In order to overcome these drawbacks, meta-heuristic or advanced optimization techniques originating from Artificial intelligence techniques are being developed periodically (*as mentioned in section 1.3*). The advantages of these techniques are that they can be applied in combination with many classical optimization techniques and has the ability of solving problems that have no solution [98].

In many real life engineering problems, it is desirable to optimize two or more objective functions simultaneously. These are known as Multi-objective optimization problems and research have established that nature-based heuristic optimization methods provide better results than classical methods. Some optimization methods that have been successfully used for Multi-objective optimization are Genetic Algorithm (GA) [33], Particle Swarm Optimization (PSO), Differential Evolution (DE), Ant Colony Optimization (ACO), Firefly Algorithm, Artificial Bee Colony (ABC) algorithm, Harmony Search (HS) algorithm, Bacterial Foraging algorithm, Cuckoo Search (CS) algorithm, etc.

5.2 Evolutionary programming applied to Voltage Stability:

In addition to conventional methods discussed in the previous chapters, evolutionary programming has also been used for Voltage stability analysis of power system networks (*as mentioned in section 1.3*). In voltage stability studies, optimization techniques are primarily used for parameter setting of the compensating devices, in order to obtain the best results. Optimization of FACTS controller ratings can be

done by using Evolutionary programming methods. These techniques are modern research tools developed to minimize or eliminate the drawbacks of conventional methods [99]. Genetic algorithm is found to be the most preferred among all evolutionary methods for voltage stability analysis [35, 40,100]. In addition to this method, many other population-based and nature-inspired optimization techniques have been developed (*as mentioned in section 5.1*) and successfully applied to voltage stability analysis in general, and parameter setting in particular. These evolutionary/ meta-heuristic computing techniques are highly powerful tools, capable of finding the optimum solution to a problem. The advantage of these tools is that there are no restrictions to the nature of the search space and the type of variables [42].

Some new methods used for voltage stability studies are Genetic Algorithm (GA) [37, 42,100], Differential Evolution (DE) [38], Ant Colony Optimization (ACO), Firefly Algorithm [44, 70], Particle Swarm Optimization (PSO) [101], Artificial Bee Colony (ABC) algorithm, Harmony Search (HS) algorithm, Bacterial Foraging algorithm, Cuckoo Search (CS) algorithm, etc. Comparisons have been made in literature between the effectiveness of different methods applied for finding an optimal solution [40, 41, 44]

Voltage stability analysis involves computation of maximum loading limit (MLL) and voltage stability proximity indicators, improvement of bus voltage magnitudes, enhancement real power flows through stressed lines and minimization of system losses. As a result, multi-objective evolutionary programming techniques are often

used for voltage stability studies, as this analysis can be addressed through different approaches [37, 42, 44, 101].

In this chapter, a new population-based evolutionary programming method, Teaching Learning Based Optimization (TLBO) Method is used for optimizing the ratings of the series FACTS compensators used for Line Voltage Stability Analysis. In addition to computation of the optimum ratings of the series FACTS controller (TCSC) used for voltage stability margin and real power flow improvement, it is essential that the Fast Voltage Stability Index (FVSI) of the stressed lines are also minimized with the application of TCSC in these lines. Minimization of FVSI ensures the system voltage stable. The Teaching Learning Based Optimization (TLBO) Method is used to optimize the design parameter of the series FACTS controller, TCSC applied to the weakest lines, for simultaneous minimization of the total Real Power Loss of the system and the sum of FVSI value of the compensated lines. Comparison of the performance of Multi-Objective TLBO is made with that of Genetic Algorithm (GA) applied to the same test systems.

5.3 The Teaching Learning Based Optimization (TLBO) Method

The Teaching Learning Based Optimization (TLBO) algorithm is a global optimization method originally developed by R.V. Rao, et al. [98] in 2011. All evolutionary and population-based optimization algorithms require common control parameters (population size, number of generations, elite size etc.) and some algorithm –specific parameters. Genetic Algorithm (GA) uses mutation and crossover probabilities [44], Artificial Bee Colony (ABC) requires number of bees and limit, Particle Swarm Optimization (PSO) uses the inertia of the swarm, weight

and social cognitive parameters [102], Firefly Algorithm uses the flashing characteristics of real fireflies [44, 45] etc. Hence, proper tuning of these algorithmic-specific parameters is essential as it has a great influence on the performance of these algorithms; else it may result in greater computational effort and time. The advantage of TLBO method is that there are no algorithm-specific parameters and therefore, requires less computational memory, improved convergence time without compromising on the quality of outcome[103]. This algorithm is a simple and robust technique involving fewer computations and high consistency [95]. It is also a population-based method and uses a population of solutions to achieve a global solution [103]. The major application of these method is found in different fields of engineering this algorithm is well-established in the field of optimization and is extremely useful for both single-objective as well as multi-objective optimization problems [104, 105,106].

5.3.1 The Teaching Learning Based Optimization (TLBO)

Algorithm

The TLBO algorithm is a population based method. This algorithm is inspired by teaching-learning process. The two modes of learning used here are:

- (i) Knowledge acquired from teacher (*known as the teacher phase*)
- (ii) Knowledge exchange among learners (*known as the learner phase*)

A group of learners is considered here as the population; the different subjects offered to the learners are the different design variables, and a learner's result is considered as the 'fitness value' of the problem [103, 104].

Initialization:

For any iteration i ,

m : number of subjects (design variables)

n : number of learners (i.e., population size, $k=1, 2, \dots, n$)

$M_{j,i}$: mean result of the learners in a particular subject ($j=1, 2, \dots, m$)

Teacher Phase:

This is the first part of the algorithm. Here the learners receive knowledge through the teacher and improve their knowledge, which in turn, improves the mean result of the class.

The difference between the mean result of the learners for any subject and the corresponding result of the teacher for the same subject is given by:

$$Diff_mean_{j,k,i} = r_i \cdot (X_{j,kbest,i} - T_f M_{j,i}) \quad (5.1)$$

$$X'_{j,k,i} = X_{j,k,i} + Diff_mean_{j,k,i} \quad (5.2)$$

Where,

$X_{j,k,i}$: result of k^{th} learner in the j^{th} subject for the i^{th} iteration

$X_{j,kbest,i}$: result of the best learner in subject j

T_f : Teaching factor, value of T_f can be either 1 or 2

r_i : random number selected between 0 and 1

$X'_{j,k,i}$: updated value of $X_{j,k,i}$

This updated value is accepted if it gives an improved function value.

All the accepted function values at the end of the Teacher phase are used as the input to the learner phase.

Learner Phase:

In this phase the interaction of learners with one another takes place. The random interactions among learners improve their knowledge. Random selection of two learners, A and B are made such that $X'_{total-A,i} \neq X'_{total-B,i}$ (where $X'_{total-A,i}$ and $X'_{total-B,i}$ are the updated function values of $X_{total-A,i}$ and $X_{total-B,i}$ of A and B at the end of the Teacher phase).

For minimization problems,

$$X''_{j,A,i} = X'_{j,A,i} + r_i(X'_{j,A,i} - X'_{j,B,i}) \quad (5.3)$$

$$\text{if } X'_{total-A,i} < X'_{total-B,i}$$

$$X''_{j,A,i} = X'_{j,A,i} + r_i(X'_{j,B,i} - X'_{j,A,i}) \quad (5.4)$$

$$\text{if } X'_{total-B,i} < X'_{total-A,i}$$

Where, r_i : random number selected between 0 and 1.

Algorithm-specific control parameters are not required in the TLBO method; only the common control parameters such as population size and the number of generations are sufficient to yield satisfactory results. The flowchart of the TLBO algorithm is shown in Appendix B (*Fig B.2*).

5.3.2 Multi-objective TLBO problem formulation

Here, multi-objective TLBO technique is applied for simultaneous minimization of Total Real Power Loss and Total FVSI of the weak lines selected for compensation. The critical lines are identified by computing the Fast Voltage Stability Index (FVSI) of each line in the system under study (*as discussed in Section 4.3*). Series FACTS compensator, TCSC is applied to the two weakest lines (*as discussed in section 4.4.1*). The design parameter gamma (γ_{TCSC}) of TCSC is optimized by multi-objective TLBO for simultaneous minimization of Real Power Loss and FVSI. Minimization of real power loss improves the line flows and enhances power transfer capability of the system. Minimization of FVSI improves the bus voltage magnitudes and voltage stability of the system, and prevents line outage and system collapse under stressed conditions.

(i) Multi-objective TLBO problem formulation:

The objective function is:

$$\text{Min } F = w \cdot \sum_{k=1}^{nL} P_{Lk} + (1-w) \cdot \sum_{l=1}^{SL} FVSI_l \quad (5.5)$$

Where,

F : objective function

P_{Lk} : Real power loss of line k

nL : no. of lines

SL : stressed lines where TCSCs are connected

$FVSI_l$: FVSI value of line l

$w, (1-w)$: weight adjustments for P_{Lk} and $FVSI_l$

Constraints:

The minimization problem is subject to the following equality and inequality constraints:

(i) Equality constraints:

The equality constraints represent the load flow equations, as given below for the i^{th} bus:

$$P_{Gi} - P_{Di} = \sum_{j=1}^{nB} V_i V_j Y_{ij} \cos(\theta_{ij} + \delta_i - \delta_j) = 0 \quad (5.6)$$

$$Q_{Gi} - Q_{Di} = \sum_{j=1}^{nB} V_i V_j Y_{ij} \sin(\theta_{ij} + \delta_i - \delta_j) = 0 \quad (5.7)$$

Where,

P_{Gi}, Q_{Gi} : active and reactive powers of the i^{th} generator

P_{Di}, Q_{Di} : active and reactive powers of the i^{th} load bus

θ_{ij} : Power angle

nB : no. of buses

nG : no. of generators

(ii) Inequality constraints:

$$P_{Gi}^{\min} \leq P_{Gi} \leq P_{Gi}^{\max}, \quad i \in nG$$

$$Q_{Gi}^{\min} \leq Q_{Gi} \leq Q_{Gi}^{\max}, \quad i \in nG$$

$$V_i^{\min} \leq V_i \leq V_i^{\max}, \quad i \in nB$$

$$\theta_{ij}^{\min} \leq \theta_{ij} \leq \theta_{ij}^{\max}, \quad i \in nB$$

$$\gamma_{\text{TCSC}}^{\min} \leq \gamma_{\text{TCSC}} \leq \gamma_{\text{TCSC}}^{\max}$$

(ii) TCSC modeling:

Among all important FACTS controllers, SVC (Static VAR Compensator) and TCSC are most suitable for voltage control [94]. With application of TCSC, the transmission line impedance can be modulated rapidly and continuously, and hence TCSC has gained importance above other series FACTS controllers in voltage stability studies. It consists of a capacitor (C) inserted directly into the transmission line and the TCR are mounted in parallel with the capacitor [73].

The TCSC modeling is done as described in section 4.4.1. Variable reactance method is adopted for this study.

The TCSC is connected in series with the line as a compensator for the inductive/capacitive deficit of the transmission line. The reactance of the TCSC is a function of the compensation ratio and the reactance of the transmission line where it is located [70]. The model of TCSC is shown in Fig. 4.2

In the variable reactance method the TCSC is modeled as [70, 95, 96]:

$$X_{ij} = X_{\text{line}} + X_{\text{TCSC}} \quad (5.8)$$

$$X_{\text{TCSC}} = \gamma_{\text{TCSC}} \cdot X_{\text{line}} \quad (5.9)$$

The level of applied compensation of the TCSC varies between 20% inductive reactance and 80% capacitive reactance [34].

(iii) Proposed approach of Multi-objective TLBO:

The proposed approach to the multi-objective TLBO technique performed in this chapter, for parameter optimization of TCSCs is represented by the flowchart shown in Appendix B (*Fig B.3*).

5.4 Chapter 5: Objectives

In this chapter, Voltage Stability analysis using a new evolutionary method discussed in this chapter is explored. The Teaching Learning Based Optimization (TLBO) is carried out on standard IEEE test systems. Fast Voltage Stability Index (FVSI) is used to identify the critical lines to be selected for series FACTS compensation. The objective of this chapter is to optimize the ratings of TCSCs added to the critical lines, for simultaneous minimization of the system real power loss and sum of FVSI of the critical lines. A comparison is made between the performances of the Multi-Objective TLBO and Genetic Algorithm.

5.5 Results and Discussion

Multi-objective Teaching Learning Based Optimization (TLBO) is performed on three IEEE standard test systems (IEEE 14, 30 and 57 bus systems) to compute the design parameter γ_{TCSC} of the TCSCs applied to the weakest lines selected for compensation. The value of gamma (γ_{TCSC}) is optimized such that the total real power loss of the system and the sum of FVSI of the compensated lines are minimized simultaneously. The real power flows, bus voltage magnitudes, system losses and total FVSI are then computed with the application of TCSCs of optimized parameter rating. The results are compared with those of the uncompensated system under same loading conditions. Multi-objective optimization using Genetic Algorithm for the same objective function and constraints is performed on the test systems, and a comparison is made between the two evolutionary programming methods.

Voltage variations in lines are due to small or large disturbances, contingencies and most importantly, due to active and reactive power variations at the load end. The OLTC has to operate several times so as to regulate voltage variations throughout the day [110]. It has been found that the FVSI computed has the highest magnitude in the weakest lines and therefore these lines have been selected for series FACTS compensation using TCSC. Some of these lines have OLTC connected to them and the TCSC has been connected to these lines in order to reduce the number of tap changer operations.

5.5.1 Case Study: IEEE 14 bus system

The IEEE 14 bus system consists of 14 buses, 20 lines, 4 generators and 3 transformers. The PV buses are 2, 3, 6 and 8 and the rest are PQ (load) buses.

Newton Raphson load flow analysis is performed on this system under overload conditions. 170% loading (both Real and Reactive) is applied uniformly to all the load buses and FVSI is calculated for these lines. It is seen that line 8 (connecting load buses 4 and 7) and line 9 (connecting load buses 4 and 9) have the highest value of FVSI. So these lines are selected for reactive power compensation. Series FACTs controllers, TCSCs of random capacity are installed on the selected weak lines 8 and 9. Multi-objective TLBO is performed within the constraints mentioned in Section 5.3, to optimize the design parameter γ of the TCSC, for simultaneous minimization of total real power loss of the system and Sum FVSI of the compensated lines under overload conditions. The tests are carried out with different weights and it is found that the optimum value of γ_{TCSC} is -0.76884154. NR load

flow is again performed on the test system for the same loading condition, with the optimized rating of TCSCs applied to lines 8 and 9, to obtain the voltage values, power flows and line losses.

Table 5.1: Voltage magnitudes of the connected buses (IEEE 14 bus system)

Line No.	Bus No.	Voltage (p.u)	
		Without TCSC	With TCSC in weak lines ($\gamma_{TCSC} = -0.76884154$)
8 (4-7)	4	0.8965	0.9138
	7	0.8942	0.9369
9 (4-9)	9	0.8596	0.9181

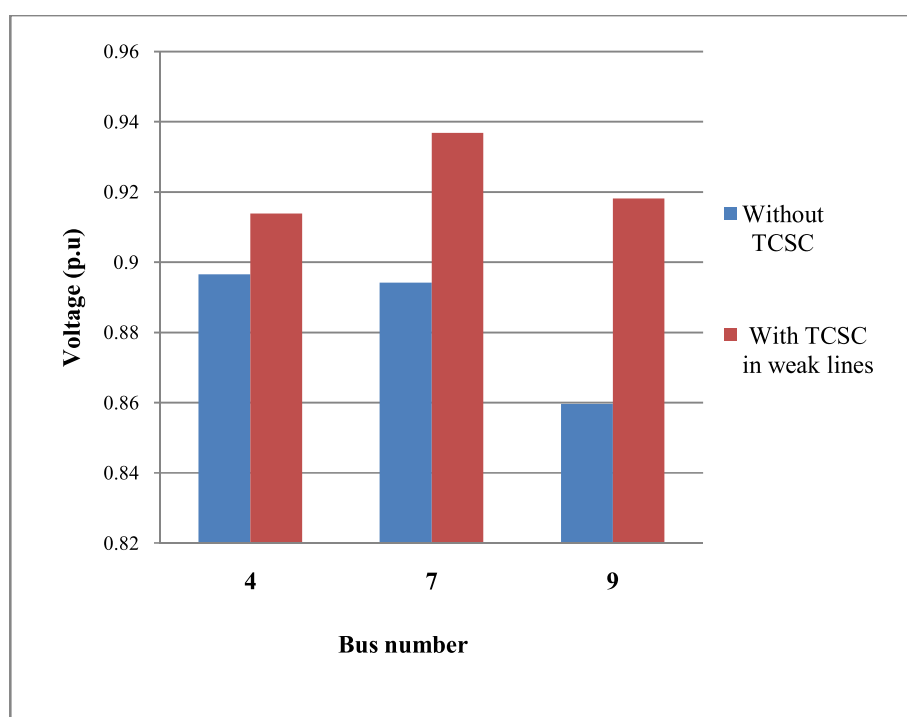


Fig 5.1: Voltage profile of the connected buses (IEEE 14 bus system)

Table 5.2: Result of Multi-Objective TLBO (IEEE 14 bus system)

Results (p.u.) (<i>Multi objective TLBO</i>)	Without TCSC	With TCSC in weak lines ($\gamma_{TCSC} = -0.76884154$)
Total Real power loss	0.52584	0.50929
Sum FVSI	1.1769	0.4046

Table 5.1 and Fig 5.1 represent the voltage magnitudes and voltage profile of the buses connecting the compensated lines, under overload conditions, before and after application of TCSCs. The results indicate voltage improvement in the buses with the optimum application of TCSCs.

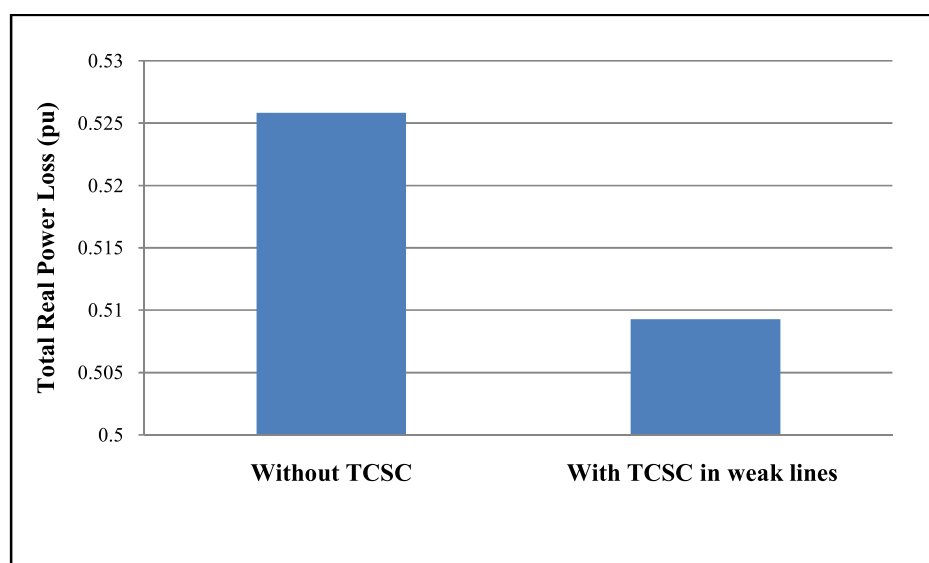
**Fig 5.2: Total Real Power Loss profile (IEEE 14 bus system)**

Table 5.2 represent the results of the Multi-objective TLBO analysis applied to the IEEE 14 bus test system. Real power loss of the system is minimized and Total FVSI value of the critical lines are also reduced simultaneously, indicating that the

voltage stability of the system has improved and the maximum loading limit enhanced, with optimum ratings of TCSC.

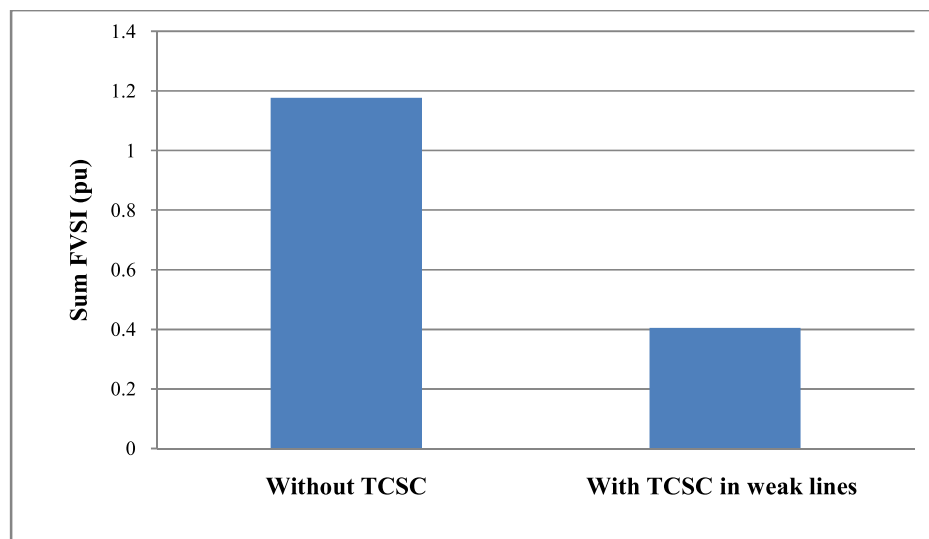


Fig 5.3: Sum FVSI profile of compensated lines (IEEE 14 bus system)

Fig 5.2 and Fig. 5.3 are representation of the objectives of this chapter, achieved through Multi-objective TLBO.

Table 5.3: Reactive Power Losses (IEEE 14 bus system)

Line No.	Reactive Power Loss (MVAR)	
	Without TCSC	With TCSC in weak lines
8	5.627	1.993
9	5.238	3.503
Total	212.289	192.658

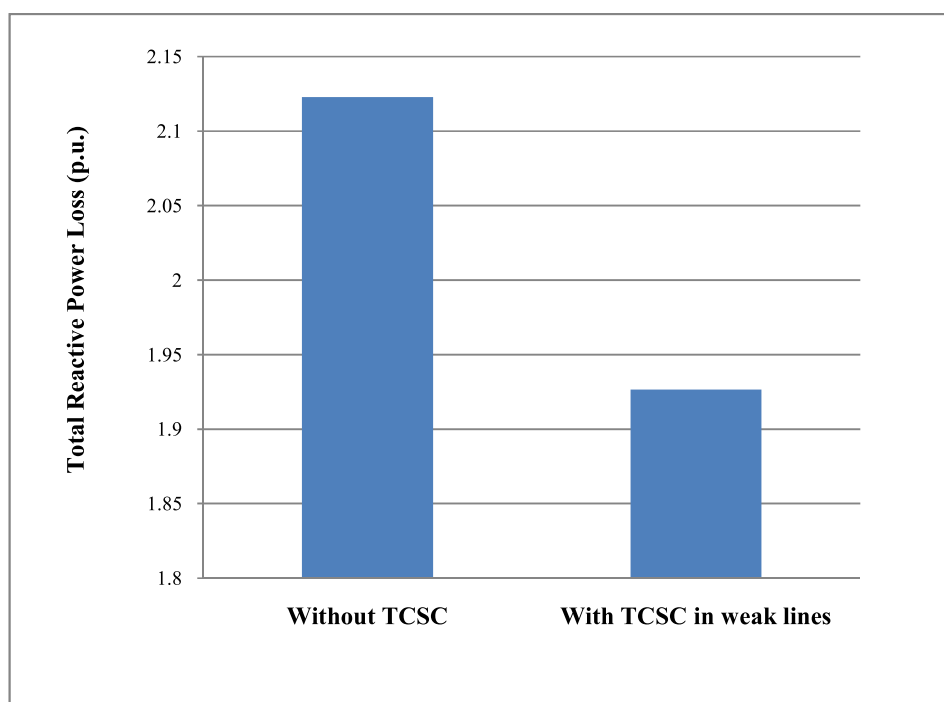


Fig 5.4: Total Reactive Power Loss profile (IEEE 14 bus system)

It is observed from Table 5.3 and Fig 5.4, that the reactive power losses of the compensated lines and the total reactive power loss of the system are also minimized in the process.

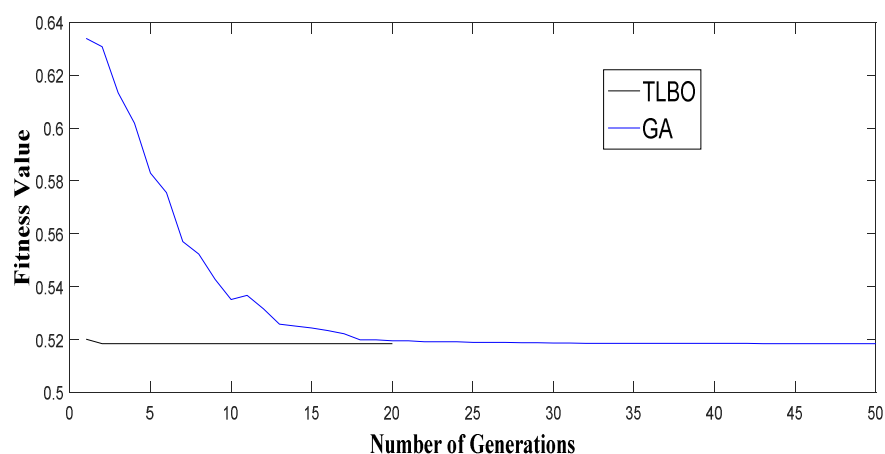


Fig 5.5: Convergence characteristics of Multi-objective TLBO & GA for IEEE 14 bus system

The convergence characteristics of Multi-objective TLBO method applied to the IEEE 14 bus system are shown in Fig. 5.5. The same optimization is performed using Genetic algorithm (GA). It is observed that TLBO technique requires less number of iterations (=02) as compared to GA, which requires 42 iterations. This indicates that the Multi-objective TLBO technique is simple and robust and require less computation time, without compromising on the quality of the results.

5.5.2 Case Study:IEEE 30 bus system

The same test data is used here as in the previous chapters. For IEEE 30 bus system, FVSI computation under overload conditions (150%, both Real and Reactive) yield that line 12 (connecting PQ buses 6 and 10), line 15 (connecting PQ buses 4 and 12) and line 36 (connecting PQ buses 28 and 27) are the most critical lines, having highest values of FVSI among load buses. Therefore these lines are selected for optimum TCSC compensation. Multi-objective TLBO analysis is performed on this system with application of TCSCs in lines 12, 15, and 36, for the same objective function as discussed in Section 5.4.1.

It is found that at 150% loading γ_{TCSC} value is optimized at -0.76892845 for simultaneous minimization of total real power loss and Sum FVSI of the compensated lines. NR load flow is performed to compute the voltage magnitudes, power flows and line losses, and the results are compared with those of the uncompensated system.

Table 5.4: Voltage magnitudes of the connected buses (IEEE 30 bus system)

Line No.	Bus No.	Voltage (p.u)	
		Without TCSC	With TCSC in weak lines ($\gamma_{TCSC} = -0.76892845$)
12	6	0.967	0.9834
	10	0.9753	1.0087
15	4	0.9692	0.9802
	12	1.0003	1.0439
36	28	0.9636	0.9807
	27	0.9548	1.0039

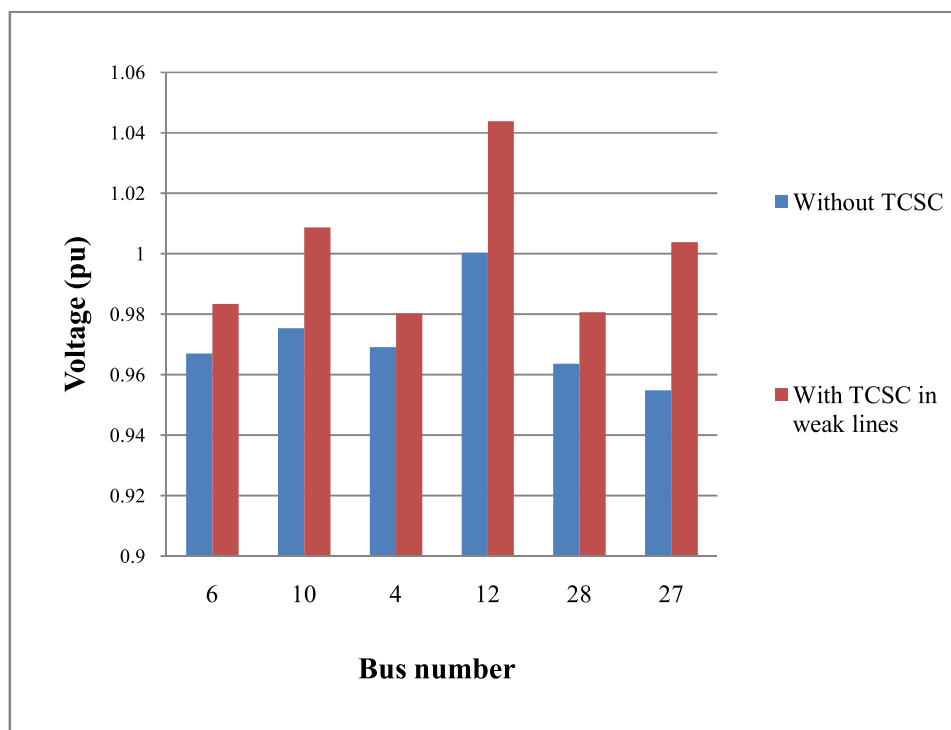
**Fig 5.6: Voltage profile of the connected buses (IEEE 30 bus system)**

Table 5.4 and Fig 5.6 represent the voltage magnitude and profile of the connected buses of the critical lines, under overload conditions, without and with application of optimized ratings of TCSC. An improvement in voltage magnitude and profile is observed when TCSC of optimized ratings have been applied to the stressed lines.

Table 5.5: Result of Multi-Objective TLBO (IEEE 30 bus system)

Result (pu) (Multi objective TLBO)	Without TCSC	With TCSC in weak lines ($\gamma_{TCSC} = -0.76892845$)
Total Real power loss	0.46203	0.45468
Sum FVSI (lines 12, 15 & 36)	1.7251	0.7018

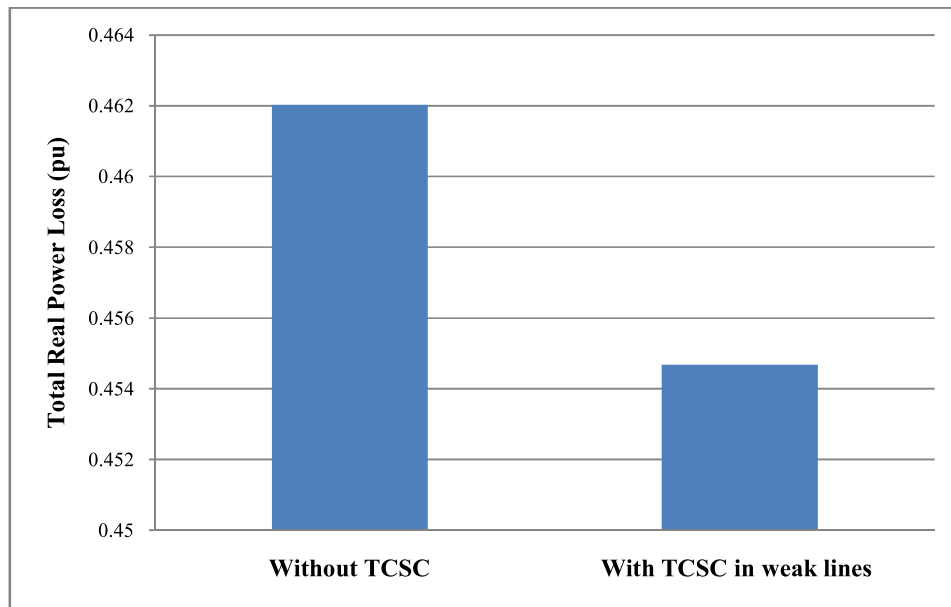


Fig 5.7: Total Real Power Loss profile (IEEE 30 bus system)

Table 5.5 represent the results of the Multi-objective TLBO technique applied to the system under test. The simultaneous objectives of real power loss minimization and Sum FVSI reduction is achieved in this case study.

The system active power loss reduces from 0.46203 p.u., for the uncompensated system, to 0.45468 p.u. when optimum ratings of TCSC are applied to the most critical lines, as seen in Fig 5.7.

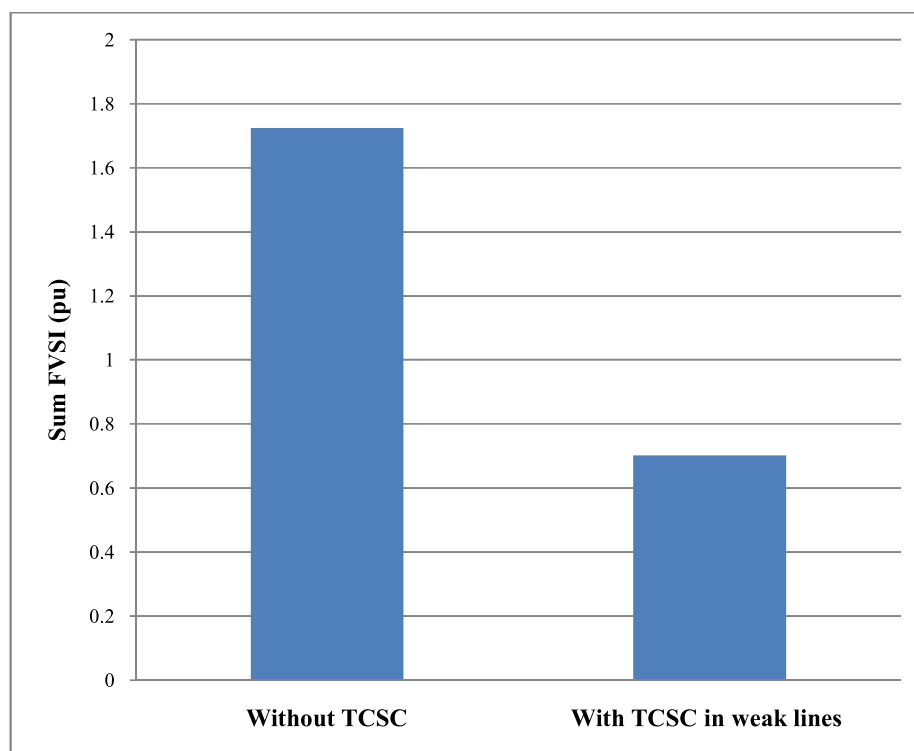


Fig 5.8: Sum FVSI profile of compensated lines (IEEE 30 bus system)

The sum of FVSI values of the weak lines are reduced from 1.7251 p.u. to 0.7018 p.u. with the same compensation, as observed in Fig 5.8. This indicates that the voltage stability of the system under overload conditions have been enhanced with optimum application of the series FACTS controller TCSC.

Table 5.6: Reactive Power Losses (IEEE 30 bus system)

Line No.	Reactive Power Loss (MVar)	
	Without TCSC	With TCSC in weak lines
12	3.247	2.141
15	11.596	10.961
36	3.189	1.311
System	176.893	165.270

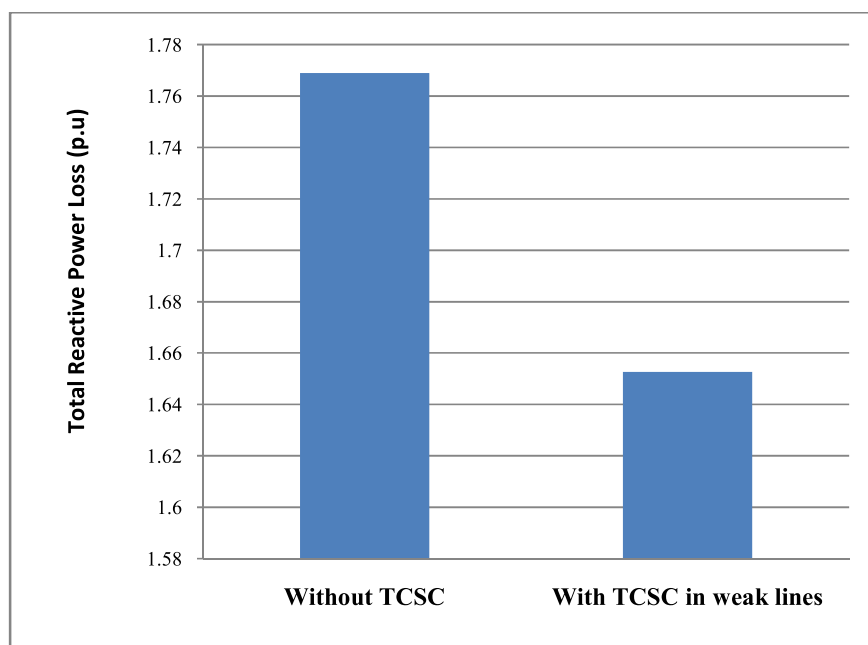
**Fig 5.9: Total Reactive Power Loss profile (IEEE 30 bus system)**

Table 5.6 and Fig 5.9 represent the reactive power losses of these lines and of the system; and these are also observed to have minimized. Therefore, it can be concluded that voltage stability enhancement has been achieved under stressed conditions.

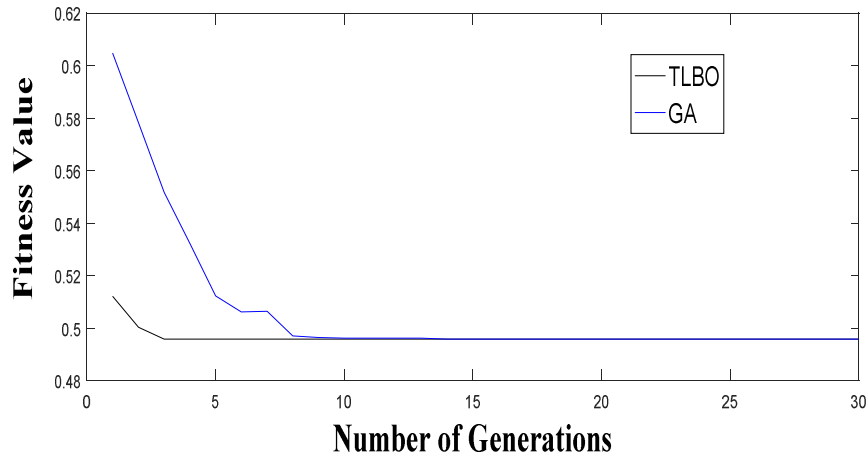


Fig 5.10: Convergence characteristic of Multi-Objective TLBO & GA for IEEE 30 bus system

The convergence characteristics of Multi-objective TLBO method applied to the IEEE 30 bus system is shown in Fig. 5.10. When the same optimization problem is executed using GA, the number of iterations required are 13, compared to Multi-objective TLBO (which requires 3 iterations), indicating the superiority of TLBO technique over GA.

5.5.3 Case Study: IEEE 57 bus system

Fast Voltage Stability Index (FVSI) is calculated for the load lines of IEEE 57 bus system under overload conditions (120% loading, both Real and Reactive). Line 35 (connecting buses 24 and 25) and line 46 (connecting buses 32 and 34) are found to have the maximum value of FVSI both under normal and overload conditions, as discussed in Section 4.4.3. Therefore, lines 35 and 46 are selected for series FACTS compensation (TCSC).

Multi-objective TLBO technique is then applied to this test system for parameter optimization for the same objective function and within the constraints discussed in Section 5.3. The result of Multi-objective optimization yields γ_{TCSC} to have a value

of -0.70682451 for simultaneous minimization of Total real power loss and Sum FVSI of the compensated lines. NR load flow is performed on the test system under the same loading conditions, and with the optimized ratings of TCSCs placed in the critical lines to obtain the bus voltage magnitudes, line flows and line losses.

Table 5.7: Voltage magnitudes of the connected buses (IEEE 57 bus system)

Line No.	Bus No.	Voltage (p.u)	
		Without TCSC	With TCSC in weak lines ($\gamma_{TCSC} = -0.70682451$)
35	24	0.953	0.9586
	25	0.8902	0.9334
46	34	0.9085	0.9130
	32	0.8726	0.9212

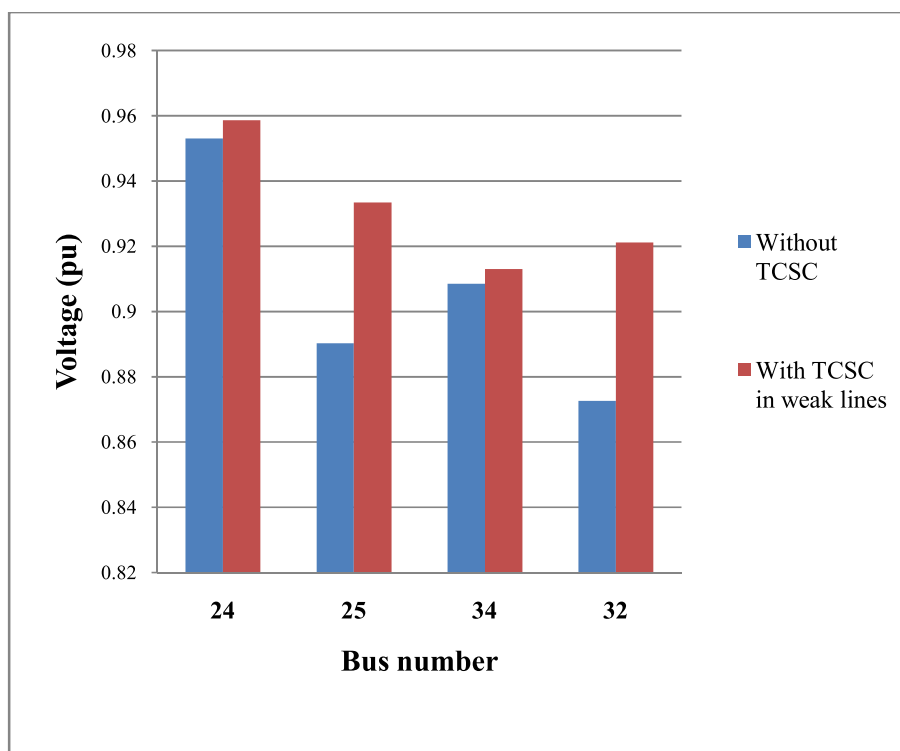


Fig 5.11: Voltage profile of the connected buses (IEEE 57 bus system)

Table 5.7 and Fig 5.11 represent the voltage magnitude and profile of the connected buses of the critical lines, before and after application of optimized series FACTS compensation using TCSC. The bus voltage magnitudes show improvement indicating that voltage stability is enhanced even under overload conditions.

Table 5.8: Result of Multi-Objective TLBO (IEEE 57 bus system)

Result (pu) (Multi objective TLBO)	Without TCSC	With TCSC in weak lines ($\gamma_{TCSC} = -0.70682451$)
Total Real power loss	0.61093	0.60810
Sum FVSI (Lines 35 & 46)	0.9101	0.3434

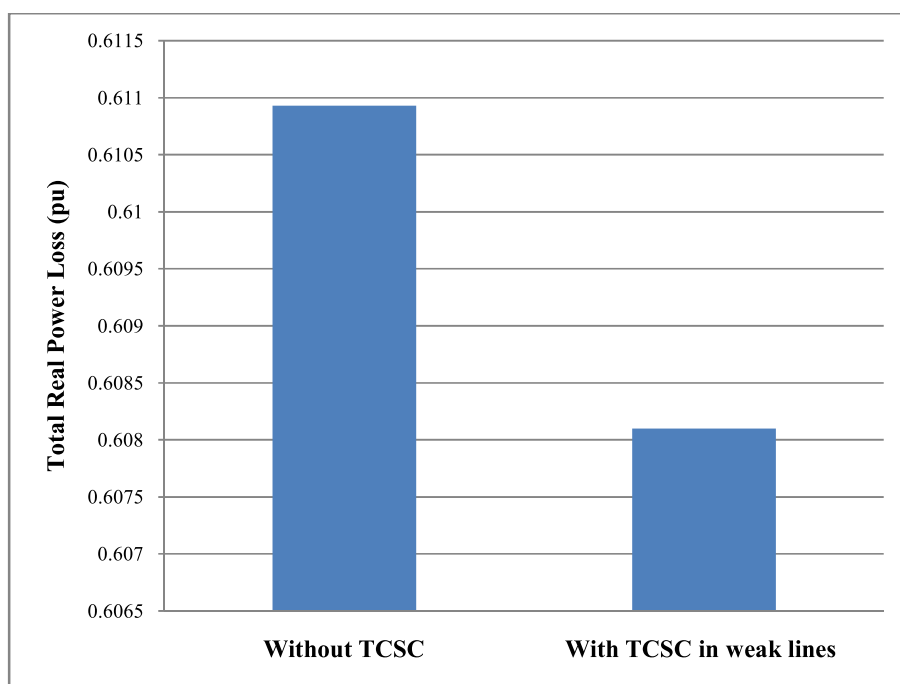


Fig 5.12: Total Real Power Loss profile (IEEE 57 bus system)

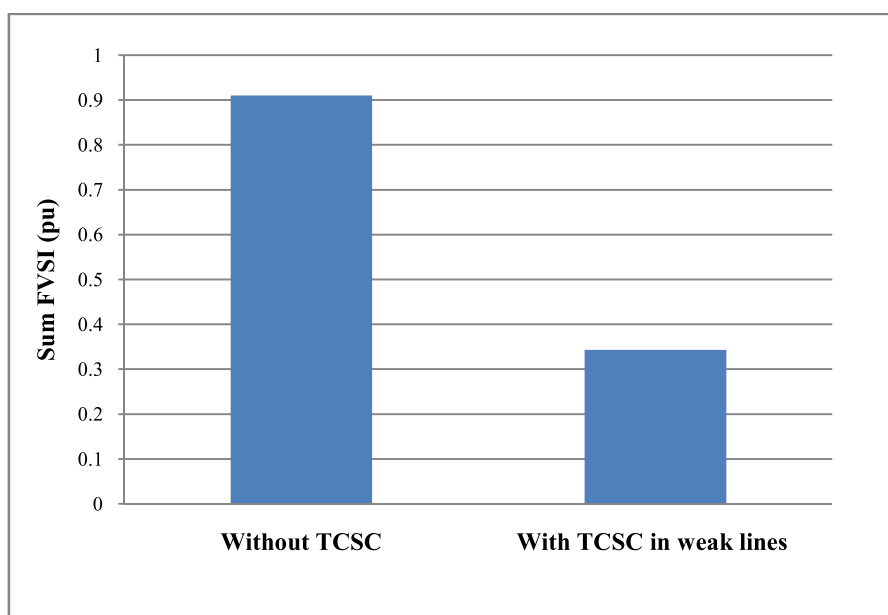


Fig 5.13: Sum FVSI profile of compensated lines (IEEE 57 bus system)

The results of the Multi-objective TLBO are tabled, as shown in Table 5.8. It is observed from Fig 5.12 and Fig 5.13, that total Real power loss and Sum FVSI values of the critical lines have been minimized with the application of optimized ratings of TCSC.

Table 5.9: Reactive Power Losses (IEEE 57 bus system)

Line No.	Reactive Power Loss (MVAR)	
	Without TCSC	With TCSC in weak lines
35	2.479	0.958
46	1.235	0.359
System	281.204	277.015

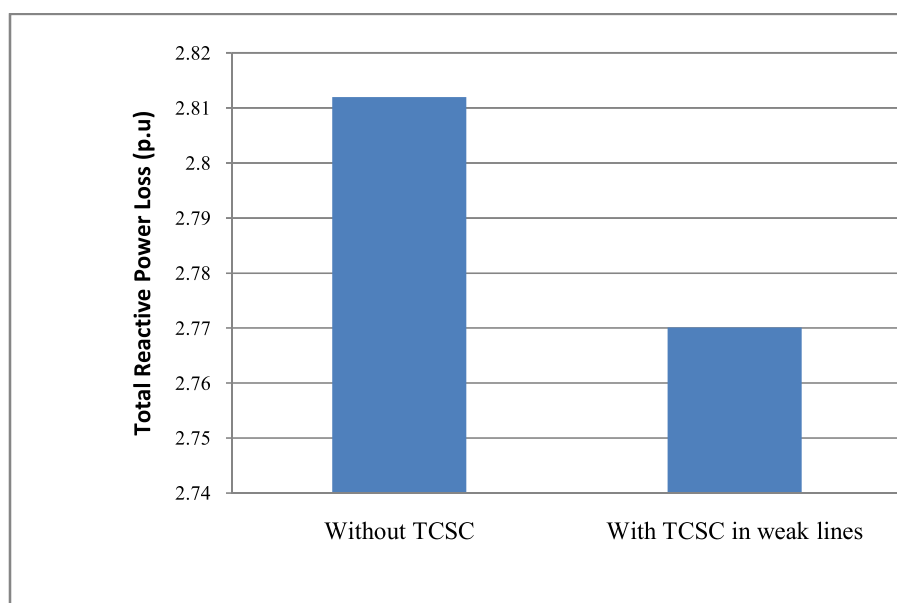


Fig 5.14: Total Reactive Power Loss profile (IEEE 57 bus system)

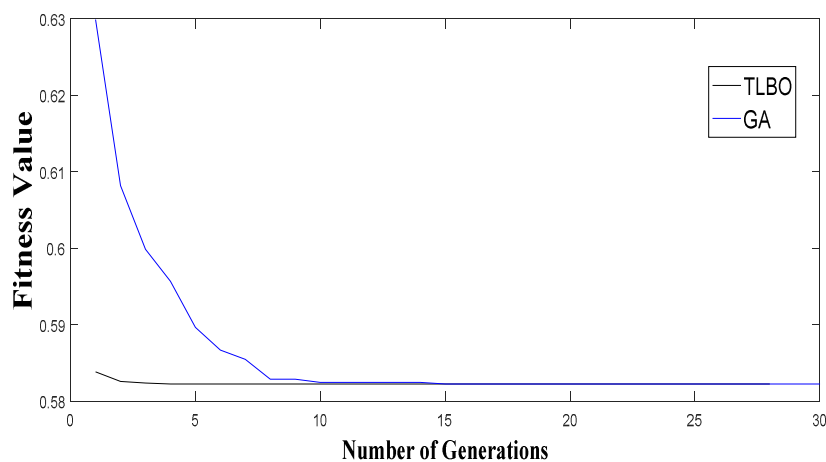


Fig 5.15: Convergence characteristic of Multi-Objective TLBO & GA (IEEE 57 bus system)

The total Reactive power losses of the system and of the critical lines are also reduced, as shown in Table 5.8 and Fig 5.14.

The convergence characteristics of Multi-objective TLBO method applied to the IEEE 57 bus system is shown in Fig. 5.15. As in the other cases, Multi-Objective

GA method is applied to the system with the same objective function and constraints. It is observed that multi-objective GA method requires more number of iterations (= 14) than Multi-objective TLBO (= 04) for the same exercise. This confirms the superiority of TLBO method over GA method of optimization.

Table 5.10: Reactive Compensation provided by TCSC

System	Line No.	X_{TCSC} (pu)
IEEE 14	8	0.04834
	9	0.12857
IEEE 30	12	0.12848
	15	0.059155
	36	0.091504
IEEE 57	35	0.346534
	46	0.27940

Table 5.10 represents the additional reactive compensation provided by the series FACTS device TCSC on the critical lines. Performance improvement is achieved through this compensating technique.

5.6 Conclusion

Voltage stability improvement of transmission lines under stress include enhancement of voltage stability margin together with minimization of transmission loss. The optimal location and rating of TCSCs play a vital role in achieving these

objectives. Therefore, voltage stability analysis using Evolutionary Programming methods are often used for this purpose. In this chapter, Multi-objective Teaching Learning Based Optimization (TLBO) Algorithm is used in determining the optimum ratings of the TCSCs to be applied to the critical lines, so that the system real power loss and the sum of FVSI of the critical lines are minimized simultaneously, under overload conditions.

The objectives of this evolutionary, population-based optimization method have been successfully achieved when applied to the three test systems selected for this work. The results have followed the same pattern in all the cases. Total real power losses of the systems and the sums of FVSI of the critical lines have been minimized simultaneously with application of the optimized ratings of TCSCs. In addition, the voltage magnitudes of the connected buses of the compensated lines have improved. The total reactive power loss of the system and those of the compensated lines have also reduced in the process.

In any evolutionary algorithm, the convergence rate is accorded the utmost importance without compromising on the quality of objectives. Therefore, a comparison is made between the Multi-objective TLBO method and Genetic Algorithm (GA) method for the same problem. The Multi-objective TLBO performed in this chapter is able to achieve its objectives at minimum convergence time as compared to GA for all the cases under study. This work also highlights the simplicity of Multi-objective TLBO method and its effectiveness while applying it to Voltage Stability Studies.

Chapter 6

Conclusion

(Summary of Work and Scope for Future Study)

6.1 Summary of Work

The importance of voltage stability analysis in power system planning and research has been highlighted in this work. The voltage stability problem has been analysed in different stages viz. Weak Bus Identification, Bus Voltage Stability Analysis and Line Voltage Stability Analysis. Voltage stability analysis using FACTS compensation has also been performed here. Besides the conventional methods, the voltage stability problem has been addressed using a new evolutionary programming technique. The conclusions drawn from the chapters are as summarized below:

- Chapter 2 is devoted to Weak Bus Identification. The voltage stability problem has been defined and discussed here. Conventional methods of voltage stability analysis have been studied. Two standard test systems, IEEE 30 and 57 bus systems have been identified for analysis. The weak bus identification process has been performed using Modal Analysis and the

results compared with Continuation Power Flow (CPF) Analysis. The Eigen values have been plotted, yielding the status of each system, with respect to voltage stability. The effectiveness of the conventional methods for weak bus identification has been successfully established in this chapter.

- In chapter 3, Bus Voltage Stability Analysis has been performed on standard IEEE 30 and 57 bus systems. Reactive power compensation and its importance in voltage stability studies are highlighted here. The critical buses approaching voltage collapse are selected for reactive power compensation using shunt FACTS controllers, SVC and STATCOM. The behaviour of the systems under different types of compensation has been observed. P-V curves for different types of compensation have been traced, yielding the maximum loading limit for different types of compensation.

From the above exercise, it has been found that reactive power compensation using FACTS devices play an important role in Bus Voltage Stability Analysis of a power system; and is the most appropriate mechanism for enhancement of bus voltage magnitudes and improvement of maximum loading margin of the critical bus.

- Chapter 4 has been dedicated to Line Voltage Stability Analysis. As the number of transmission lines are more in number than the number of buses, line outages are more frequent and common than bus voltage collapses. Therefore, line voltage stability is of utmost importance for the proper and stable performance of a power system network. Line Voltage Stability

analysis performed in this chapter have been divided into two parts: identification of critical lines and enhancing real power flows and voltage stability limit of these lines by applying series FACTS compensators, TCSC and SSSC to them. The tests have been carried out on IEEE 30 and 57 bus systems. A very widely used Line voltage stability indicator, the Fast Voltage Stability Index (FVSI), has been used here for identification of the most critical lines. These critical lines have been selected for series FACTS compensation using TCSC and SSSC of random compensation. Improvement in real power flows through the critical lines with application of TCSC and SSSC have been achieved; in addition to minimization of system losses and enhancement of line voltage stability with improvement in FVSI values of the critical lines. The objectives of the chapter; i.e. to demonstrate the importance of Line Voltage Stability analysis in power systems, have been achieved.

- In Chapter 5, the Evolutionary programming method for Voltage Stability analysis has been explored for parameter optimization of FACTS devices. A new, population-based optimization technique, the Teaching Learning Based Optimization (TLBO) method is adopted here for the purpose. Fast Voltage Stability Index (FVSI) has been used to identify the most critical lines and series FACTS compensation using optimal ratings of TCSC are applied to these lines. The Multi-Objective TLBO technique has been used for simultaneous minimization of system Real power loss and Sum FVSI of the critical lines, without and with compensation using TCSC. The tests have

been performed on standard IEEE 14, 30 and 57 bus systems. The percentage compensation for TCSC has been optimized for the multi-objective problem under overload conditions and the performances of the different test systems have been observed. The objectives of the Multi-Objective TLBO problem have been demonstrated with success, ensuring line voltage stability enhancement in each case. The same optimization problem has been executed using Genetic Algorithm and the superiority of the TLBO technique has also been established.

6.2 Scope for future study

This work has demonstrated the effectiveness of Static Voltage Stability Analysis of power system networks. Dynamic voltage stability analysis on the test systems considered here, can be performed for contingencies on the given lines and buses. A comparison can be made with the application of series-shunt FACTS compensator, Unified Power Flow Controller (UPFC).

Furthermore, considering the evolutionary programming part, the improvement of one objective may result in deterioration of another. Therefore, pareto optimal solutions for the same objective function, discussed in Chapter 5 can be explored using Multi-Objective TLBO method. In addition to parameter optimization for TCSC, optimum location of the FACTS devices can be included as another objective for the problem discussed in this work.

References

- [1] **H.G. Kwatny, A.K. Pasrija, Leon Y. Bahar**, “*Static Bifurcations In Electric Power Networks: Loss Of Steady-State Stability And Voltage Collapse*”, IEEE Transactions on Circuits and Systems, Vol. CAS-33, No. 10, October 1986
- [2] **I. Dobson and H.D. Chiang**, “*Towards A Theory Of Voltage Collapse In Electric Power Systems*”, School of Electrical Engineering, Cornell University U.S.A, 26 April 1989
- [3] **H.D. Chiang, Ian Dobson, Robert J. 'Ilio~nas, J.S. Thorp and L. F.-Ahmed**, “*On Voltage Collapse In Electric Power Systems*”, IEEE Transactions on Power Systems, Vol. 5, No. 2, May 1990
- [4] **Ian Dobson**, “*Observations on the Geometry of Saddle Node Bifurcation and Voltage Collapse in Electrical Power Systems*”, IEEE Transactions on circuits and systems -I: Fundamentals theory and applications, Vol. 39, No. 3, March 1992
- [5] **Ian Dobson**, “*The Irrelevance Of Load Dynamics For The Loading Margin To Voltage Collapse And Its Sensitive*”, Bulk Power System Voltage Phenomena III: Voltage Stability, Security & Control, Davos, Switzerland, August 1994
- [6] **V. Ajjarapu**, “*A Study of Dynamic Aspects Related to Voltage Collapse in Power Systems*”, presented at 28th Conference on Decision and Control, Tampa, Florida, 1989
- [7] **B. Gao, G.K. Morison, and P. Kundur**, “*Voltage Stability Evaluation Using Modal Analysis*”, IEEE Transactions on Power Systems, Vol. 7, No. 4, November 1992, pp. 1529–1542.
- [8] **V. Ajjarapu and C. Christy**, “*The Continuation Power Flow: A Tool For Steady State Voltage Stability Analysis*”, IEEE Transactions on Power Systems, Vol. 7, no. 1, pp. 416–423, Feb. 1992.

- [9] **G. K. Morison, B. Gao and P. Kundur**, "*Voltage Stability Analysis Using Static And Dynamic Approaches*", IEEE Transactions on Power Systems, Vol. 8, No. 3, August 1993, pp. 1159–1171.
- [10] **B. Ha Lee and K. Y. Lee**. "*Dynamic And Static Voltage Stability Enhancement Of Power Systems*", IEEE Transactions on Power Systems, Vol. 8, No. 1, February 1993
- [11] **C. Canizares**, "*On Bifurcations, Voltage Collapse And Load Modelling*", IEEE Transactions in Power Systems, Vol. 10, pp. 512-522, 1995.
- [12] **C. Canizares, A. C. Z. de Souza, and V. H. Quintana**, "*Comparison of Performance Indices for Detection of Proximity to Voltage Collapse*", IEEE Transactions on Power Systems, Vol. 11, No.3, August 1996
- [13] **P. Kundur, J. Paserba, V. Ajjarapu, G. Andersson, A. Bose, C. Canizares, N. Hatziaargyriou, D. Hill, A. Stankovic, C. Taylor, T. van Cutsem, and V. Vittal**, "*Definition And Classification Of Power System Stability Ieee/Cigre Joint Task Force On Stability Terms And Definitions*," IEEE Transactions on Power Systems, Vol. 19, no. 2, pp. 1387 – 1401, August 2004.
- [14] **P. Kessel, H. Glavitsch**, "*Estimating The Voltage Stability Of A Power System*", IEEE Transactions on Power Delivery, Vol. PWRD-1, No. 3, July 1986
- [15] **G.B. Jasmon , F. L. H Callistus, C .Lee**, "*Prediction Of Voltage Collapse In Power Systems Using A Reduced System Model*", University of Malaya, Malaysia.
- [16] **M.Moghavvemi, O.Faruque**, "*Real-Time Contingency Evaluation And Ranking Technque*", IEE Proc.-Gener. Transm. Distrib..Vol. 145, No. 5. September 1998
- [17] **M. Moghavvemi, F. M. Omar**, "*Technique For Contingency Monitoring And Voltage Collapse Prediction*", IEE Proc.-Gener. Transm. Distrb., Vol. 145, No. 6, November. 1998
- [18] **I. Musirin, T.K. Abdul Rahman**, "*Novel Fast Voltage Stability Index (FVSI) For Voltage Stability Analysis In Power Transmission System*", 2002 Student Conference on Research and Development Proceedings, Shah Alam, Malaysia

- [19] **A.S. Yome and N. Mithulananthan**, "*Comparison Of Shunt Capacitor, SVC And STATCOM In Static Voltage Stability Margin Enhancement*", International Journal of Electrical Engineering Education 41/2
- [20] **A.S. Yome, N. Mithulananthan, Kwang Y. Lee**, "*Static Voltage Stability Margin Enhancement Using STATCOM, TCSC and SSSC*", 2005 IEEE/PES Transmission and Distribution Conference & Exhibition: Asia and Pacific Dalian, China.
- [21] **M. Ndubuka**, "*Voltage Stability Improvement Using Static Var Compensator In Power Systems*", Leonardo Journal of Sciences, Issue 14, January-June 2009, p. 167-172, ISSN 1583-0233
- [22] **N.M. Ndubuka**, "*Effects Of Static Synchronous Compensator (STATCOM) On Voltage Stability And Transmission Losses Of Electrical Power Systems*", International Journal of Electrical and Power Engineering, 5(1): 13-17, 2011, ISSN: 1990-7958
- [23] **M.Kowsalya, K.K.Ray, U. Shipurkar and Saranathan**, "*Voltage Stability Enhancement By Optimal Placement Of UPFC*", Journal of Electrical Engineering & Technology Vol. 4, No. 3, pp. 310~314, 2009.
- [24] **C. Nandi, S. Deb, M.D. Barma, and A.K. Chakraborty**, "*Study And Simulation Of The SVC And STATCOM Effect Of Voltage Collapse And Critical Fault Clearing Time*", International Journal of Modelling and Optimization, Vol.2, No.4, August 2012
- [25] **J.V. Parate, A.S. Sindekar**, "*Reactive Power Control And Transformation Loss Reduction With Realization Of SVC And TCSC*", IJEST, Vol. 4, No 07, July 2012, ISSN-0975-5462
- [26] **J. Sutter, J. Nderu. C. Murali**, "*Placement Of Facts Devices For Voltage Profile Improvement And Loss Reduction*", International Journal of Emerging Technology and Advanced Engineering , www.ijetae.com , ISSN: 2250-2459, Vol 5, Issue 10, October 2015)

- [27] **C. A. Cañizares**, “*Applications Of Optimization To Voltage Collapse Analysis, Panel Session: Optimization Techniques In Voltage Collapse Analysis*”, IEEE/PES Summer Meeting, San Diego, July 14, 1998.
- [28] **L.C. A. Ferreira, A.C. Zambroni de Souza, S. Granville and J.W.M. Lima**, “*Interior Point Method Applied To Voltage Collapse Problems And System -Losses- Reduction*”, IEE Proc.-Gener, Trans, Distrib, Vol. 149, No. 2, March 2002
- [29] **Yongchun Su, S. Cheng, J. Wen, Y. Zhang**, “*Reactive Power Generation Management for the Improvement of Power System Voltage Stability Margin*”, Proceedings of the 6th World Congress on Intelligent Control and Automation, June 21 - 23, 2006, Dalian, China
- [30] **T. O. Ting, K. P. Wong, C. Y. Chung**, “*Locating Type-1 Load Flow Solutions Using Hybrid Evolutionary Algorithm*”, Proceedings of the Fifth International Conference on Machine Learning and Cybernetics, Dalian, 13-16 August 2006, 1-4244-0060-0/06/ IEE 4093
- [31] **L. Zhijian, Yu Jilai, S. Hongchun**, “*Coordination Control Between PSS And SVC Based On Fuzzy-Satisfactory Degree And MOEA*”, 978-1-4244-2487-0/09/2009 IEEE
- [32] **A. H. Khazali, A. Parizad, M. Kalantar**, “*Optimal Reactive/Voltage Control By An Improved Harmony Search Algorithm*”, The Centre of Excellence for Power System Automation and Operation, Iran University of Science and Technology (IUST), Narmak 16846, Tehran, Iran
- [33] **S.C. Satapathy, A. Naik, K. Parvathi**, “*A Teaching Learning Based Optimization Based On Orthogonal Design For Solving Global Optimization Problems*”, Springer Plus 2013, 2:130

- [34] **V.A. Preethi, S. Muralidharan, S. Rajasekar**, “*Application Of Genetic Algorithm To Power System Voltage Stability Enhancement Using Facts Devices*”, International Conference on Recent Advancements in Electrical Electronics and Control Engineering, 2011
- [35] **A. Ozturk, P. Erdogmus, M.A. Yalcum**, “*Investigation of Voltage Stability Limit Values in Electrical Power Systems Using Generic Algorithm*”, www.researchgate.net, 2010
- [36] **S.R. Najafi, M. Abedi, S.H. Hosseinian**, “*A Novel Approach To Optimal Allocation Of SVC Using Genetic Algorithm And Continuation Power Flow*”, First International Power and Energy Conference PEC, 2006
- [37] **J.P. Roselyn, D. Devraj, S.S. Dash**, “*Multi-Objective Genetic Algorithm for Voltage Stability Enhancement using Rescheduling and FACTS Devices*”, Ain Shams Engineering Journal (2014) 5, 789-801
- [38] **B.Bhattacharyya, V.K Gupta, S. Kumar**, “*UPFC with Series and Shunt FACTS Controllers for the Economic Operation of a Power*”, Ain Shams Engineering Journal, www.elsevier.com, 2014
- [39] **T. Nireekshana, G.K. Rao, S.S.N. Raju**, “*Enhancement Of ATC With FACTS Devices Using Real- Code Genetic Algorithm*”, Electrical Power and Energy Systems, 43 (2012), 1276-1284.
- [40] **K.K Ray, M.Kowsalya, D.P Kothari**, “*Voltage Stability Margin Enhancement through Optimal Location of VAR Compensation*”, Journal of Electrical Engineering, 2008, www.je.ro, ISSN: 1582-4594
- [41] **B. Mallaiah, P.R. Reddy**, “*Voltage Stability Enhancement Through Optimization Techniques*”, ITSI Transactions on Electrical and Electronics Engineering (ITSI-TEEE), ISSN: 2320-8945, Vol. 1, Issue 3, 2013

- [42] **P. Acharjee**, “*Identification Of Maximum Loadability Limit And Weak Buses Using Security Constraint Genetic Algorithm*”, *Electrical Power and Energy Systems*, Elsevier, 2011
- [43] **J.J. and K.H. Reddy**, “*Differential Evolution Approach to Optimal Reactive Power Dispatch With Voltage Stability Enhancement By Modal Analysis*”, *International Journal of Engineering Research and Applications (IJERA)*, ISSN: 2248-9622, Vol.3, Issue 4, July – August 2013
- [44] **L. Jebaraj, C.C.A. Ranjan, and K.Sriram**, “*Application Of Firefly In Voltage Stability Environment Incorporating Circuit Element Model Of SSSC With Variable Susceptance Model Of SVC*”, *Hindawi Publishing Corporation Advance in Electrical Engineering*, Vol. 2014, Article ID 349787
- [45] **H. Deenadhayalam**, “*Real Power Minimization Using Firefly Algorithm*”, *IJAICT*, Vol.1, Issue 8, December 2014, ISSN: 2348-9928
- [46] **R. Sirjani, N.T Bolan**, “*An Improved Cuckoo Search Algorithm For Voltage Stability Enhancement In Power Transmission Networks*”, *International Journal of Electrical, Computer, Energetic, Electronic and Communication Engineering*, Vol.10, No.5, 2016
- [47] **M.C, Murithi C.M, Abungu N.O, N.G.N**, “*Amalgamated Optimal Load Shedding Using Cuckoo Search With Levy Flight Algorithm for Frequency And Voltage Stability Improvement*”, *International Journal of Emerging Technology and Advanced Engineering (UETAE)*, www.ijetae.com, ISSN: 2250-2459, Vol.5, Issue 12, December 2015
- [48] **I.N. Trivedi, P.Jangir, and S.A. Parmar**, “*Optimal Power Flow With Enhancement Of Voltage Stability And Reduction Of Power Loss Using Ant-Lion Optimizer*”, *Cogent Engineering*, 2016

- [49] **W. Warid, H. Hizam, N.M., and N.I Abdul-Wahab**, “*Optimal Power Flow Using The Jaya Algorithm*”, *Energies*, www.mdpi.com/journal/energies, 2016
- [50] **P. Kundur**, “*Power System Stability and Control*”, EPRI Power System Engineering Series, McGraw-Hill, 1994.
- [51] **T. van Cutsem and C. Vournas**, “*Voltage Stability of Electric Power Systems*”, Springer, 1998.
- [52] **M.A. Kamarposhti, M. Alinezhad, H.Lesani, Nemat Talebi**, “*Comparison Of SVC, STATCOM, TCSC, And UPFC Controllers For Static Voltage Stability Evaluated By Continuation Power Flow Method*”, IEEE Electrical and Power & Energy Conference, 2008
- [53] **S. Chakrabarti**, “*Notes On Power System Voltage Stability*”, [Online]. Available (Jan. 2011)
https://www.researchgate.net/publication/260661284_Notes_on_power_system_Voltage_stability
- [54] **D. Bica**, “*Steady –State Analysis Of Voltage Stability By Reactive Participation Factor*”, *The 6th Edition Of The Interdisciplinary International Conference “Petru Major”* University of Tirgu Mures, Romania, 2012
- [55] **U. P. Anand , P. DharmameshKumar**, “ *Voltage Stability Assessment Using Continuation Power Flow*”, *International Journal of Advanced Research in Electrical , Electronics and Instrumentation Engineering*, ISSN: 2320-3765, Vol.3, Issue 8, August 2013
- [56] **P. Duraipandy, D. Devraj**, “*Power System Loading Margin Enhancement Using Shunt Facts Controllers*”, *Ird India (IAEEEE)*, ISSN: 2278-8948, Vol.3, Issue 3, 2014

- [57] **B. Telang, P. Khampariya**, “*Voltage Stability Evaluation Using Modal Analysis*”, International Journal of Scientific Research Engineering & Technology (IJSRET), ISSN: 2278-0882, Vol. 4, Issue 4, April 2015
- [58] **H.A.Hassan, Z.H.Osman, Abd El- Aziz Lasheen**, “*Sizing Of STACOM To Enhance Voltage Stability Of Power Systems For Normal And Contingency Cases*”, Scientific Search, www.scrip.org/journal/sgre, 2014
- [59] **S.B. Bhaladhare, A.S.Telang, P.P.Bedekar**, “*P-V, Q-V, A Novel Approach For Voltage Stability*”, National Conference on Innovation Paradigms in Electrical & Technology (NCIPET-2013) Proceedings published by International Journal Of Computer Applications (IJCA), 2013
- [60] **M.M. Salama, E.M. Saeid, H.M Mahmoud, A.S. Allaw**, “*Estimating The Voltage Stability Of Electrical Power Systems Using Field Programme Get Array (F.P.G.A) Technique*”, Engineering Research Journal, Shoubra Faculty of Engineering, Benha University, Egypt, Vol. 19, July 2013, pp. 13-23
- [61] **C. Reis, F.P. Maciel Barbosa**, “*A Comparison Of Voltage Stability Indices*”, IEEE MELECON 2006, May 16-19, Spain
- [62] **K.Z. Heetun, S.H.E. A. Aleem , A. F. Zobaa**, “*Voltage Stability Analysis Of Grid –Connected Wind Farms With FACTS: Static And Dynamic Analysis*”, Energy and Policy Research, Taylor & Francis, ISSN: 2381-5639, June 2016
- [63] **H.M. and Iman Soltani**, “*Continuation Power Flow Method With Improved Voltage Stability Analysis In Two Area Power System*”, International Journal of Electrical Energy, Vol.1, No.1, March 2013
- [64] **H. Marefatijou, M. Sarvi**, “*Power Flow Study And Performance Of STATCOM And TCSC In Improvement Voltage Stability And Load Ability Amplification In Power System*”, International Journal of Applied Power Engineering (IJAPE), Vol.2, No.1, April 2013, ISSN: 2252-8792

- [65] **A. Chakrabarti, D.P. Kothari, A.K. Mukhopadhyay, A. De**, “*An Introduction To Reactive Power Control And Voltage Stability In Power Transmission Systems*”, PHI Learning Private Limited, ISBN-978-81-203-4050-3
- [66] **M.Z. Laton, I.Musirin, T.K.A. Rahman**, “*Voltage Stability Assessment Via Continuation Power Flow Method*”, International Journal of Electrical and Electronics Systems Research, Vol.1, June 2008
- [67] **S.D.Patel, H.H. Raval, A. G.Patel**, “*Voltage Stability Analysis Of Power System Using Continuation Power Flow Method*”, International Journal for Technological Research In Engineering, ISSN: 2347-4718, Vol.1, Issue 9, May 2014
- [68] **F.Milano**, “*An Open Source Power System Analysis Toolbox*”, IEEE Transactions on Power Systems, Vol. 20, No. 3, August 2005
- [69] **L. Jebaraj, C. Christoper Asir Rajan, S.S**, “*Real Power Loss And Voltage Stability Limit Optimization Incorporating TCSC And SVC Through DE Algorithm Under Different Operating Conditions Of A Power System*”, IOSR Journal of Electrical and Electronics Engineering (IOSRJEEE), ISSN:2278-1676, Vol. 1, Issue 5, July-August 2012
- [70] **R.Selvarasu, M.S.Kalavathi.**, “*TCSC Placement For Loss Minimum Using Self Adaptive Firefly Algorithm*”, Journal of Engineering Science and Technology, Vol.10, No.3, 2015
- [71] **S.K. El Sayed**, “*Comparison of TCSC and UPFC for Increasing Power Transfer Capability and Damping Power System Oscillation*”, New York Science Journal, ISSN: 1554-0200, 2014
- [72] **S.B Bhaladhare, P.P. Bedekar**, “*Enhancement Of Voltage Stability Through Optimal Location Of SVC*”, International Journal of Electronic and Computer Science Engineering, IJECSE, Vol.2, ISSN: 2277-1956

- [73] **S. Akter, A. Saha, P. Das**, “*Modelling Simulation And Comparison Of Various Facts In Power System*”, International Journal of Engineering Research & Technology (IJERT), Vol. 1 Issue 8, October -2012, ISSN 2278-0181
- [74] **Aswin R, Jo Joy**, “*Comparison between STATCOM And TCSC On Static Voltage Stability Using MLP Index*”, International Journal of Advanced Research in Electrical, Electronics and Instrumentation Engineering, ISSN: 2320-3765, Vol.2, Special Issue 1, December 2013
- [75] **B.K. Mehta, P.J. Patel**, “*Static Voltage Stability Improvement In Power System Using STATCOM FACTS Controller*”, Journal of Information, Knowledge and Research in Electrical Engineering, ISSN: 0975-6736, Vol. 02, Issue -02, November 2012 To October 2013
- [76] **J.M. Ranirez, and J.L.M.Perez**, “*Application Of The Three –Phase STACOM In Voltage Stability*”, www.aedic.org, www.researchgate.net, 229020984
- [77] **A.H. Sekhar, A.L. Devi**, “*Performance Improvement Of Transmission System Using TCSC With Firing Angle Control*”, Journal of Theoretical and Applied Information Technology, e-ISSN 1817-3195, 2005-2016
- [78] **K.V.R. Reddy, M.P.Lalita, PB Chennaiah**, “*Improvement Of Voltage Profile Through The Optimal Placement Of FACTS Using L-Index Method*”, International Journal of Electrical and Computer Engineering (IJECE), Vol.4, No.2, ISSN: 2088-8707, April 2014
- [79] **Le Ngoc Giang, N. T. D. Thuy, T.T Ngoat**, “*Assessment Study of STATCOM Effectiveness In Improving Transient Stability For Power System*”, TELKOMNIKA, Vol.11, No.10, October 2013, pp. 6095~6104, e-ISSN: 2087-278X

- [80] **J.E. Essilfie, J. Tlustý, P.Santarius**, “*Using SVC To Improve Voltage Stability Of The Ghana Power Network*”, Czech Technical University in Prague(1), VSB-Technical University of Ostrava, ISSN: 0033-2097, R- 89, NR5/2013
- [81] **D. Sahasrabude, P. Pandey**, “*Voltage Stability Enhancement By VAR Management Using SVC And STATCOM*”, International Journal of Advanced Research and Technology (JERT), ISSN: 2278-0181, Vol. 2, Issue: 9, September, 2013
- [82] **F. Milano**, “*Power System Analysis Toolbox Documentation For PSAT*”, version 2.0.0 _1, March 24, 2006
- [83] **K.G. T, Z.J. Khan**, “*Optimization Of Reactive Power By Using SVC And TCSC Devices For Reducing Transmission Loss*”, International Journal of Core Engineering & Management (IJCEM), Vol.2, Issue 3, June 2015, ISSN: 2348-9510
- [84] **H.H. Goh, Q.S. Chua, S.W. Lee, B.C. Kok, K.C. Goh, K.T.K. Teo**, “*Evaluation For Voltage Stability Indices In Power Systems Using Artificial Neural Network*”, ELSEVIER-Procedia Engineering, 118(2015)1127-1136
- [85] **C. Reis and M. Barbosa**, “*Assessment Of Voltage Of Electrical Power Systems: A Simulational Survey*”, IEEE Xplore, 18 Dec 2009
- [86] **P.R.Sharma, R.K. Ahuja, S. Vashissth, V. Hudda**, “*Computation Of Sensitive Node For IEEE- 14 BUS System Subjected To Load Variation*”, International Journal of Innovative Research in Electrical, Electronics, Instrumentation And Control Engineering, Vol.2, Issue 6, June 2014,ISSN 2321-5526
- [87] **A.M. Chebbo, M.R. Irving, M.J.H. Sterling**, “*Voltage Collapse Proximity Indicator: Behaviour And Implications*”, IEE Proceedings-c, Vol.139, No.3, May1992

- [88] **H.H. Goh, Q.S. Chua, S.W. Lee, B.C. Kok, K.C. Goh, K.T.K. Teo,** “*Comparative Study Of Line Voltage Stability Indices For Voltage Collapse Forecasting In Power Transmission System*”, International Journal of Electrical , Computer, Energetic, Electronic and Communication Engineering Vol. 9, No. 2, 2015
- [89] **N. D. Hatziaargyriou, T. Van Cutsem,** “*Indices For Predicting Voltage Collapse Including Dynamic Phenomena*”, Technical Report TF-38-02-11, CIGRE, 1994.
- [90] **I. Dobson, T. V. Cutsem, C. Vournas, C. L. DeMarco, M. Venkatasubramanian, T. Overbye, C.A. Canizares,** “*Voltage Stability Assessment: Concepts, Practices And Tools*”, Chapter 2, [Online] Available <https://www.researchgate.net/publication> , January 2002
- [91] **M.H. Haque,** “*Use of Local Information to Determine the Distance to Voltage Collapse*”, The 8th International Power Engineering Conference IPEC 2007, pp.407-411
- [92] **K.R.Vadivelu., G.V. Marutheswar,** “*Fast Voltage Stability Index Based Optimal Reactive Power Planning Using Differential Evolution*”, An International Journal (ELELU), Vol.3, No.1, February 2014
- [93] **S. Choudhary, Samina E. Mubeen, M. Jain,** “*Evaluation Of TCSC Power Flow Control Capability*”, Innovative Systems Design and Engineering, Vol.4, No.6, 2013, ISSN: 2222-1727
- [94] **I.A. Shah, Y.R. Prajapati,** “*Implementation Of TCSC For Enhancement Of ATC*”, International Journal of Engineering and Electronics Engineers, IJEEE, Vol. 07, ISSN-2321-2055(E), Jan-June 2015
- [95] **N. Rajasree, M.D. Reddy,** “*Simultaneous Placement Of TCSC And UPFC In Transmission System Using Teaching –Learning Based Optimization Technique*”, Discovery The International Daily 2015, ISSN 2278-5469

- [96] **P. Singh, L.S. Titare, L.D. Arya**, “*Mitigation of Transmission Lossess with Voltage Stability Consideration Using TLBO*”, Power and Energy Systems: Towards Sustainable Energy (PESTSE 2014).
- [97] **N.A. Kumar, M.R. Kumar, M.Y, J. Dinesh**, “*Comparative Study On The Effectiveness Of TCSC And UPFC Controllers*”, International Journal of Computer Application, Vol. 67–No.5, April 2013
- [98] **R.V. Rao**, “*Teaching Learning Based Optimization Algorithm And Its Engineering Applications*”, © Springer International Publishing Switzerland 2016, ISBN: 978-3-319-22731-3, ISBN 978-3-319-22732-0 (eBook), DOI 10.1007/978-3-319-22732-0
- [99] **BV. Srikanth, A.L. Devi**, “*Voltage Stability Analysis And Bifurcation Techniques: A Detailed Survey*”, International Journal of Latest Trends in Engineering and Technology (IJLTET), ISSN: 2278-621x, Vol-7, Issue-3 June 2016.
- [100] **E.N. Kumar, R.D, and R. Mani**, “*Optimal Location And Improvement Of Voltage Stability By UPFC Using Genetic Algorithm (GA)*”, Indian Journal of Science and Technology, Vol. 8 (11), 56463, June 2015, ISSN (Print) - 0974-6846
- [101] **A. Jagadeesh. And G.V.N. Kumar**, “*Optimal Placement Of Static VAR Compensation Using Genetic Algorithm And Particle Swarm Optimization Techniques*”, Elixir, ISSN-2229-712x, 2012
- [102] **M.Kowsalya, K.K. Ray, D.P.Kothari**, “*Voltage Stability Enhancement Through Optimal Location Of Var Compensator*”, IEEE Xplore, DOI: 10.1109/ICSET.2008.4747033, 09 Jan. 2009
- [103] **S.C. Satapathy, A. Naik, K. Parvathi**, “*A Teaching Learning Based Optimization Based On Orthogonal Design For Solving Global Optimization Problems*” , Springer Plus 2013, 2:130

- [104] **K. Lenin, B.R. Reddy, M.S. Kalavathi**, “*Improved Teaching Learning Based Optimization (Tlbo) Algorithm For Solving Optimal Reactive Power Dispatch Problem*”, Vol. 1, 2013, ISSN 2345-3877
- [105] **M.R. Nayak, C.K. Nayak, P.K. Rout**, “*Application Of Multi-Objective Teaching Learning Based Optimization Algorithm To Optimal Power Flow Problem*”, Elsevier, Science Direct Procedia Technology 6(2012) 255-264
- [106] **K.R. Krishnanand, B.K. Panigrahi, P.K. Rout, A. Mohapatra**, “*Application Of Multi-Objective Teaching- Learning-Based Algorithm To An Economic Load Dispatch Problem With Incommensurable Objectives*”, SEMCCO 2011, Part 1, LNCS 7076, pp 697-705, Springer-Verlag Berlin Heidelberg 2011
- [107] **M. Kumari**, “*Global Journal Of Engineering Science And Researchers Distributed Generation Planning Using Teaching Learning Based Optimization With Voltage Stability Consideration*”, Impact Factor -3.155, ISSN: 2348-8034, October 2015
- [108] **B. Mohanty, S.Tripathy**, “*A Teaching Learning Based Optimization Technique For Optimal Location And Size Of DG In Distribution Network*”, Journal of Electrical and Information Technology, March 2016
- [109] **Y.L. Reddy, M. Sydulu**, “*Teaching –Learning –Based Optimization Algorithm For Reconfiguration In Radial Distribution Systems For Loss Reduction*”, International Journal of Advanced Engineering and Global Technology, ISSN: 2309-4893, Vol-2, Issue-4, April 2014.
- [110] **Y. Muhammad, M.N. Arbab**, “*Optimization in Tap Changer Operation of Power Transformer using Reactive Power Compensation by FACT devices*”, IEEE, 4th Control and System Graduate Research Colloquium, Shah Alam, Malaysia, 19-20 Aug, 2013